ARMY RESEARCH LABORATORY

Conceptual Design Approach for Small-Caliber Aeroballistics With Application to 5.56-mm Ammunition

by Paul Weinacht, James F. Newill, and Paul J. Conroy

ARL-TR-3620   **September 2005**

NOTICES

Disclaimers

Army Research Laboratory

Aberdeen Proving Ground, MD 21005-5066

ARL-TR-3620 **September 2005**

Conceptual Design Approach for Small-Caliber Aeroballistics With Application to 5.56-mm Ammunition

Paul Weinacht, James F. Newill, and Paul J. Conroy
Weapons and Materials Research Directorate, ARL

REPORT DOCUMENTATION PAGE		*Form Approved* *OMB No. 0704-0188*

1. REPORT DATE *(DD-MM-YYYY)* September 2005	2. REPORT TYPE Final	3. DATES COVERED (From - To) 2003–2005
4. TITLE AND SUBTITLE Conceptual Design Approach for Small-Caliber Aeroballistics With Application to 5.56-mm Ammunition		**5a. CONTRACT NUMBER**
		5b. GRANT NUMBER
		5c. PROGRAM ELEMENT NUMBER
6. AUTHOR(S) Paul Weinacht, James F. Newill, and Paul J. Conroy		**5d. PROJECT NUMBER** 1L1612618AH
		5e. TASK NUMBER
		5f. WORK UNIT NUMBER
7. PERFORMING ORGANIZATION NAME(S) AND ADDRESS(ES) U.S. Army Research Laboratory ATTN: AMSRD-ARL-WM-BC Aberdeen Proving Ground, MD 21005-5066		**8. PERFORMING ORGANIZATION REPORT NUMBER** ARL-TR-3620
9. SPONSORING/MONITORING AGENCY NAME(S) AND ADDRESS(ES)		**10. SPONSOR/MONITOR'S ACRONYM(S)**
		11. SPONSOR/MONITOR'S REPORT NUMBER(S)

12. DISTRIBUTION/AVAILABILITY STATEMENT

Approved for public release; distribution is unlimited.

13. SUPPLEMENTARY NOTES

14. ABSTRACT

A conceptual design approach for small-caliber ammunition is presented. The analysis is based on analytical solutions of the point mass trajectory equations obtained using a power law model of the drag coefficient variation with Mach number. The method is validated by comparison with numerical trajectory predictions for the 5.56-mm M855. Using existing data, several important observations regarding small arms drag characteristics are quantified. The results of the analysis form the basis for a conceptual design approach for examining the aeroballistics of small-caliber munitions. Application is then made to 5.56-mm ammunition. Results are presented that examine the design boundaries for 5.56-mm ammunition in terms of trajectory match relative the 5.56-mm M855. By considering interior ballistics constraints and dependence of muzzle velocity on launch mass, the design space is further refined. The results allow the projectile performance to be characterized in terms of impact velocity and energy, gravity drop, trajectory mismatch at range, and cross-wind sensitivity.

15. SUBJECT TERMS

aerodynamics, aeroballistics, small-caliber ammunition

16. SECURITY CLASSIFICATION OF:			17. LIMITATION OF ABSTRACT	18. NUMBER OF PAGES	19a. NAME OF RESPONSIBLE PERSON Paul Weinacht
a. REPORT UNCLASSIFIED	**b. ABSTRACT** UNCLASSIFIED	**c. THIS PAGE** UNCLASSIFIED	UL	74	**19b. TELEPHONE NUMBER** (*Include area code*) 410-278-4280

Contents

List of Figures

List of Tables

INTENTIONALLY LEFT BLANK.

1. Introduction

The current generation of 5.56-mm ammunition for the M16 and M4 rifles has provided the U.S. Army with high performance projectiles for several decades. Currently, the U.S. Army is investigating possible replacements for the existing family of 5.56-mm ammunition. Some of the factors driving the replacement include cost and performance. The reduction of the environmental impact associated with the materials currently used in 5.56-mm ammunition, in particular the heavy metal lead core, is an additional important consideration and is being addressed by the U.S. Army's Green Ammunition programs.

As part of the design effort, conceptual design studies are being performed to define the design space and highlight the important design variables. A recent study (*1*) has provided the framework for examining the exterior ballistic performance in a conceptual design environment where many details of the design have not been fully established. This allows the gross characteristics of the round to be examined and the design tradeoffs regarding the aeroballistics to be more fully quantified and understood. In the current effort, interior ballistic considerations have also been incorporated as well. The analysis also considers relatively simple metrics that allow the terminal performance to be assessed in a very general qualitative manner. These types of metrics are appropriate for a conceptual design approach, although, clearly, more detailed analysis is required to quantify the terminal performance as the design process evolves.

The basis of the current approach is a simple but accurate method for predicting the trajectories for high velocity direct-fire munitions (*1*). The method allows the trajectories to be characterized in terms of three parameters: the muzzle velocity, the muzzle retardation (or velocity fall-off), and a parameter defining the shape of the drag curve. The method provides an excellent means of assessing the exterior ballistic performance in a conceptual design environment where details of the designs have not been completely defined.

In the following sections, the analytical approach for solving the three-degree-of-freedom (3DOF) trajectory equations is briefly described and benchmarked with numerical predictions of the trajectory of the 5.56-mm M855 projectile. The drag characteristics of existing small arms bullets are then analyzed and several important observations regarding the drag characteristics are quantified. Results are then presented for a family of potential 5.56-mm ammunition designs. The first set of results examines the performance of 5.56-mm ammunition assuming the muzzle velocity is an independent parameter. The boundaries of the design space are defined in terms of trajectory match with the existing M855 projectile. The second set of results considers the effect of interior ballistic considerations and constraints on the muzzle velocity resulting from the dependence of muzzle velocity on projectile mass. Both sets of results provide important design guidance for current efforts in 5.56-mm ammunition development.

2. Technical Approach

The flat fire trajectory of a projectile can be characterized as follows (*2*):

$$\begin{bmatrix} \text{The Complete} \\ \text{Flat Fire Trajectory} \end{bmatrix} = \begin{bmatrix} \text{The Flat Fire} \\ \text{Point Mass Trajectory} \end{bmatrix} + \begin{bmatrix} \text{Lateral} \\ \text{Throwoff} \end{bmatrix} + \begin{bmatrix} \text{Aerodynamic} \\ \text{Jump} \end{bmatrix} + \begin{bmatrix} \text{Epicyclic} \\ \text{Swerve} \end{bmatrix} + \begin{bmatrix} \text{Drift} \end{bmatrix}. \tag{1}$$

The flat fire point mass trajectory accounts for the most dominant characteristics of the trajectory and is most heavily influenced by the mass and drag characteristics of the projectile. It includes such effects as gravity drop and cross-wind drift. It is this portion of the trajectory that is the focus of the current concept design approach. The aerodynamic jump and lateral throwoff of the projectile produce angular deviations of the flight path from the intended line of flight due to launch disturbances and mass asymmetries within the projectile, respectively. Bias errors associated with these effects are normally removed through the rifle zeroing process. These effects can also produce random errors that contribute to the ammunition dispersion. Normally, these effects would not be considered in any detail in a conceptual design process as the relative magnitude of these effects can only be quantified later in the design cycle. Additionally, the relative magnitude of the lateral throwoff is heavily influenced by manufacturing quality considerations. The epicyclic swerve represents fluctuating motions of the projectile about the trajectory due to the angular motion of the projectile. For a stable projectile, these motions are typically small relative to the mean path of the projectile. The drift produces a small horizontal deflection of the projectile that is fairly consistent from shot to shot. The deflection is typically small compared with cross-wind drift.

The flat fire point mass trajectory can be obtained by solving the 3DOF equations. This approach considers only the linear displacement of the projectile's center of gravity along the flight path and ignores the angular motion of the projectile. Using this approach, the projectile is characterized by its muzzle velocity, mass, and the variation of its drag coefficient with Mach number. Typically, the integration of the 3DOF equations is performed numerically. However, it is also possible to obtain analytical solutions of the 3DOF equations under the assumption of direct fire using an assumed form of the drag coefficient variation with Mach number (*1*). For supersonic flight, it can be shown that the drag coefficient variation with Mach number can be modeled as a function of Mach number to a power as shown in equation 2. For constant atmospheric conditions, the sound speed is constant, and the Mach number and velocity are directly proportional. In this case, the drag coefficient varies with Mach number and velocity in the same manner.

$$C_D \propto \frac{1}{M^n} \propto \frac{1}{V^n}. \tag{2}$$

Figure 1 shows the variation of the drag coefficient with Mach number for the 5.56-mm M855. The Firing Tables Branch (FTB), U.S. Army Armament Research, Development, and Engineering Center (ARDEC) "aeropack" data (*3*) used to construct firing tables for the round are shown along with aerodynamic spark range data (*4*). The fit of the FTB aeropack drag coefficient data obtained using the power law formulation shown in equation 2 is also shown. The computed exponent for the M855 is 0.53 for the range between Mach 2.8 (muzzle velocity) and Mach 1.1. The power law fit shows excellent agreement over this Mach number range.
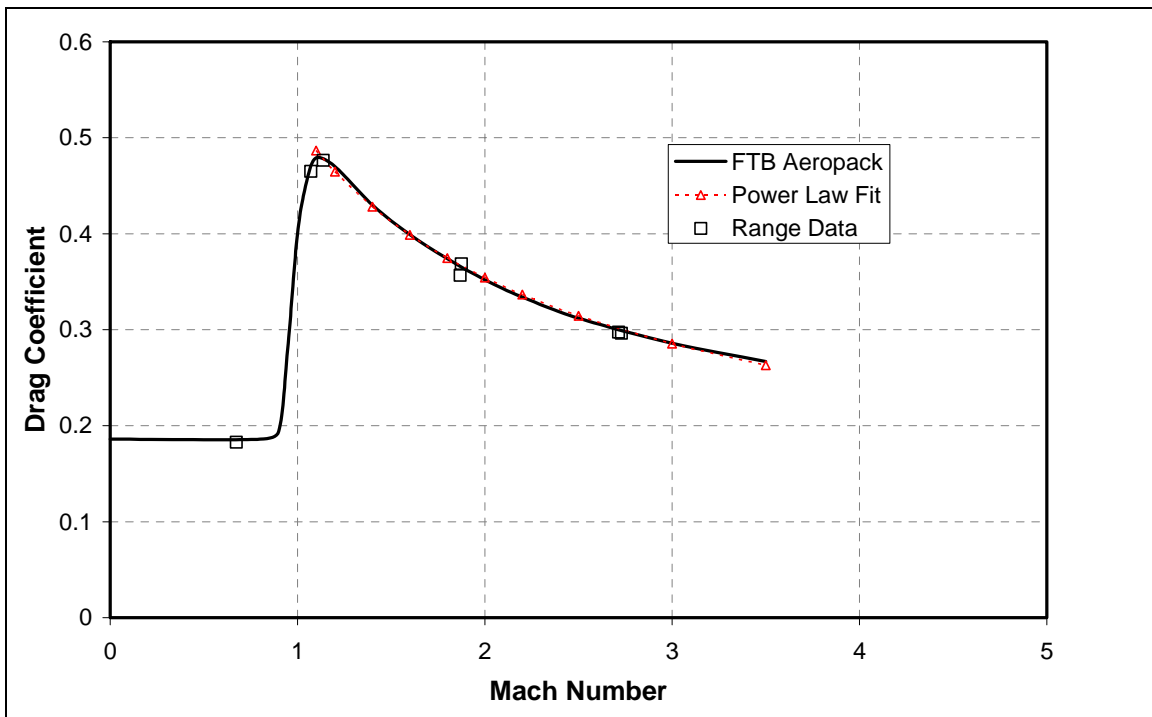
Figure 1. Fit of drag coefficient for the M855.

Weinacht et al. (*1*) examined the drag coefficient variation of a wide variety of munitions and found that the drag coefficient exponent varied between 0.0 and 1.0 for supersonic flight. Additional results specifically aimed at small arms ammunition have been obtained as part of the current study. These results are discussed in a subsequent section.

Using this approach, analytical solution of the governing equations can be obtained resulting in closed form equations for the dependent variables characterizing the projectile trajectory. These include the velocity V, time of flight t, gravity drop $s_{g\text{-drop}}$, vertical displacement of the projectile along the trajectory s_y, and vertical deflection due to cross wind s_z, as a function of range s_x, as shown in equations 3–7.

3

$$V = V_0 \left\{ 1 + n \left(\frac{dV}{ds} \right)_0 \frac{s_x}{V_0} \right\}^{\frac{1}{n}}. \tag{3}$$

$$t = \frac{1}{(n-1)\left(\dfrac{dV}{ds} \right)_0} \left[\left\{ 1 + n \left(\frac{dV}{ds} \right)_0 \frac{s_x}{V_0} \right\}^{1-\frac{1}{n}} - 1 \right]. \tag{4}$$

$$s_{g-drop} = \frac{-g}{2(n-2)(n-1)\left(\dfrac{dV}{ds} \right)_0^2} \left[\left\{ 1 + n \left(\frac{dV}{ds} \right)_0 \frac{s_x}{V_0} \right\}^{\frac{2(n-1)}{n}} - 1 - 2(n-1) \left(\frac{dV}{ds} \right)_0 \frac{s_x}{V_0} \right]. \tag{5}$$

$$s_y = s_x \tan \theta_0 + s_{g-drop}. \tag{6}$$

$$s_z = w_z \left[t - \frac{s_x}{V_0} \right]. \tag{7}$$

Through the analysis, it can be shown that these trajectory characteristics are functions of only three primary variables, the projectile's muzzle velocity V_0, muzzle retardation $\left(\dfrac{dV}{ds} \right)_0$, and the exponent defining the shape of the drag curve n. The trajectory is also a function of two independent parameters, the gravitational constant g, and the cross-wind velocity w_z. The gun elevation angle θ_0 also appears in equation 6 and can be treated as another independent parameter. However, the gun elevation angle θ_0 required to hit a target at range can be related to the three primary variables: the muzzle velocity, muzzle retardation, and drag coefficient exponent. In this regard, the gun elevation angle itself can be treated as a dependent variable. The muzzle velocity and muzzle retardation have the strongest influence on the trajectory and the exponent defining the shape of the drag curve can be shown to be a higher-order effect whose influence is less important that the first two variables, particularly at shorter ranges.

The muzzle retardation is dependent on the projectile mass and muzzle drag coefficient as shown in equation 8.

$$\left(\frac{dV}{ds} \right)_0 = -\frac{1}{2m} \rho V_0 S_{ref} C_D \big|_{V_0}. \tag{8}$$

Thus, the effect of both projectile mass and muzzle drag coefficient on the trajectory are represented by a single parameter, the muzzle retardation. The effect on the trajectory of a 20% increase in the drag coefficient is the same as a 20% decrease in the projectile mass.

The approach was validated in Weinacht et al. (*1*) for large-caliber tank-fired munition such as the M829A1, M830, M865, and M830A1 by comparing the results of the analytical method with

numerical solutions obtained with the 6DOF option of the aerodynamic and trajectory prediction code PRODAS (*5*). Excellent agreement between the two approaches was found. In fact, in most cases, the uncertainty or variability in the muzzle velocity and muzzle retardation (in particular, the muzzle drag coefficient) produces more error than the approximations made to obtain the analytical integrations, although both of these errors are typically small.

Similar validation for small-caliber munitions was performed as part of the current study. Predictions of the trajectory history were made for the 5.56-mm M855 munition using the analytical approach and 6DOF predictions from PRODAS. To provide a fair basis for comparison, both simulations used the identical muzzle velocity and projectile mass. The drag coefficient exponent used in the analytical approach was obtained by fitting the drag coefficient variation with Mach number obtained from U.S. Army ARDEC FTB "aeropack" data for the M855. The aeropack data is used to compute the firing tables for the round. This data was also used to determine the muzzle drag coefficient and, subsequently, the muzzle retardation used in the analytical approach. This drag data was also used for the PRODAS simulations. The 6DOF simulations also require additional aerodynamic data. Updated aerodynamics based on aerodynamic range firings (*4*) were used for the PRODAS 6DOF simulations, although these data have little effect on the point mass trajectory parameters considered here. Figures 2–6 show the velocity history, time of flight, gravity drop, vertical displacement for 300- and 600-m range trajectories, and cross-wind deflection due to 10-m/s cross wind as a function of range. Excellent agreement is seen between the PRODAS simulations and the analytical predictions.
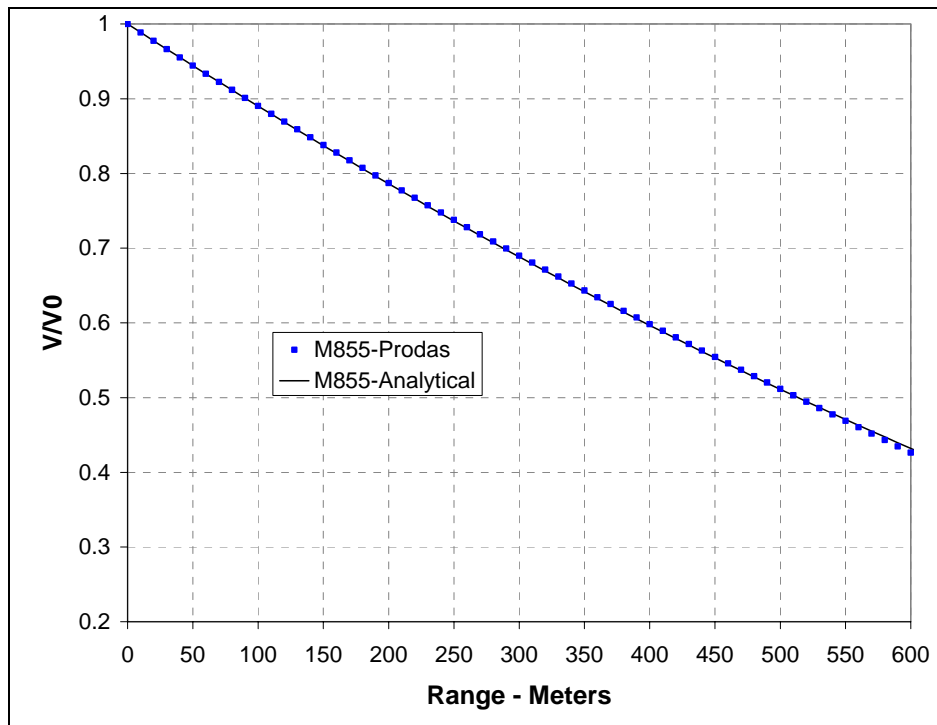
Figure 2. Fractional remaining velocity as a function of range, M855.
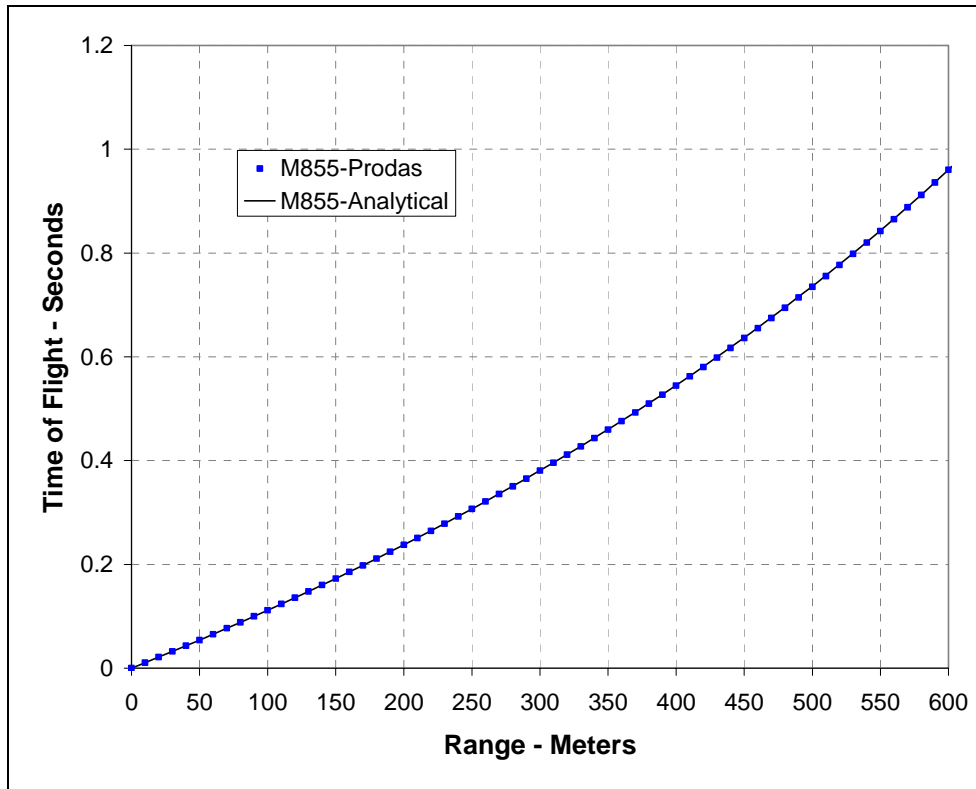
Figure 3. Time of flight vs. range, M855.
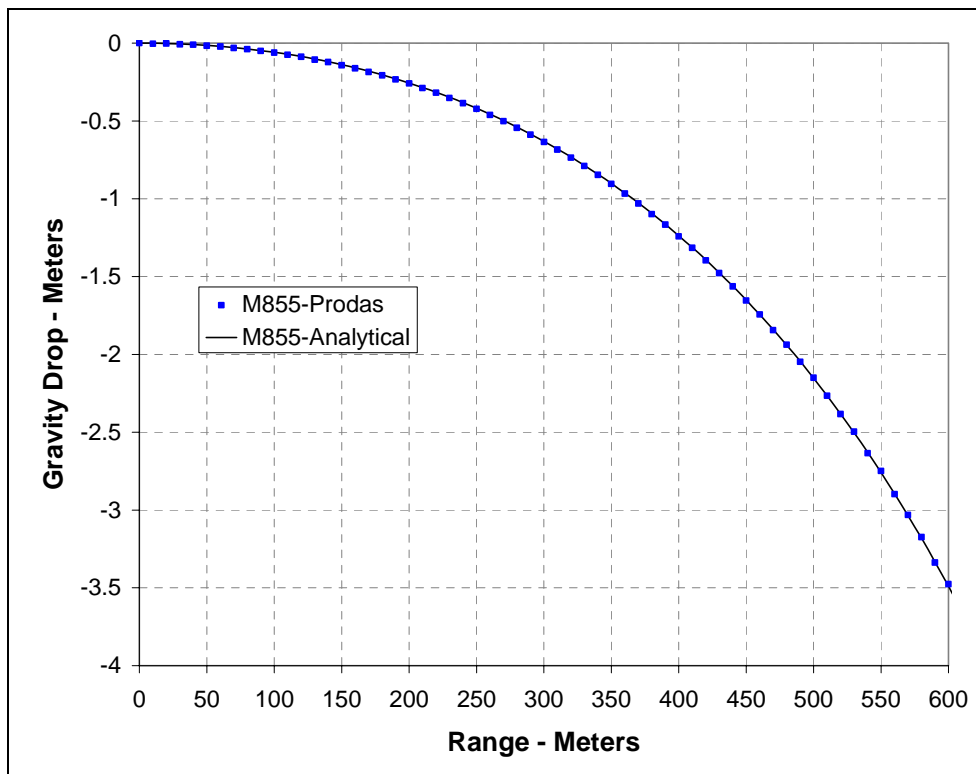
Figure 4. Gravity drop vs. range, M855.
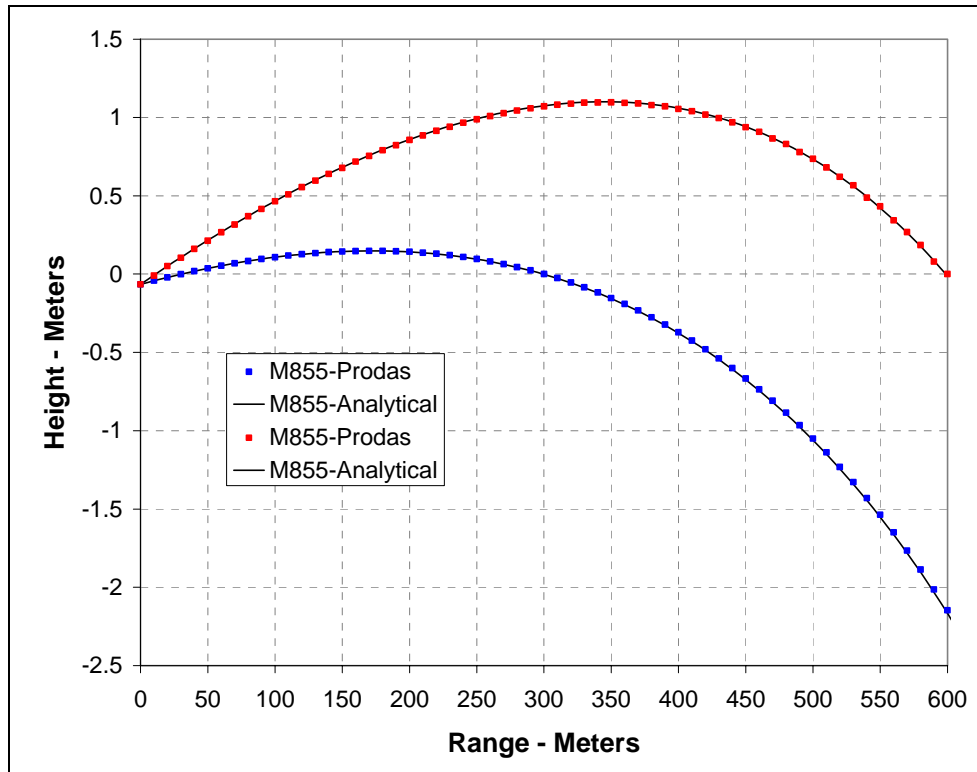
Figure 5. Trajectories to hit 300- and 600-m targets, M855.
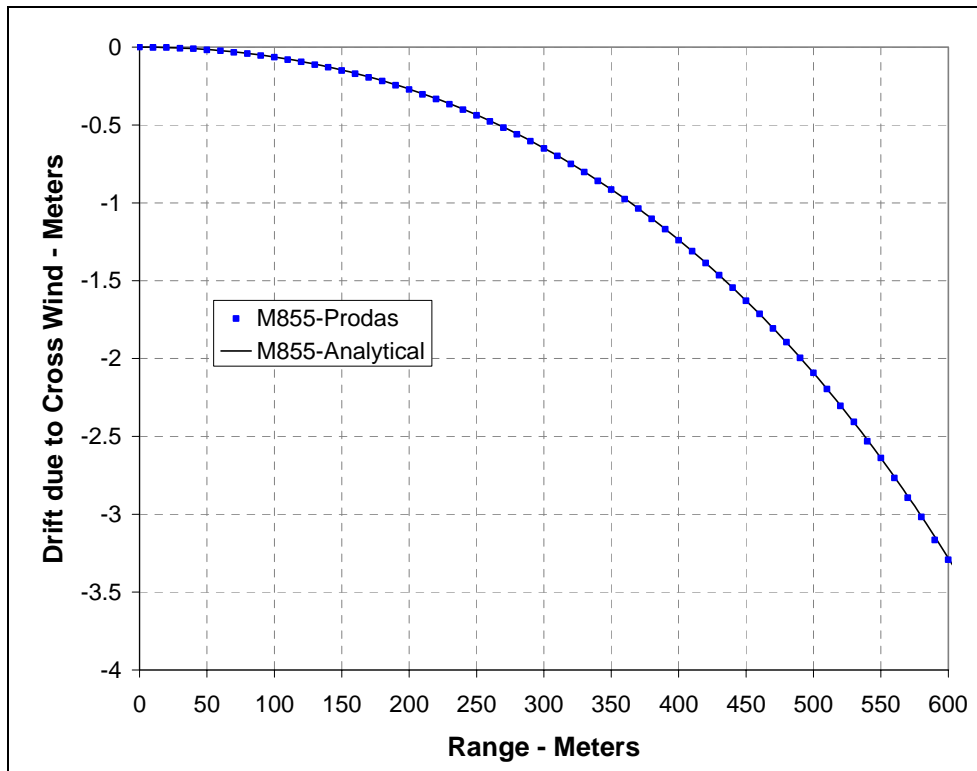
Figure 6. Cross-wind drift due to 10-m/s cross wind, M855.

Figure 7 also shows two important contributions to the vertical and horizontal displacement of the projectile along the trajectory obtained from the 6DOF predictions. These two contributions are the horizontal drift due to yaw of repose and the deflection (vertical or horizontal) due to aerodynamic jump. Prediction of these displacements requires additional details of the projectile physical properties and aerodynamics beyond those required for 3DOF trajectory predictions presented here. Typically, these details are not available in the conceptual design process considered here, but are defined as the design evolves. In any event, these effects exist and must be considered in the conceptual design even if they can't be predicted in the conceptual design process.
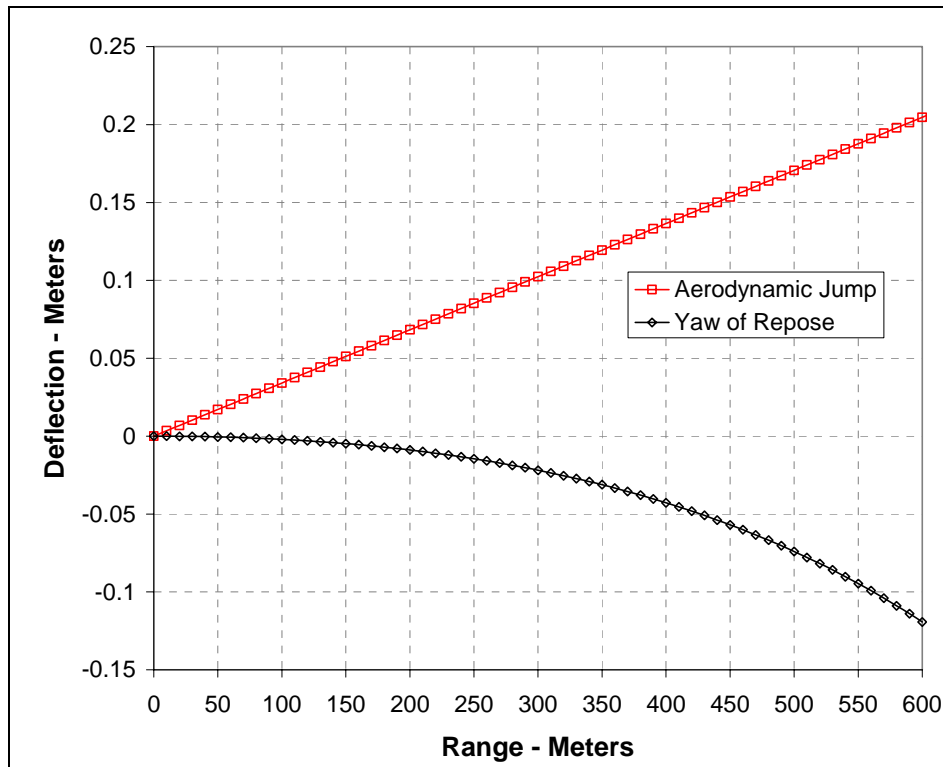
Figure 7. Drift due to yaw of repose and aerodynamic jump due to 50-rad/s angular rate at muzzle, M855.

There are two notable sources of error or uncertainty in applying the approach of Weinacht et al. (*1*). The first is the approximation made to obtain closed form analytical solution of the point mass trajectory equations. This approximation assumes that the component of velocity produced by gravity is small and can be ignored when computing the aerodynamic drag of the projectile. This approximation is valid for flat fire and has been shown to produce very little error when compared with more exact numerical solutions of the governing equations.

The second source of error is associated with modeling the variation of the drag coefficient with Mach number using a power law approach. The analysis of Weinacht et al. (*1*) shows that the drag variation of a wide variety of munitions can be accurately modeled using this approach.

8

Furthermore, the predicted trajectories obtained using this approach show surprisingly little sensitivity to the exponent used in the power law approach. This implies that the shape of the drag curve is not a dominant factor in predicting the trajectory, particularly when compared with the muzzle velocity and muzzle retardation. This is significant because when the current approach is used in a conceptual design approach, the design process can focus on muzzle velocity and muzzle retardation as the significant design variables defining the point mass trajectories. The second source of uncertainty must be considered whether analytical or numerical solutions of the point mass equations are sought. In either case, the variation of the drag coefficient with Mach number must be specified. The power law approach represents a very useful approach for conceptual design because of its simplicity and accuracy in representing the drag variation with Mach number. The geometric details required to obtain a more accurate drag variation are unavailable at this point in the design cycle.

Figures 8–10 show the relative effect of uncertainty in the muzzle velocity, muzzle retardation, and the exponent defining the shape of the drag curve on the predicted velocity, gravity drop, and cross-wind drift, respectively. Here, the results show differences between the baseline M855, a projectile with 10% more muzzle velocity, a projectile with 10% higher retardation, and a projectile with a drag coefficient exponent of 0.25 (relative to the baseline drag coefficient of 0.53). The selected differences are indicative of uncertainties that might be present in a conceptual design environment where the physical characteristics of the munition are not completely defined. (They should not be interpreted as representative of any variability in performance of the M855.) The selected drag coefficient exponents represent a relatively large difference given the ability to appropriately estimate this parameter. Analysis presented in the following section provides a means of estimating this parameter with greater fidelity than that represented by the differences presented here.

The results show a greater sensitivity to muzzle velocity and muzzle retardation although the magnitude of the sensitivity depends somewhat on the dependent variable being considered. Gravity drop appears to be more heavily influenced by muzzle velocity than muzzle retardation since the gravity drop is strongly affected by the time of flight, which, to first order, is a function of muzzle velocity and range. Cross-wind drift shows significant sensitivity to both muzzle velocity and muzzle retardation. The greatest sensitivity of the results to the drag coefficient exponent relative to the muzzle velocity and muzzle retardation is seen for the velocity history shown in figure 8. At ranges up to about 300 m, the difference between predicted velocities for the baseline results and the results with a drag coefficient exponent of 0.25 is less than 2%. The differences increase to about 10% at 600 m. The sensitivity of the results to drag coefficient exponent is less for the cross-wind drift and gravity drop. These results provide further demonstration that the muzzle velocity and muzzle retardation are dominant independent variables defining the characteristics of the 3DOF trajectory.
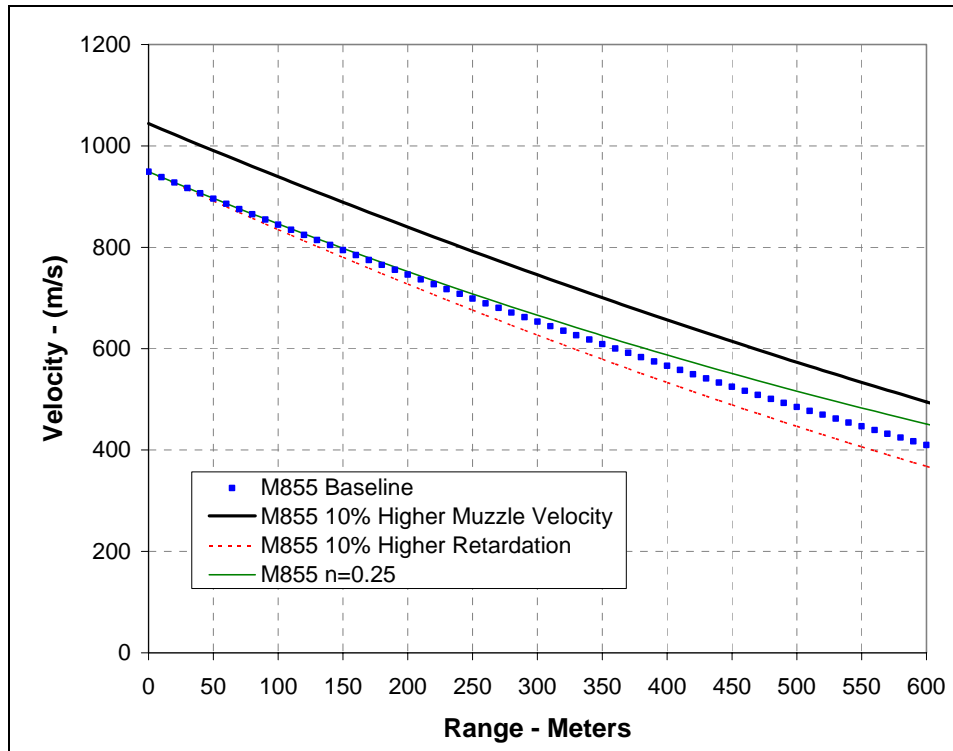
Figure 8. Velocity vs. range for baseline M855, M855 with 10% higher muzzle velocity, M855 with 10% higher retardation, and M855 with n = 0.25.
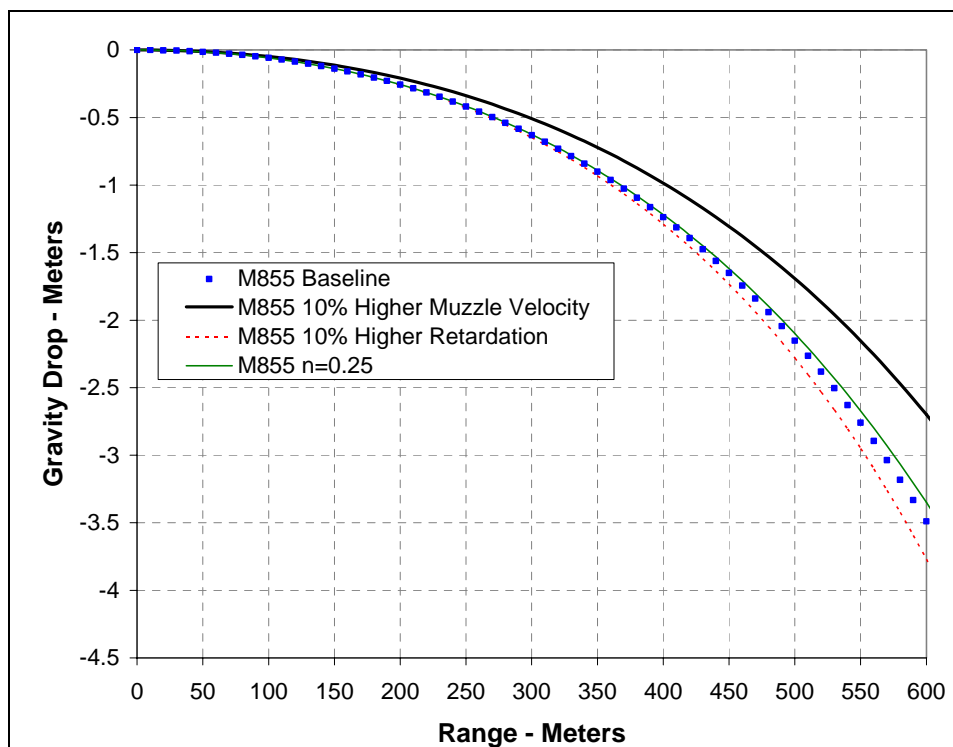
Figure 9. Gravity drop vs. range for baseline M855, M855 with 10% higher muzzle velocity, M855 with 10% higher retardation, and M855 with n = 0.25.
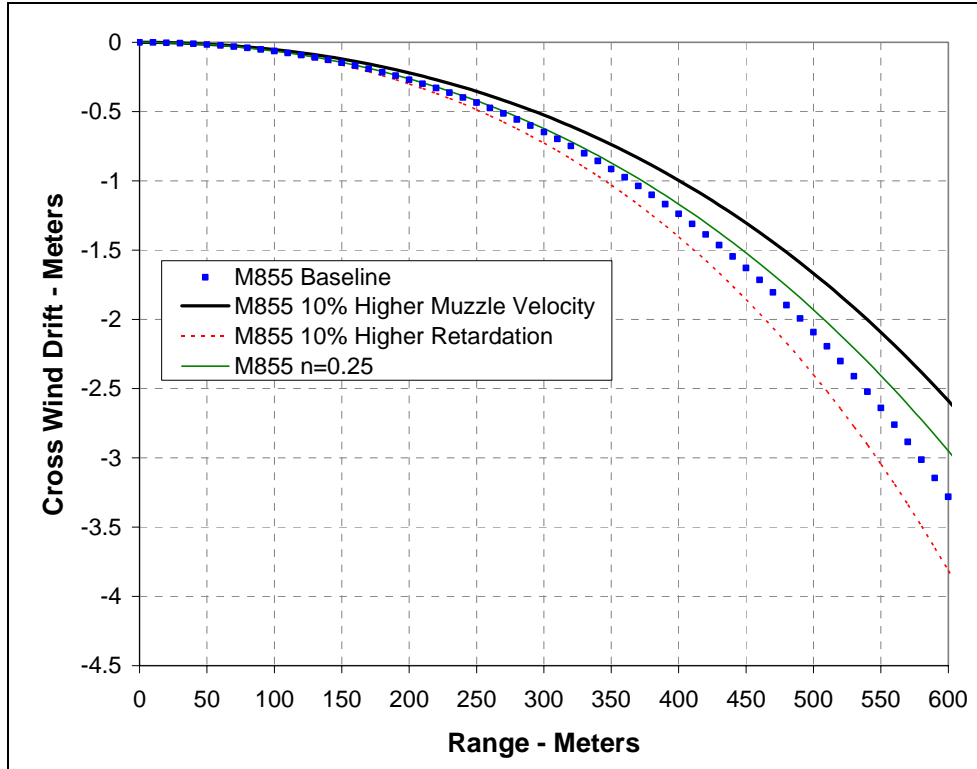
Figure 10. Cross-wind drift (10-m/s cross wind) vs. range for baseline M855, M855 with
10% higher muzzle velocity, M855 with 10% higher retardation, and M855
with n = 0.25.

3. Drag Characteristics of Small-Caliber Ammunition

The analysis of Weinacht et al. (*1*) examined a wide range of munition types, geometric shapes, and calibers and found that the exponent defining the variation of the drag coefficient in the supersonic regime varied between 0 and 1. For the current study, which is focused on small arms munitions, an addition study of the variation of the drag coefficient with Mach number (velocity) has been performed using data available from a commercial small arms ammunition manufacturer. This information includes ballistic coefficients and trajectory vs. range data.

The ballistic coefficient C typically provided by small arms ammunition manufacturers is defined in equation 9.

$$C = \frac{m}{D^2} \frac{1}{i_{Form}} . \tag{9}$$

The ratio of the mass to reference diameter squared is referred to as the sectional density. The sectional density for a given bullet is either quoted by the manufacturer or is easily calculated from manufacturer's data. It depends purely on the physical properties of the bullet and is a

constant for a given bullet type. Generally, the sectional density increases with bullet caliber because the bullet mass increases at a rate proportional to the cube of the caliber whereas the denominator of the sectional density increases with the square of the caliber. The variation of sectional density with bullet caliber reflects only a general trend. Variations of sectional density within a fixed bullet caliber are common because the length and material composition (and hence mass) vary between different bullet designs.

The form factor i_{Form} in the ballistic coefficient represents the ratio of the drag coefficient of the actual round to the drag coefficient corresponding to a reference drag curve. For most commercial arms manufacturers, this reference drag curve is the G1 drag curve. The form factor for a low-drag streamlined bullet is generally about 0.6, indicating that the drag coefficient of the bullet is 60% of the reference drag coefficient. For bullets with very large nose bluntness, the form factor can be larger than 1.0. In contrast to the sectional density, there is likely little variation of the form factor between bullet calibers for the same shape bullet. The ratio represented by the form factor generally varies with Mach number. Typically, the form factor quoted by most small arms ammunition manufacturers represents the average value of this ratio over a range of velocities or Mach numbers. In some cases, the velocity regime may be broken into several intervals with a different ballistic coefficient and form factor assigned to each velocity interval.

Many manufacturers quote a single ballistic coefficient (and hence form factor) for each bullet. Presumably, this single value represents the ballistic coefficient or form factor over a representative velocity range for the bullet. If a single form factor is used, the drag curve of the actual projectile is simply increased or decreased by a multiplicative constant over the reference drag curve. Thus, many commercial small arms ammunition manufacturers essentially assume that the shape of the drag curve for their bullet is identical to the shape of the reference G1 drag curve. In the context of the power law drag variation used in the current approach, these manufacturers essentially assume that the shape of the drag curve is represented by the drag coefficient exponent for the G1 drag curve, n = 0.36 for flight velocities between Mach 1.5 and 3.0. As concluded in Weinacht et al. (*1*), the exponent defining the shape of the drag curve has a relatively small effect on the accuracy of the trajectory prediction compared to the muzzle velocity and muzzle retardation, especially at short ranges. In a sense, the analysis of reference Weinacht et al. (*1*) provides some measure of justification of the approach of quoting a single ballistic coefficient and representing the shape of the drag curve of all small arms bullets with the G1 drag function.

At least one small arms ammunition manufacturer, Sierra Bullets, quotes several ballistic coefficients for each round that are valid over specified velocity regimes. Essentially, the manufacturer is attempting to account for differences in the shape of the actual drag curve relative to the reference G1 drag curve. This implies that if the drag curve is modeled using a power law representation, the drag coefficient exponent may be different from the exponent associated with the G1 drag curve. If the quality of the drag data used to derive the form factors

12

and ballistic coefficients is good, the resulting trajectory predictions are likely to be more accurate using multiple ballistic coefficients than the predictions made using a single ballistic coefficient.

An important observation regarding the drag coefficient exponent can be made by examining the ballistic coefficient data. For a given bullet, if the ballistic coefficient decreases with decreasing velocity in the supersonic regime, the drag coefficient exponent will be greater than the value of the exponent for the reference drag curve (n = 0.36). This is because the form factor of the bullet is increasing with decreasing velocity (or Mach number) and the drag coefficient is increasing faster with decreasing Mach number than the reference drag coefficient. Conversely, if the ballistic coefficient increases with decreasing velocity, the drag coefficient exponent will be less than the value of exponent for the reference drag curve (0.36). In this case, the form factor of the bullet is decreasing with decreasing velocity (or Mach number). This may indicate that the drag coefficient is either increasing more slowly with Mach number than the reference drag coefficient or perhaps even decreasing with Mach number.

The database of ballistic coefficients and trajectory data provided by Sierra Bullets provides a wealth of data from which very useful information can be derived on the drag properties of small arms bullets. An extensive set of ballistic coefficients and trajectory data is provided by the manufacturer for a wide variety of projectile shapes and calibers (*6*, *7*). This trajectory data is derived from the manufacturer's ballistic coefficient data and includes velocity, gravity drop, and cross-wind drift vs. range.

In the current study, the velocity vs. range data were curve fit to the functional form shown in equation 3 using a nonlinear least-squares approach. Since the muzzle velocity of the bullet is specified in the data, only the muzzle retardation and the exponent defining the shape of the drag curve were treated as variables in the fitting process. For each bullet type, trajectory data were available for a range of muzzle velocities. However, in the fitting process, only a single trajectory was typically fit. Where available, the trajectory data corresponding to 3100-ft/s muzzle velocities were selected. The 3100-ft/s muzzle velocity is close to the muzzle velocity of the M855 which is the focus of the current study. Sensitivity of the results to muzzle velocity was examined and is discussed below. In some cases, trajectories were not available at muzzle velocities as high as 3100 ft/s and, in these cases, the trajectory for the closest available muzzle velocity was selected. Any velocity data below Mach 1.1 (1241 ft/s) was ignored to avoid the transonic/subsonic velocity regime where drag coefficient changes rapidly with Mach number. For each trajectory, six to nine range locations were fit for each projectile.

Following the fitting process, the manufacturer's trajectory data was compared with the prediction made with the analytical method using both the muzzle retardation and drag coefficient exponent obtained from the corresponding fit and the specified muzzle velocity. Comparisons were made for the velocity, gravity drop, and cross-wind drift vs. range and root mean square (RMS) errors were computed for the individual trajectories. The average of the

RMS errors from the individual trajectories for the impact velocity, gravity drop, and cross-wind drift were 0.85 ft/s, 0.04 in, and 0.03 in, respectively.

Tables 1–8 display the data obtained from the fitting process for eight different bullet calibers. Shown in these tables are the exponent and muzzle retardation obtained from the fitting process along with the muzzle velocity. Since the fitting process was accomplished for different muzzle velocities for some rounds, the muzzle retardation was normalized to a reference muzzle velocity V_{Ref} of 3100 ft/s. This corresponds to the muzzle velocity of the majority of the trajectory selected for the fitting process. It is also close to the muzzle velocity of the M855. The normalized muzzle retardation provides a means of comparing the muzzle retardation between the rounds on a consistent basis. Muzzle retardation was adjusted for muzzle velocity as shown in equation 10 using the power law formulation for the drag coefficient.

$$\left(\frac{dV}{ds}\right)_{V_{Ref}} = \left(\frac{dV}{ds}\right)_0 \left(\frac{V_{Ref}}{V_0}\right)^{1-n}. \tag{10}$$

Table 1. Results from curve-fitting velocity data, 0.224-caliber projectiles.

Projectile	C_D Exponent (n)	$\left(\dfrac{dV}{ds}\right)_0$ ([m/s]/m)	V_0 (m/s)	SD (lb/in²)	Results Normalized to V_{Ref}		
					$\left(\dfrac{dV}{ds}\right)_{V_{Ref}}$ ([m/s]/m)	$C_D\big|_{V_{Ref}}$	i_{Form}
40-gr Hornet	0.099	–2.9038	945.1	0.114	–2.9038	0.521	1.049
40-gr HP	0.267	–2.1609	945.1	0.114	–2.1609	0.388	0.781
45-gr Hornet	0.093	–2.2819	823.2	0.128	–2.5865	0.522	1.049
45-gr SMP	0.266	–2.0273	945.1	0.128	–2.0273	0.409	0.822
45-gr SPT	0.498	–1.6415	945.1	0.128	–1.6415	0.331	0.666
50-gr SMP	0.389	–1.7355	945.1	0.142	–1.7355	0.388	0.781
50-gr SPT	0.429	–1.5034	945.1	0.142	–1.5034	0.336	0.677
50-gr Blitz	0.429	–1.5034	945.1	0.142	–1.5034	0.336	0.677
55-gr SPT	0.404	–1.3860	945.1	0.157	–1.3860	0.343	0.690
55-gr Blitz	0.404	–1.3860	945.1	0.157	–1.3860	0.343	0.690
55-gr SMP	0.252	–1.6219	945.1	0.157	–1.6219	0.401	0.807
55-gr FMJBT	0.523	–1.3147	945.1	0.157	–1.3147	0.325	0.654
55-gr SBT	0.461	–1.3325	945.1	0.157	–1.3325	0.330	0.663
55-gr HPBT	0.321	–1.7866	945.1	0.157	–1.7866	0.442	0.889
60-gr HP	0.372	–1.3693	945.1	0.171	–1.3693	0.369	0.742
63-gr SMP	0.317	–1.4336	945.1	0.179	–1.4336	0.404	0.813
52-gr HPBT Match King	0.410	–1.5131	945.1	0.148	–1.5131	0.353	0.710
53-gr HP Match King	0.425	–1.5004	945.1	0.151	–1.5004	0.357	0.718
69-gr HPBT Match King	0.284	–1.1054	945.1	0.196	–1.1054	0.341	0.687
80-gr HPBT Match King	0.514	–0.7754	945.1	0.228	–0.7754	0.278	0.560

Table 2. Results from curve-fitting velocity data, 0.243-caliber projectiles.

Projectile	C_D Exponent (n)	$\left(\dfrac{dV}{ds}\right)_0$ ([m/s]/m)	V_0 (m/s)	SD (lb/in^2)	Results Normalized to V_{Ref}		
					$\left(\dfrac{dV}{ds}\right)_{VRef}$ ([m/s]/m)	$C_D\big|_{V_{Ref}}$	i_{Form}
60-gr HP	0.186	−1.8474	945.1	0.145	−1.8474	0.422	0.850
75-gr HP	0.242	−1.5379	945.1	0.181	−1.5379	0.440	0.884
80-gr SPTSSP	0.560	−1.1137	914.6	0.194	−1.1299	0.345	0.693
80-gr SBT Blitz	0.570	−1.0141	914.6	0.194	−1.0285	0.314	0.631
85-gr HPBT	0.235	−1.1776	945.1	0.206	−1.1776	0.381	0.768
85-gr SPT	0.499	−1.0492	945.1	0.206	−1.0492	0.340	0.684
90-gr FMJBT	0.507	−0.8545	945.1	0.218	−0.8545	0.293	0.590
100-gr SPT	0.587	−0.8786	945.1	0.242	−0.8786	0.335	0.674
100-gr SBT	0.594	−0.7615	945.1	0.242	−0.7615	0.290	0.584
100-gr SMP	0.099	−1.2170	945.1	0.242	−1.2170	0.464	0.933
70-gr HPBT Match King	0.293	−1.2981	945.1	0.169	−1.2981	0.346	0.697
107-gr HPBT Match King	0.443	−0.6241	945.1	0.259	−0.6241	0.255	0.512

The drag coefficient at the reference muzzle velocity was extracted from the normalized muzzle retardation using equation 11.

$$C_D\big|_{V_{Ref}} = \frac{-2m}{\rho V_{Ref} S_{ref}}\left(\frac{dV}{ds}\right)_{V_{Ref}}. \tag{11}$$

The form factor evaluated at the reference muzzle velocity was obtained by taking the ratio of the drag coefficient obtained from equation 11 and the drag coefficient from the G1 drag curve evaluated at the reference velocity, $C_{DG1}\big|_{V_{Ref}} = 0.53$.

$$i_{Form} = \frac{C_D\big|_{V_{Ref}}}{C_{DG1}\big|_{V_{Ref}}}. \tag{12}$$

Comparisons were also made between the ballistic coefficients quoted by the manufacturer and the ballistic coefficients obtained from the fitting process. In general, the results agreed very well, typically within 3% or less. However, several rounds, typically the flat nose projectiles, showed differences in the ballistic coefficient coefficients of as much as 12%. For these rounds, the manufacturer's ballistic coefficient shows large changes (20% or greater) across adjacent velocity intervals traversed by the projectile for the trajectory used in the fitting process. In these cases, the ballistic coefficient derived from the fitting process was bracketed by the manufacturer's ballistic coefficients in adjacent velocity intervals near the muzzle velocity.

Table 3. Results from curve-fitting velocity data, 0.308-caliber projectiles.

Projectile	C_D Exponent (n)	$\left(\dfrac{dV}{ds}\right)_0$ ([m/s]/m)	V_0 (m/s)	SD (lb/in^2)	Results Normalized to V_{Ref}		
					$\left(\dfrac{dV}{ds}\right)_{V_{Ref}}$ ([m/s]/m)	$C_D\big|_{V_{Ref}}$	i_{Form}
110-gr RN	0.125	−2.2966	945.1	0.166	−2.2966	0.599	1.206
110-gr FMJ	0.125	−2.0914	853.7	0.166	−2.2863	0.597	1.200
110-gr HP	0.157	−1.8672	945.1	0.166	−1.8672	0.487	0.980
125 -gr HP	−0.359	−2.1834	762.2	0.188	−2.9247	0.867	1.745
125 -gr SPT	0.485	−1.1747	945.1	0.188	−1.1747	0.348	0.701
150 -gr FN	−0.275	−1.3202	701.2	0.226	−1.9315	0.687	1.383
150-gr RN	0.024	−1.6469	945.1	0.226	−1.6469	0.586	1.179
150-gr SPT	0.314	−0.9856	945.1	0.226	−0.9856	0.351	0.706
150-gr SBT	0.522	−0.8628	945.1	0.226	−0.8628	0.307	0.618
150-gr FMJBT	0.489	−0.8115	945.1	0.226	−0.8115	0.289	0.581
165-gr SBT	0.269	−0.8343	945.1	0.248	−0.8343	0.327	0.657
165-gr HPBT	0.453	−0.9097	945.1	0.248	−0.9097	0.356	0.716
170-gr FN	−0.247	−1.1877	701.2	0.256	−1.7236	0.695	1.399
180-gr RN	−0.246	−1.3663	945.1	0.271	−1.3663	0.583	1.174
180-gr SPT	0.292	−0.8201	945.1	0.271	−0.8201	0.350	0.705
180-gr SBT	0.368	−0.6592	945.1	0.271	−0.6592	0.282	0.566
200-gr SBT	0.409	−0.5911	945.1	0.301	−0.5911	0.280	0.564
220-gr RN	−0.109	−1.0000	853.7	0.331	−1.1194	0.584	1.175
150-gr HPBT Match King	0.519	−0.8003	945.1	0.226	−0.8003	0.285	0.573
155-gr HPBT Palma Match King	0.445	−0.7330	945.1	0.226	−0.7330	0.261	0.525
168-gr HPBT Match King	0.529	−0.7108	945.1	0.253	−0.7108	0.283	0.570
175-gr HPBT Match King	0.493	−0.6518	945.1	0.264	−0.6518	0.271	0.544
180-gr HPBT Match King	0.357	−0.6818	945.1	0.271	−0.6818	0.291	0.586
190-gr HPBT Match King	0.423	−0.6175	945.1	0.286	−0.6175	0.278	0.560
200-gr HPBT Match King	0.418	−0.5828	945.1	0.301	−0.5828	0.277	0.556
220-gr HPBT Match King	0.419	−0.5238	945.1	0.331	−0.5238	0.273	0.550
240-gr HPBT Match King	0.426	−0.4630	945.1	0.361	−0.4630	0.264	0.530

Table 4. Results from curve-fitting velocity data, 0.311-caliber projectiles.

Projectile	C_D Exponent (n)	$\left(\dfrac{dV}{ds}\right)_0$ ([m/s]/m)	V_0 (m/s)	SD (lb/in^2)	Results Normalized to V_{Ref}		
					$\left(\dfrac{dV}{ds}\right)_{V_{Ref}}$ ([m/s]/m)	$C_D\big|_{V_{Ref}}$	i_{Form}
125-gr SPT	0.267	−1.1366	853.7	0.185	−1.2246	0.356	0.717
150-gr SPT	0.451	−0.8991	853.7	0.222	−0.9508	0.332	0.668
174-gr HPBT Match King	0.478	−0.5930	792.7	0.257	−0.6500	0.263	0.530
180-gr SPT	0.394	−0.7260	792.7	0.266	−0.8077	0.338	0.681

Table 5. Results from curve-fitting velocity data, 0.323-caliber projectiles.

Projectile	C_D Exponent (n)	$\left(\dfrac{dV}{ds}\right)_0$ ([m/s]/m)	V_0 (m/s)	SD (lb/in^2)	$\left(\dfrac{dV}{ds}\right)_{V_{Ref}}$ ([m/s]/m)	$C_D\big|_{V_{Ref}}$	i_{Form}
					Results Normalized to V_{Ref}		
150-gr SPT	0.518	−0.9734	945.1	0.205	−0.9734	0.315	0.634
175-gr SPT	0.445	−0.8611	945.1	0.240	−0.8611	0.325	0.654
220-gr SBT	0.404	−0.6325	945.1	0.301	−0.6325	0.300	0.604

Table 6. Results from curve-fitting velocity data, 0.338-caliber projectiles.

Projectile	C_D Exponent (n)	$\left(\dfrac{dV}{ds}\right)_0$ ([m/s]/m)	V_0 (m/s)	SD (lb/in^2)	$\left(\dfrac{dV}{ds}\right)_{V_{Ref}}$ ([m/s]/m)	$C_D\big|_{V_{Ref}}$	i_{Form}
					Results Normalized to V_{Ref}		
215-gr SBT	0.430	−0.6777	945.1	0.269	−0.6777	0.287	0.577
250-gr SBT	0.446	−0.5811	945.1	0.313	−0.5811	0.286	0.576
300-gr HPBT Match King	0.426	−0.4288	945.1	0.375	−0.4288	0.253	0.510

Table 7. Results from curve-fitting velocity data, 0.375-caliber projectiles.

Projectile	C_D Exponent (n)	$\left(\dfrac{dV}{ds}\right)_0$ ([m/s]/m)	V_0 (m/s)	SD (lb/in^2)	$\left(\dfrac{dV}{ds}\right)_{V_{Ref}}$ ([m/s]/m)	$C_D\big|_{V_{Ref}}$	i_{Form}
					Results Normalized to V_{Ref}		
200-gr FN	0.041	−1.7963	945.1	0.203	−1.7963	0.575	1.157
250-gr SBT	0.258	−0.9379	945.1	0.254	−0.9379	0.375	0.755
300-gr SBT	0.413	−0.6782	914.6	0.305	−0.6913	0.332	0.668

Table 8. Results from curve-fitting velocity data, 0.458-caliber projectiles.

Projectile	C_D Exponent (n)	$\left(\dfrac{dV}{ds}\right)_0$ ([m/s]/m)	V_0 (m/s)	SD (lb/in^2)	$\left(\dfrac{dV}{ds}\right)_{V_{Ref}}$ ([m/s]/m)	$C_D\big|_{V_{Ref}}$	i_{Form}
					Results Normalized to V_{Ref}		
300-gr HP/FN	−0.481	−2.1156	731.7	0.204	−3.0906	0.995	2.001

In general, the data show that the exponent defining the shape of the drag curve varies between –0.5 and 0.6 for these small arms bullets. When comparing the geometric shape of the bullet to both the drag coefficient exponent and form factor, there appears to be some correlation. Figure 11 shows a tabular listing of the drag coefficient exponent and the form factor along with a picture of each round for the 27 0.308-caliber projectiles considered in the study. The tabular listing is shown in order of increasing drag coefficient exponent. The negative drag coefficient exponents all corresponded to blunt nosed (flat or rounded) projectiles with the largest negative values observed for the flat faced projectiles. The negative drag coefficient exponent indicates a decreasing drag coefficient with decreasing Mach number as opposed to the more typical increasing trend with decreasing Mach number. A decreasing trend of the drag coefficient with Mach number in the supersonic regime has been previously documented for flat nose projectiles (*9, 10*). The round nose (spherically blunted) projectiles exhibit a drag coefficient exponent close to 0 which is similar to the drag coefficient exponent for a spherical ball projectile previously discussed in Weinacht et al. (*1*). As the projectile becomes more streamlined, the drag coefficient exponent increases. The low drag boattailed projectiles with long noses have drag coefficient exponents approaching 0.5. Figure 11 also appears to show a correlation between drag coefficient exponent and form factor. Although figure 11 shows data for a single projectile caliber, similar observations were made for the other projectile calibers examined in the study.

n	I_{form}	n	I_{form}	n	I_{form}
-0.36	1.74	0.27	0.66	0.43	0.53
-0.27	1.38	0.29	0.70	0.45	0.52
-0.25	1.40	0.31	0.71	0.45	0.71
-0.25	1.17	0.36	0.59	0.49	0.70
-0.11	1.18	0.37	0.57	0.49	0.58
0.02	1.18	0.41	0.56	0.49	0.54
0.12	1.20	0.42	0.56	0.52	0.57
0.12	1.21	0.42	0.55	0.52	0.62
0.16	0.98	0.42	0.56	0.53	0.57
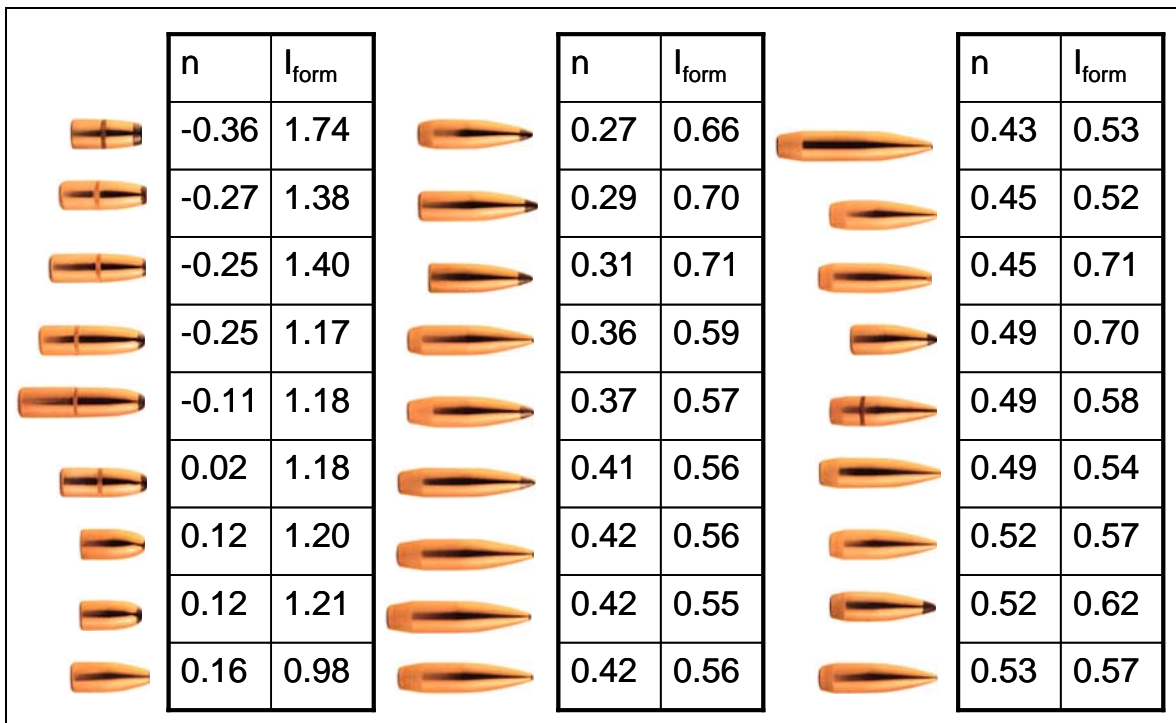
Figure 11. Drag coefficient exponent and form factor for various 0.308-projectiles; bullet photographs from Sierra Bullets (*8*).

Figure 12 shows the correlation between the drag coefficient exponent and the form factor for each of the eight calibers of munitions examined in the current study. The results appear to be independent of bullet caliber. A curve fit of the data was obtained using a second-order polynomial. The resulting polynomial is shown in equation 13. The maximum error in the drag coefficient exponent n from the fit is 0.25 with a standard deviation of 0.085.

$$n = 0.0848\, i_{Form}^2 - 0.932\, i_{Form} + 0.9841 . \qquad (13)$$
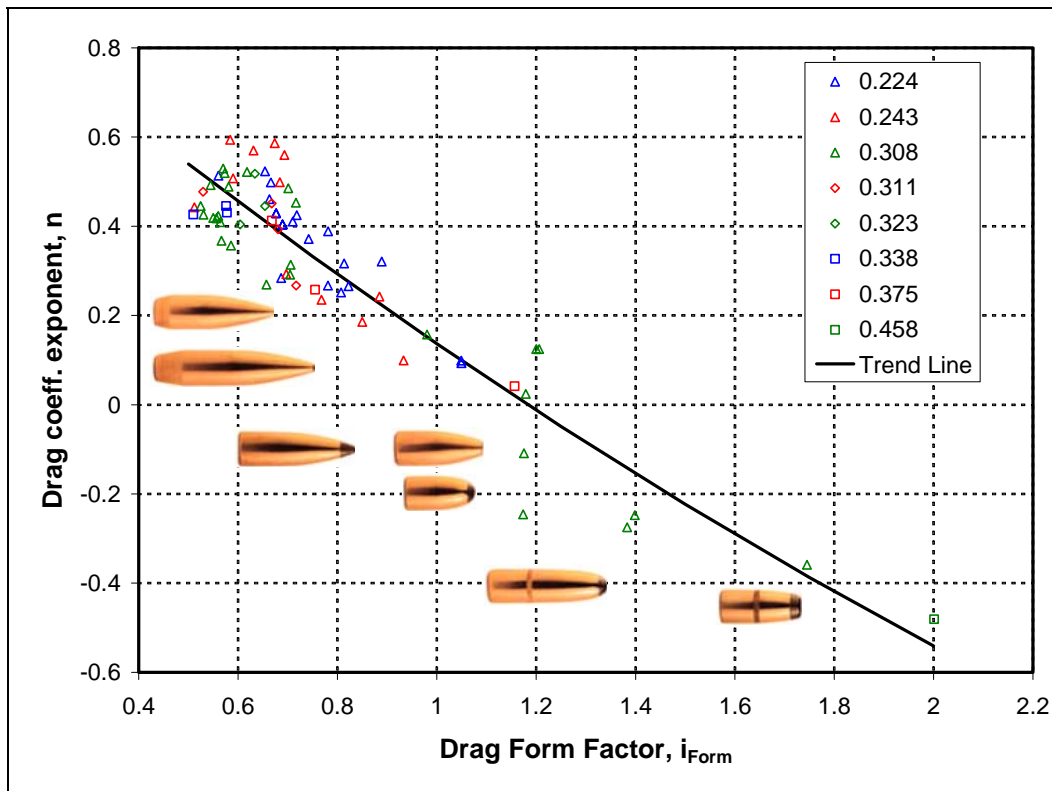
Figure 12. Drag coefficient exponent, n, vs. drag form factor with illustration of effect of bullet shape; bullet photographs from Sierra Bullets (*8*).

The significance of the correlation is that the drag coefficient exponent can be estimated from the ballistic coefficient since the form factor is easily determined from equation 9 using the sectional density of the projectile. This is particularly important when a manufacturer only quotes a single value of the ballistic coefficient and uses the standard G1 drag function to predict trajectory data—a common practice within the commercial small arms ammunition industry. The results presented here indicate the possibility of improving the trajectory predictions using the power law formulation with the exponent estimated from the correlation in equation 13. This is particularly important when the exponent estimated using the correlation varies significantly from the 0.36 exponent corresponding to the G1 drag function. It is also important to understand that the correlation in equation 13 is best suited for small arms axisymmetric bullets, since it was

derived using data for these types of bullets. It may be completely inappropriate for other classes of munitions such as kinetic energy projectiles.

The sensitivity of the results obtained in the fitting process to muzzle velocity was examined by fitting several trajectories corresponding to different muzzle velocities for several bullet types. Some of the results of this study are shown in tables 9–12. The tables show the drag coefficient exponent and muzzle retardation obtained from the fitting process for each muzzle velocity. The results also show the muzzle retardation, drag coefficient, and form factor normalized to the reference muzzle velocity of 3100 ft/s. Table 9 shows a typical result. The drag coefficient exponent shows only minor variation over the range of muzzle velocities available for this round. The muzzle retardation from the fit shows a decreasing trend with decreasing muzzle velocity. However, when each of the muzzle retardations is normalized to the reference velocity using equation 10, the only small variations in the normalized retardation are seen as the muzzle velocity is varied. Both the drag coefficient and form factor when normalized to the reference velocity also show correspondingly little variation with muzzle velocity.

Table 9. Sensitivity of muzzle velocity on results from trajectory fitting, 0.308 150-gr HPBT Match King.

				Results Normalized to V_{Ref}		
V_0 (m/s)	C_D Exponent (n)	$\left(\dfrac{dV}{ds}\right)_0$ ([m/s]/m)	SD (lb/in^2)	$\left(\dfrac{dV}{ds}\right)_{V_{Ref}}$ ([m/s]/m)	$C_D\big|_{V_{Ref}}$	i_{Form}
1067	0.532	−0.8512	0.226	−0.8042	0.286	0.576
1037	0.529	−0.8378	0.226	−0.8021	0.285	0.574
1006	0.519	−0.8259	0.226	−0.8014	0.285	0.574
976	0.534	−0.8108	0.226	−0.7989	0.284	0.572
945	0.519	−0.8003	0.226	−0.8003	0.285	0.573
915	0.532	−0.7875	0.226	−0.7997	0.285	0.573
884	0.539	−0.7763	0.226	−0.8006	0.285	0.573
854	0.534	−0.7675	0.226	−0.8048	0.286	0.576
823	0.562	−0.7502	0.226	−0.7970	0.284	0.571
793	0.581	−0.7327	0.226	−0.7887	0.281	0.565
762	0.561	−0.7222	0.226	−0.7937	0.282	0.568
732	0.524	−0.7122	0.226	−0.8046	0.286	0.576

For some bullets, trajectory data was available for a very wide range of muzzle velocities. Tables 10 and 11 show two such sets of data. In these tables, the drag coefficient exponent and the normalized retardation are fairly consistent down to muzzle velocities of 732–762 m/s. Below these velocities, the drag coefficient exponent decreases to a value near zero indicating that the drag coefficient is relatively constant with Mach number. This behavior can be traced to the G1 drag function which is used in conjunction with the form factor contained in the ballistic

coefficient to determine the variation in drag coefficient with Mach number for the individual rounds. For both of these rounds, a constant ballistic coefficient is used below 671 m/s. For the low muzzle velocities, this constant ballistic coefficient is used for the bulk of the trajectory. The drag coefficient exponent for these trajectories at the lower muzzle velocities represents the shape of the G1 drag curve at these velocities rather than the shape of the drag curve as modified through the variation in the ballistic coefficients with velocity.

Table 10. Sensitivity of muzzle velocity on results from trajectory fitting, 0.224 69-gr HPBT Match King.

				Results Normalized to V_{Ref}		
V_0 (m/s)	C_D Exponent (n)	$\left(\dfrac{dV}{ds}\right)_0$ ([m/s]/m)	SD (lb/in²)	$\left(\dfrac{dV}{ds}\right)_{V_{Ref}}$ ([m/s]/m)	$C_D\big|_{V_{Ref}}$	i_{Form}
1128	0.271	−1.2611	0.196	−1.1085	0.343	0.690
1098	0.279	−1.2329	0.196	−1.1070	0.343	0.689
1067	0.282	−1.2069	0.196	−1.1061	0.342	0.689
1037	0.283	−1.1814	0.196	−1.1057	0.342	0.688
1006	0.289	−1.1543	0.196	−1.1041	0.342	0.687
976	0.290	−1.1292	0.196	−1.1040	0.342	0.687
945	0.284	−1.1054	0.196	−1.1054	0.342	0.688
915	0.281	−1.0803	0.196	−1.1061	0.342	0.689
884	0.271	−1.0568	0.196	−1.1094	0.343	0.691
854	0.253	−1.0342	0.196	−1.1159	0.345	0.695
823	0.221	−1.0154	0.196	−1.1308	0.350	0.704
793	0.189	−0.9942	0.196	−1.1467	0.355	0.714
762	0.208	−0.9634	0.196	−1.1424	0.354	0.711
732	0.176	−0.9394	0.196	−1.1598	0.359	0.722
701	0.226	−0.9012	0.196	−1.1356	0.351	0.707
671	0.210	−0.8701	0.196	−1.1409	0.353	0.710
640	0.108	−0.8542	0.196	−1.2090	0.374	0.753

To demonstrate this point, the trajectories were constructed using the G1 drag curve with a constant ballistic coefficient of 0.225 for a 52-gr 0.224-caliber projectile. Essentially, this represents a 52-gr 0.224-caliber HPBT Match King projectile with a constant ballistic coefficient equal to the value used for the actual round at velocities above 914 m/s. The trajectories were then curve fit in a manner identical to the approach used to generate the results in tables 9–11. The results of the fits are shown in table 12. The drag coefficient exponent and normal muzzle retardation show relatively little variation with muzzle velocity until about 732–762 m/s. The values of the drag coefficient exponent are close to the value obtained by directly fitting the drag curve (n = 0.36). At lower velocities, the drag coefficient exponent approaches zero. For the results in table 12, the drag coefficient exponent represents the shape of the G1 drag curve over the velocity regime of the trajectory since the ballistic coefficient is constant.

Table 11. Sensitivity of muzzle velocity on results from trajectory fitting,
0.224 52-gr HPBT Match King.

V_0 (m/s)	C_D Exponent (n)	$\left(\dfrac{dV}{ds}\right)_0$ ([m/s]/m)	SD (lb/in^2)	Results Normalized to V_{Ref}		
				$\left(\dfrac{dV}{ds}\right)_{V_{Ref}}$ ([m/s]/m)	$C_D\big|_{V_{Ref}}$	i_{Form}
1250	0.379	−1.8095	0.148	−1.5211	0.355	0.714
1220	0.401	−1.7681	0.148	−1.5178	0.354	0.712
1189	0.421	−1.7297	0.148	−1.5144	0.353	0.711
1159	0.440	−1.6920	0.148	−1.5097	0.352	0.708
1128	0.454	−1.6578	0.148	−1.5051	0.351	0.706
1098	0.462	−1.6262	0.148	−1.5006	0.350	0.704
1067	0.468	−1.5961	0.148	−1.4962	0.349	0.702
1037	0.464	−1.5713	0.148	−1.4953	0.349	0.702
1006	0.457	−1.5471	0.148	−1.4954	0.349	0.702
976	0.438	−1.5283	0.148	−1.5013	0.350	0.704
945	0.410	−1.5131	0.148	−1.5131	0.353	0.710
915	0.374	−1.5005	0.148	−1.5316	0.357	0.719
884	0.443	−1.4520	0.148	−1.5070	0.351	0.707
854	0.415	−1.4321	0.148	−1.5199	0.354	0.713
823	0.374	−1.4157	0.148	−1.5436	0.360	0.724
793	0.321	−1.4004	0.148	−1.5782	0.368	0.741
762	0.406	−1.3521	0.148	−1.5365	0.358	0.721
732	0.343	−1.3367	0.148	−1.5813	0.369	0.742
701	0.255	−1.3258	0.148	−1.6561	0.386	0.777
671	0.140	−1.3167	0.148	−1.7684	0.412	0.830
640	0.148	−1.2718	0.148	−1.7722	0.413	0.832
610	0.024	−1.2465	0.148	−1.9116	0.446	0.897
579	0.005	−1.1979	0.148	−1.9498	0.455	0.915
549	−0.011	−1.1445	0.148	−1.9831	0.463	0.931

It is difficult to determine from the existing Sierra Bullet data whether the drag coefficient at lower velocities is well represented by the G1 drag curve. Drag results for the M855 obtained from an aeroballistic range (shown previously in figure 1) show a much stronger variation with Mach number than does the G1 drag curve. Not withstanding, the results presented here show that the drag coefficient exponent is relatively constant over a range of velocities and projectile geometries that are of interest for current study and validate the approach of characterizing the shape of the drag curve using a power law approach.

The approach taken here is to fit the velocity vs. range data to obtain the muzzle retardation and drag coefficient exponent. It may also be possible to perform fits of the drag curve directly using the form factors obtained from the ballistic coefficients and the reference drag curve. This approach yields similar results to the results presented here. However, the results show some

Table 12. Sensitivity of muzzle velocity on results from trajectory fitting, 0.224 52-gr, G1 drag curve, constant ballistic coefficient C = 0.225.

V_0 (m/s)	C_D Exponent (n)	$\left(\dfrac{dV}{ds}\right)_0$ ([m/s]/m)	SD (lb/in^2)	Results Normalized to V_{Ref}		
				$\left(\dfrac{dV}{ds}\right)_{VRef}$ ([m/s]/m)	$C_D\big|_{V_{Ref}}$	i_{Form}
1250	0.289	−1.8276	0.148	−1.4980	0.349	0.703
1220	0.307	−1.7852	0.148	−1.4962	0.349	0.702
1189	0.325	−1.7441	0.148	−1.4936	0.348	0.701
1159	0.341	−1.7044	0.148	−1.4903	0.348	0.699
1128	0.355	−1.6662	0.148	−1.4865	0.347	0.698
1098	0.367	−1.6297	0.148	−1.4824	0.346	0.696
1067	0.375	−1.5949	0.148	−1.4785	0.345	0.694
1037	0.380	−1.5622	0.148	−1.4753	0.344	0.692
1006	0.379	−1.5318	0.148	−1.4735	0.344	0.691
976	0.373	−1.5036	0.148	−1.4740	0.344	0.692
945	0.361	−1.4775	0.148	−1.4775	0.345	0.693
915	0.341	−1.4535	0.148	−1.4852	0.346	0.697
884	0.312	−1.4317	0.148	−1.4990	0.350	0.703
854	0.367	−1.3870	0.148	−1.4793	0.345	0.694
823	0.337	−1.3646	0.148	−1.4955	0.349	0.702
793	0.296	−1.3439	0.148	−1.5211	0.355	0.714
762	0.241	−1.3248	0.148	−1.5598	0.364	0.732
732	0.318	−1.2748	0.148	−1.5180	0.354	0.712
701	0.260	−1.2520	0.148	−1.5614	0.364	0.733
671	0.183	−1.2299	0.148	−1.6276	0.380	0.764
640	0.179	−1.1910	0.148	−1.6398	0.382	0.769
610	0.072	−1.1648	0.148	−1.7494	0.408	0.821
579	0.056	−1.1199	0.148	−1.7775	0.415	0.834
549	−0.102	−1.0868	0.148	−1.9787	0.461	0.929

slight sensitivity to the velocity or Mach number range used in fitting the drag curve. By fitting the velocity data over the values of range quoted by the manufacturer, a more representative velocity range of the bullet is considered.

As previously discussed, the analytical predictions of the velocity, gravity drop, and wind drift using the muzzle retardation and drag coefficient exponent extracted from the fitting process were in excellent agreement with Sierra Bullets's trajectory data. It is also possible to plot all of the manufacturer's data on a family of universal curves using the nondimensionalization that results from the analytical method of Weinacht et al. (*1*). For instance, the analytical method shows that the ratio of the impact velocity to muzzle velocity is a function of the nondimensional range coordinate $\bar{s}$ as shown in equations 14 and 15.

$$\frac{V}{V_0} = \left\{ 1 + n\left(\frac{dV}{ds}\right)_0 \frac{s_x}{V_0} \right\}^{\frac{1}{n}} = \left\{ 1 + n\bar{s} \right\}^{\frac{1}{n}} \quad n \neq 0. \tag{14}$$

$$\bar{s} = \left(\frac{dV}{ds}\right)_0 \frac{s_x}{V_0}. \tag{15}$$

Similarly, the gravity drop and the wind drift can be expressed in nondimensional terms as functions of the nondimensional range coordinate as shown in equations 16 and 17. The formulae for the special cases n = 0,1,2 shown in Weinacht et al. (*1*) also produce the same nondimensionalization as equations 14, 16, and 17, but the functional form is slightly different.

$$\frac{s_{g-drop}\left(\frac{dV}{ds}\right)_0^2}{g} = \frac{-1}{2(n-2)(n-1)}\left[\left\{1+n\bar{s}\right\}^{\frac{2(n-1)}{n}} - 1 - 2(n-1)\bar{s}\right] \quad n \neq 0,1,2. \tag{16}$$

$$\frac{s_z\left(\frac{dV}{ds}\right)_0}{w_z} = \frac{1}{(n-1)}\left[\left\{1+n\bar{s}\right\}^{1-\frac{1}{n}} - 1\right] \quad n \neq 0, n \neq 1. \tag{17}$$

When the velocity, gravity drop, and wind drift are nondimensionalized, as previously shown, and plotted vs. the nondimensional range, the result is a family of curves in terms of a single parameter, the drag coefficient exponent n. Using this approach, the velocity ratio, gravity drop and wind-drift data available from the manufacturer for eight different calibers and a variety of different projectile masses and shapes can be collapsed on individual plots for each of these three variables. Figures 13 and 14 show the velocity ratio as a function of nondimensional range. Figure 13 presents the complete range of data, while figure 14 presents a close-up view at shorter ranges. Similar plots of the results for gravity drop and wind drift are shown in figures 15–18.

This data provides additional validation of the approach. Most of the data is contained between the n = 0 and n = 0.5 curves from the analytical theory. This is consistent with the results from the fitting process. The analytical curves also offer some estimate of the error that results from estimating the drag coefficient exponent or from directly assuming that the shape of the drag curve is represented by the G1 drag function (n = 0.36 from the fitting). At close ranges, the results are relatively insensitive to the drag coefficient exponent. The error increases slightly at longer ranges.
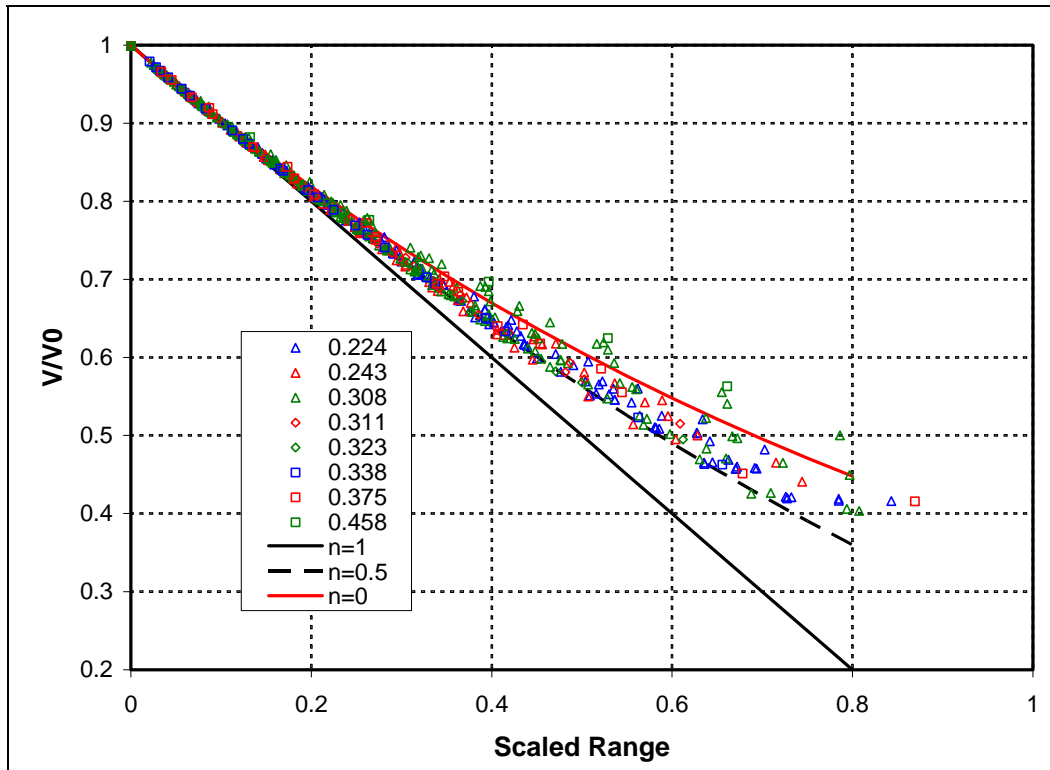
Figure 13. Scaled impact velocity as a function of scaled range.
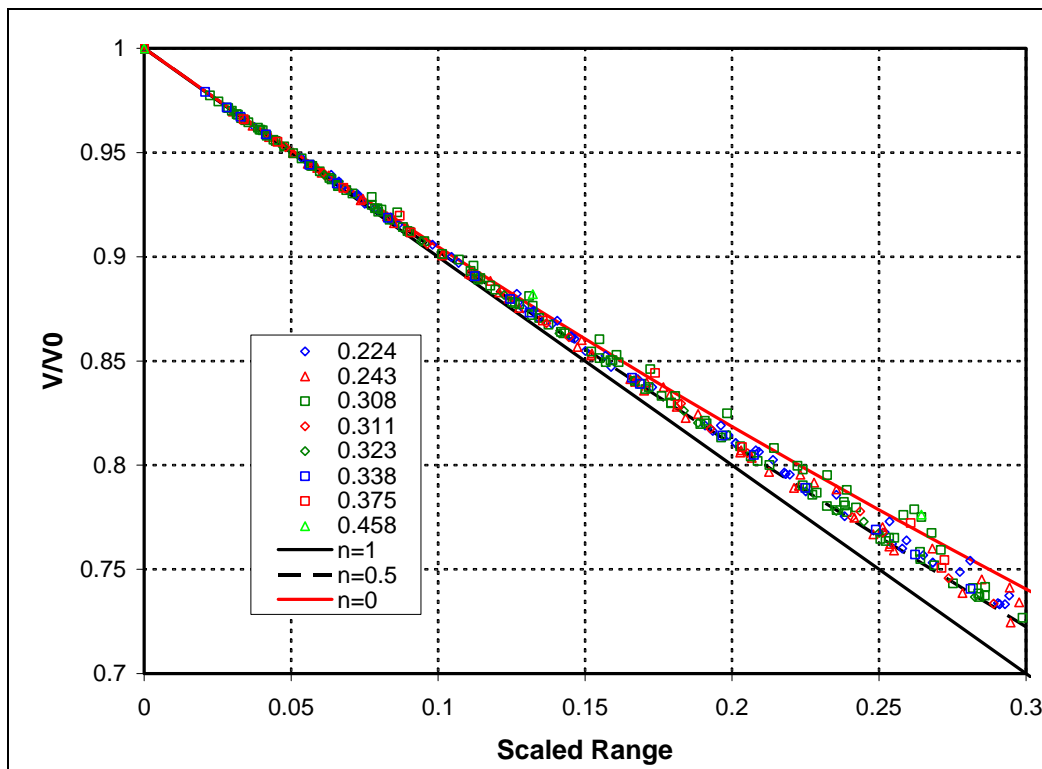

Figure 14. Scaled impact velocity as a function of scaled range (close-in).
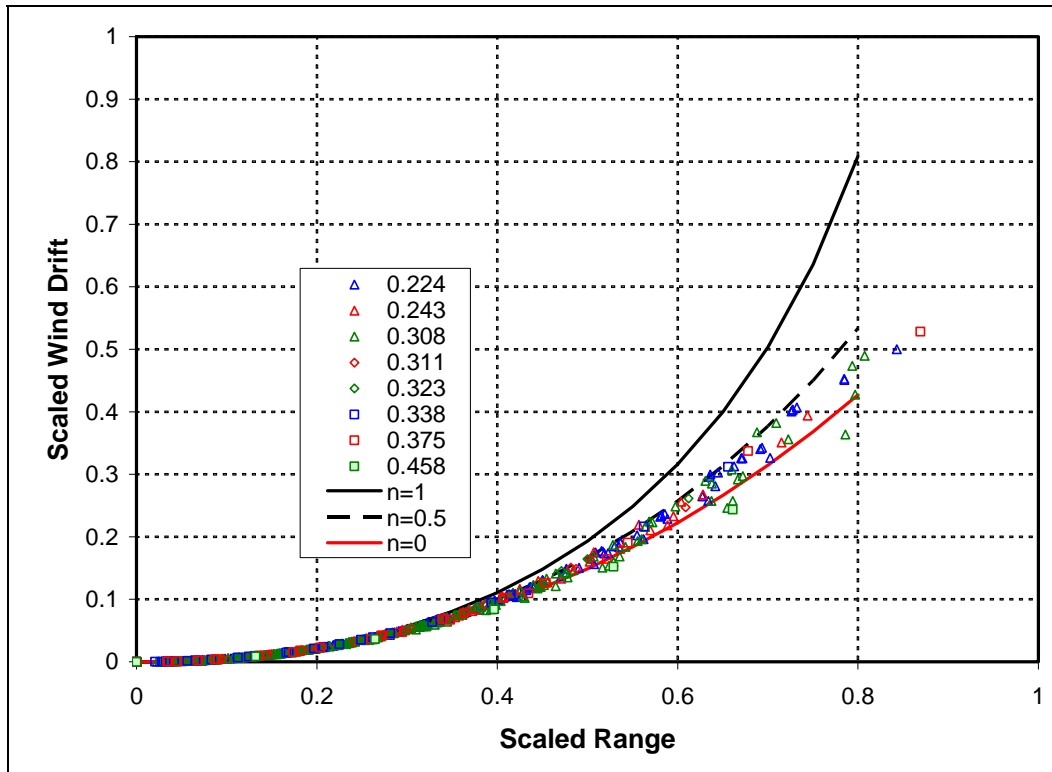
Figure 15. Scaled cross-wind drift as a function of scaled range.
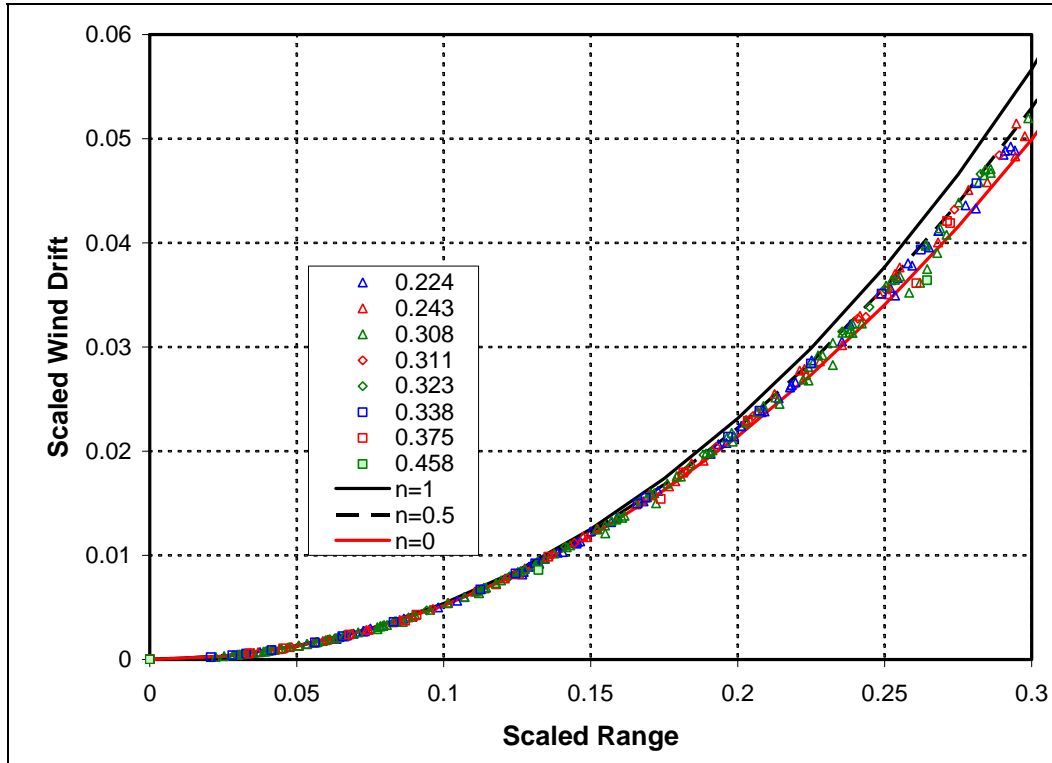

Figure 16. Scaled cross-wind drift as a function of scaled range (close-in).
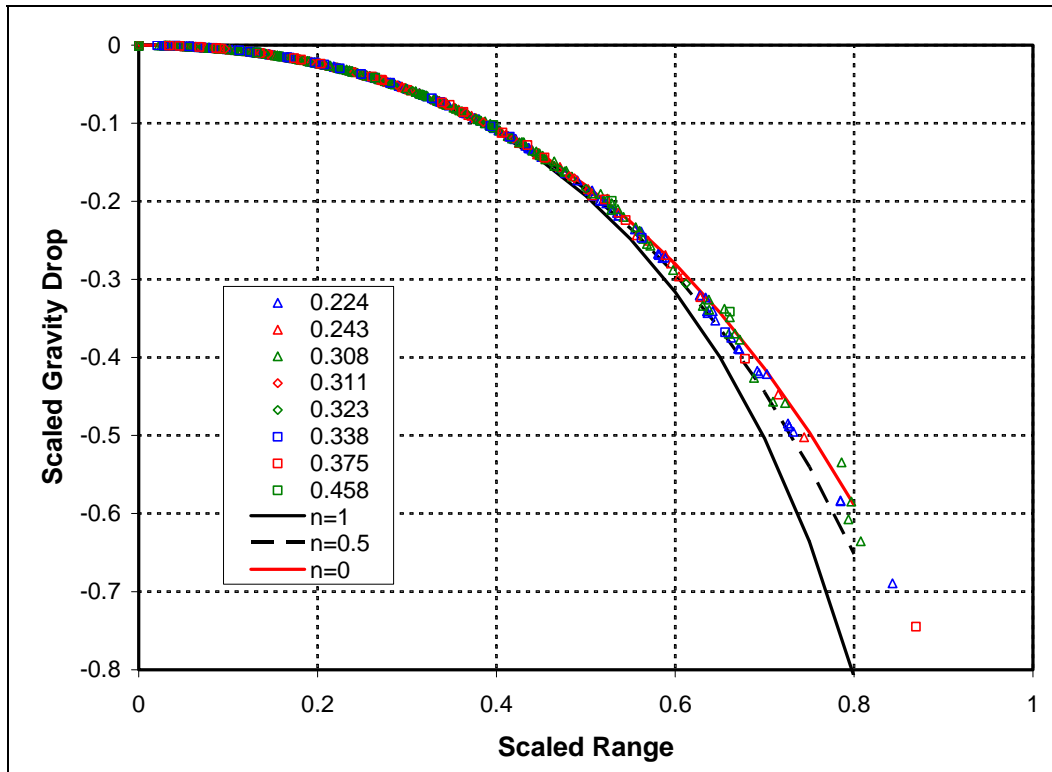
Figure 17. Scaled gravity drop as a function of scaled range.
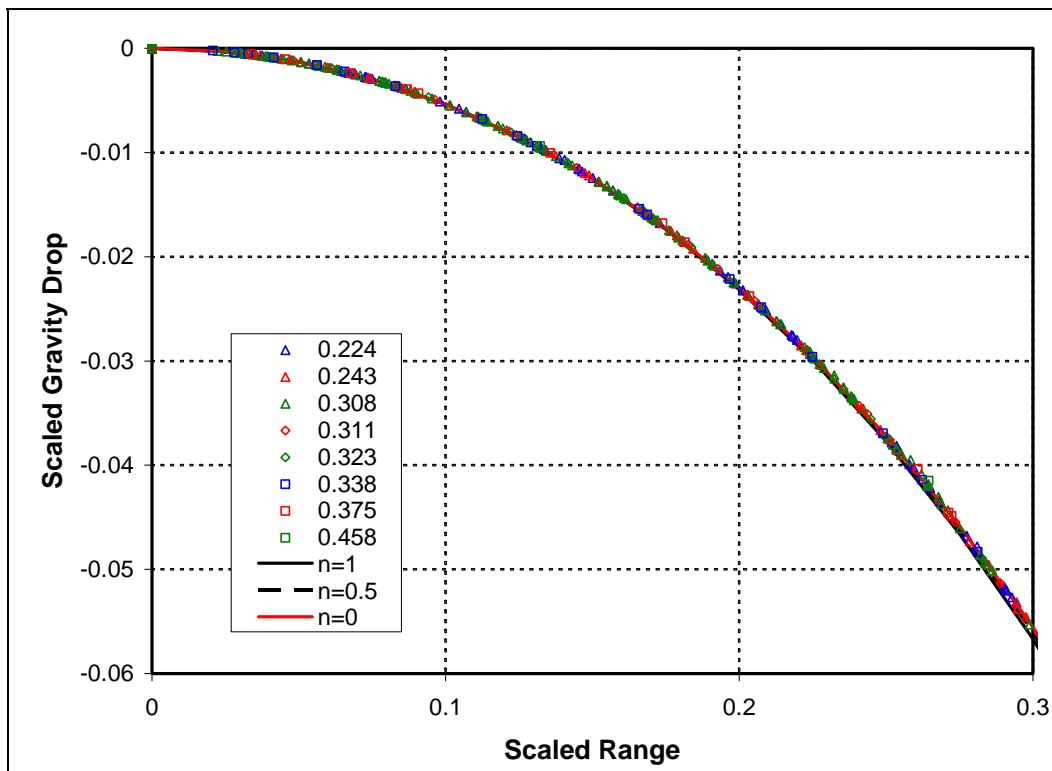
Figure 18. Scaled gravity drop as a function of scaled range (close-up).

4. Trajectory Mismatch

One approach for defining the requirements for new ammunition or modified ammunition based on a previous design is to specify that the trajectories must be similar to existing ammunition. This allows the new ammunition to be used by the Soldier with little apparent difference in its aeroballistic performance. It may also allow compatibility between the new ammunition and the existing tracer round.

For small-caliber ammunition, this requirement is often cited as ±1.0 gunner's mil mismatch in impact location for ranges up to 600 m. It is implied that the gun elevation used to meet this requirement is the same for both the modified and baseline ammunition. From a practical standpoint, this essentially assumes that the existing sights and sight adjustments for the baseline ammunition are used for the modified ammunition, or alternatively, both baseline and modified ammunition use the same firing tables. The second part of this requirement can be shown to be equivalent to requiring that the gravity drop of baseline and modified ammunition to be within ±1.0 gunner's mil mismatch in impact location for range up to 600 m. Equation 6 shows the vertical displacement in the trajectory as a function of range. This expression is valid for both baseline and modified ammunition. By assuming that the gun elevation Θ_0 is equivalent for both, the difference in the vertical impact location can be seen to be produced by the differences in the gravity drop alone.

As previously shown in equation 5, the gravity drop, like the other trajectory characteristics, is a function of the muzzle velocity, muzzle retardation and, to a lesser extent, a function of the exponent defining the shape of the drag curve. Assuming the shape of the drag curve is the same for a similar class of ammunition, the gravity drop is then a function of only the muzzle velocity and muzzle retardation. For the results presented here, the exponent defining the shape of the drag curve is assumed to be 0.53, the same as the M855.

Equation 5 provides some very important insights into the trajectory mismatch problem. First, for each muzzle velocity there exists a value of the muzzle retardation for the modified ammunition that produces the identical impact at 600 m as the M855. For each muzzle velocity there are also corresponding values of muzzle retardation that produce impacts 1.0 mils above and below the baseline M855 impact at 600 m. The value of the muzzle retardation required to obtain a specified value of mismatch at range can be obtained by solving equation 5 for the muzzle retardation. Unfortunately, because of the complicated nature of equation 5, closed form solutions for the muzzle retardation cannot be obtained and the muzzle retardation must be determined in an iterative manner.

Figure 19 shows the gravity drop as a function of range for the baseline M855 and projectiles with a ±1.0 mil mismatch at 600 m for a constant muzzle velocity equal to the baseline M855

muzzle velocity. It can be seen that all three trajectories show little deviation from each other at shorter ranges. This deviation increases with range with the maximum deviation occurring at 600 m. For the ±1.0 mil mismatch trajectories, the muzzle retardation decreases by 27% for impacts above the baseline impact and increases by 20% for impacts below the baseline impact.
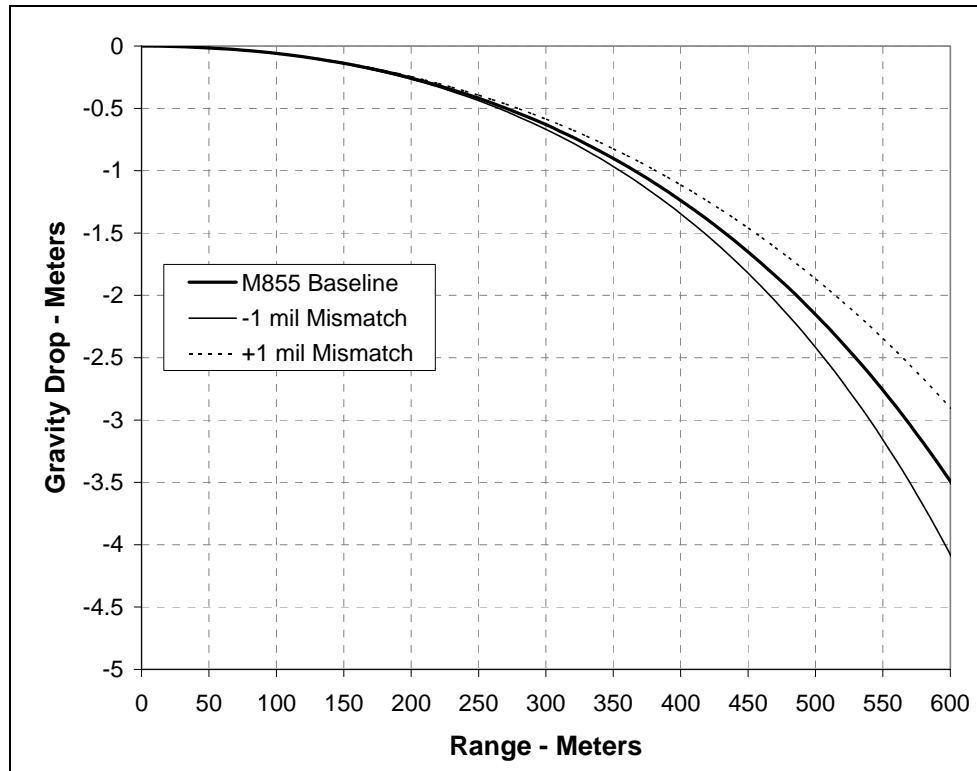
Figure 19. Gravity drop for M855 and ±1.0 mil mismatch trajectories for 949 m/s muzzle velocity.

Figure 20 shows the gravity drop in mils for the baseline M855 and projectiles with a ±1.0 mil mismatch at 600 m for a constant muzzle velocity. Considering the differences between the baseline and mismatch trajectories, the greatest mismatch occurs at maximum range (in this case, 600 m). Thus, a projectile that meets the ±1 mil mismatch requirement at 600 m also meets this requirement at all intermediate ranges.

Additional trajectories that produce ±1.0 mil mismatches at 600 m can be obtained by varying the muzzle velocity. As the muzzle velocity increases, the corresponding values of the muzzle retardation increase as well. Figure 21 shows the trajectories for –1.0 mil mismatch for three different values of muzzle velocity compared with the baseline M855 trajectory. Although the three –1.0 mil mismatch trajectories are relatively similar, as the muzzle velocity increases, the trajectory becomes flatter at shorter ranges, but shows much larger gravity drop at longer ranges.

The range of values of muzzle velocity and muzzle retardation that produce a fixed vertical impact mismatch at 600 m compared with the baseline M855 ammunition can be determined
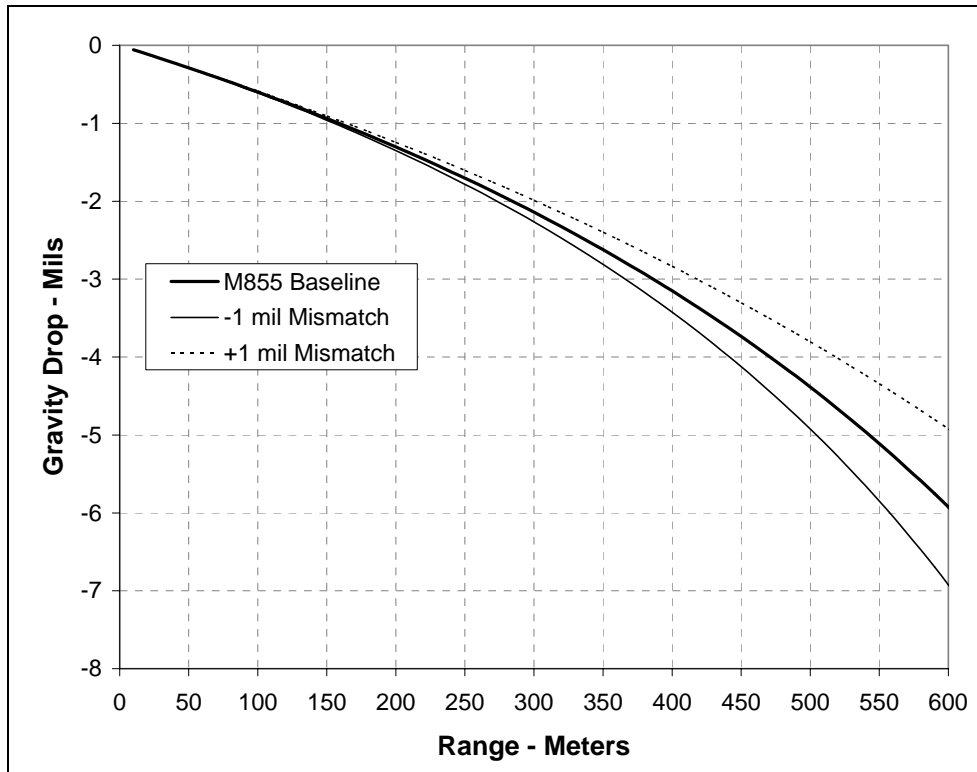
Figure 20. Gravity drop in mils for M855 and ±1.0 mil mismatch trajectories for 949 m/s muzzle velocity.
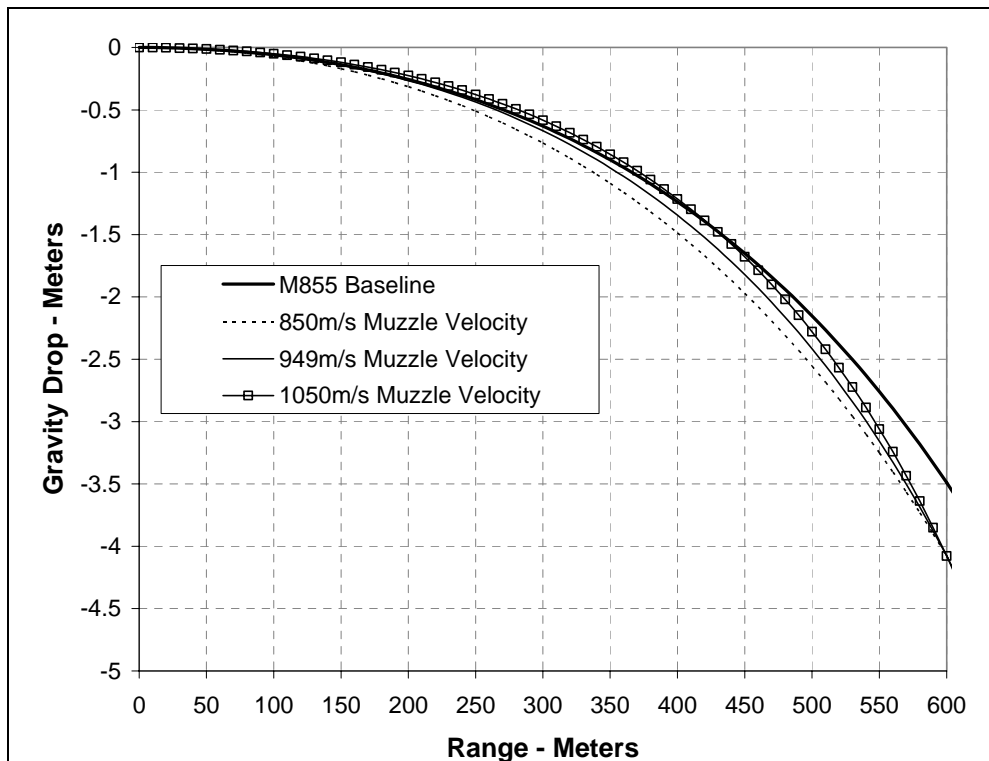
Figure 21. Gravity drop for M855 and −1.0 mil mismatch trajectories for different muzzle velocities.

from equation 5 and are represented as a contour plot shown in figure 22. Here, the lines of constant vertical impact mismatch are plotted as functions of muzzle retardation and muzzle velocity. Any combination of muzzle velocity and muzzle retardation contained between the ±1.0 mil mismatch lines will produce a vertical impact at 600 m that meets the ±1.0 mil requirement. Also shown are the values of muzzle velocity and muzzle retardation that produce the same impact location at 600 m as the baseline M855.
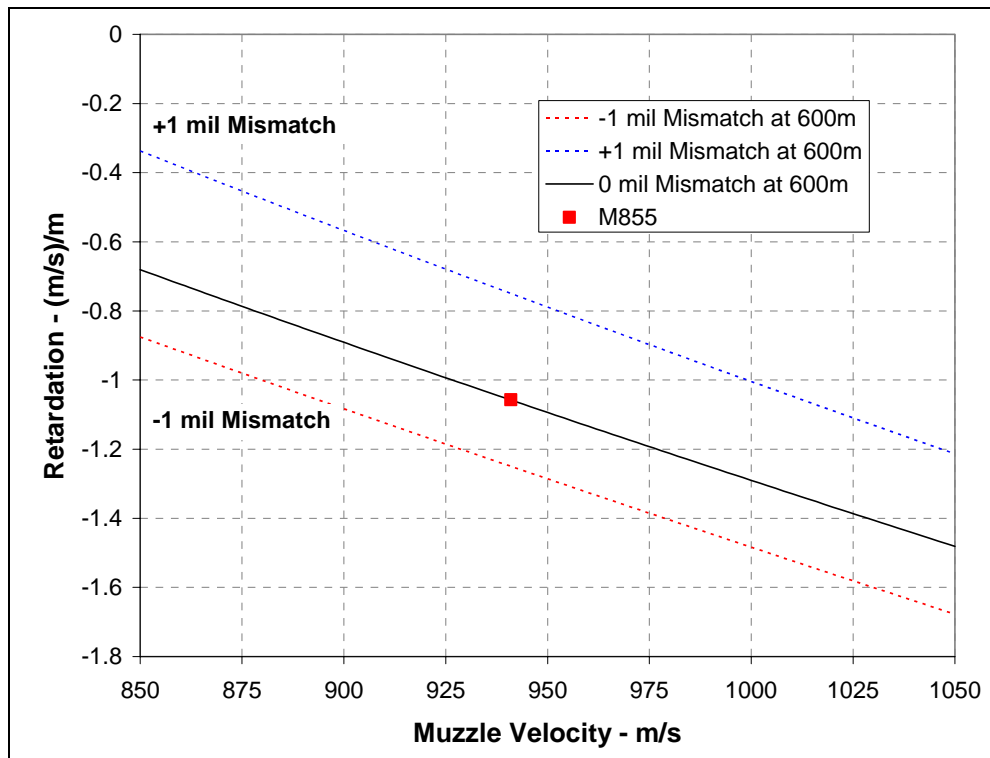
Figure 22. Acceptable range of muzzle velocity and muzzle retardation to attain ±1.0 mil mismatch.

The sensitivity of these bounds to the value of the drag coefficient exponent is shown in figure 23. Here, the bounds on muzzle velocity and muzzle retardation to meet the ±1.0 mil requirement are shown for the baseline drag coefficient exponent of 0.53 and a drag coefficient exponent of 0.25. These two drag coefficient exponents represents a rather wide variation for this parameter, especially for the streamlined low drag shapes typical of tactical small arms bullets which are more typically characterized by values of the drag coefficient exponent closer to the baseline value of 0.53. For the −1.0 mil mismatch results, the difference in the predicted retardation for a given muzzle velocity is less than 8% between the drag coefficient exponents of 0.25 and 0.53. Somewhat larger differences are observed for the +1.0 mil mismatch trajectory results at lower muzzle velocities. However, these low values of muzzle retardation necessary to achieve a +1.0 mil vertical impact above the M855 may be very difficult to obtain in practice.

31
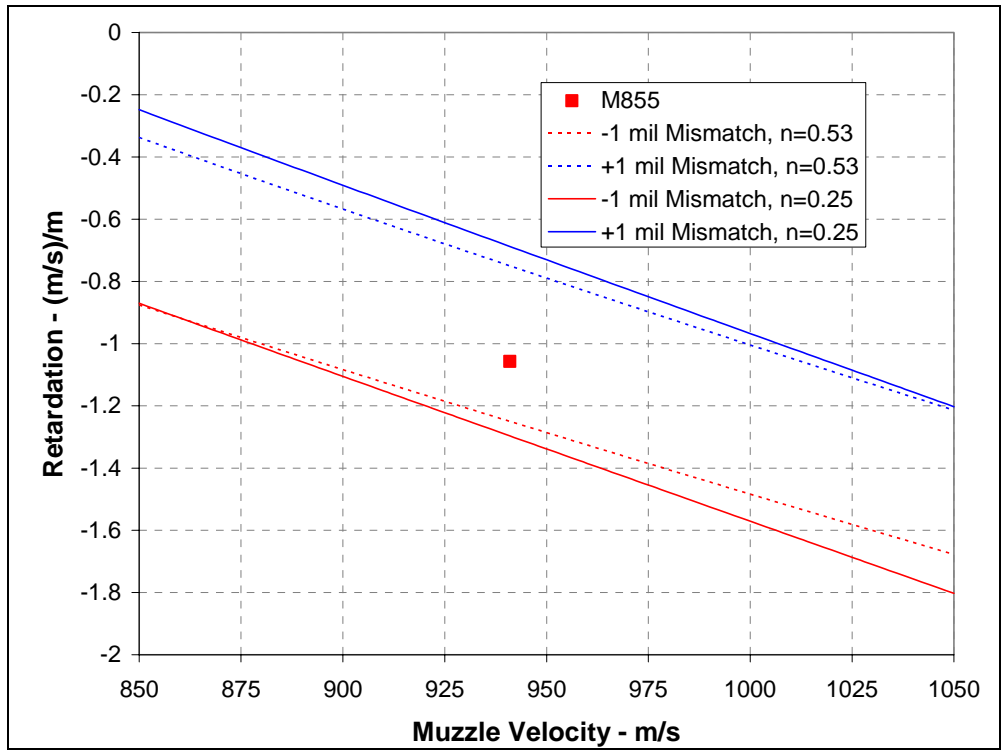
Figure 23. Sensitivity of the acceptable range of muzzle velocity and muzzle retardation for ±1.0 mil mismatch to drag coefficient exponent.

The trajectory mismatch requirement can be examined in light of current ammunition. Muzzle velocities, muzzle retardations, and vertical impact locations were obtained from the firing tables (*11*) for the M855, M856, M193, and M196 fired from the M16A2 and M4 rifles. The M856 and M196 are tracer rounds for the M855 and M193, respectively. Difference in the impact locations and muzzle retardations for identical rounds fired from the M16A2 and M4 rifles are produced by the differences in muzzle velocity. Figure 24 displays the mismatch for each of the four projectiles and two rifle combinations as a function of muzzle velocity and muzzle retardation on mismatch contours similar to those shown in figure 22. It can be seen that the companion tracer rounds are well matched to the tactical round for each of the round/rifle combinations with little difference in the relative impact locations noted. This occurs despite a rather large variation in muzzle velocity produced by firing the same round from a different rifle.

In addition to trajectory mismatch, the aeroballistician must also consider the wind sensitivity of the projectile. In general, firing a projectile with a higher muzzle velocity and lower (less negative) muzzle retardation will produce less wind drift. However, the previous results demonstrate that for a constant value of trajectory mismatch, as the muzzle velocity increases, the muzzle retardation increases (becomes more negative). Equation 7 can be applied to determine the relative wind drift as a function of muzzle velocity for constant values of trajectory mismatch.

32
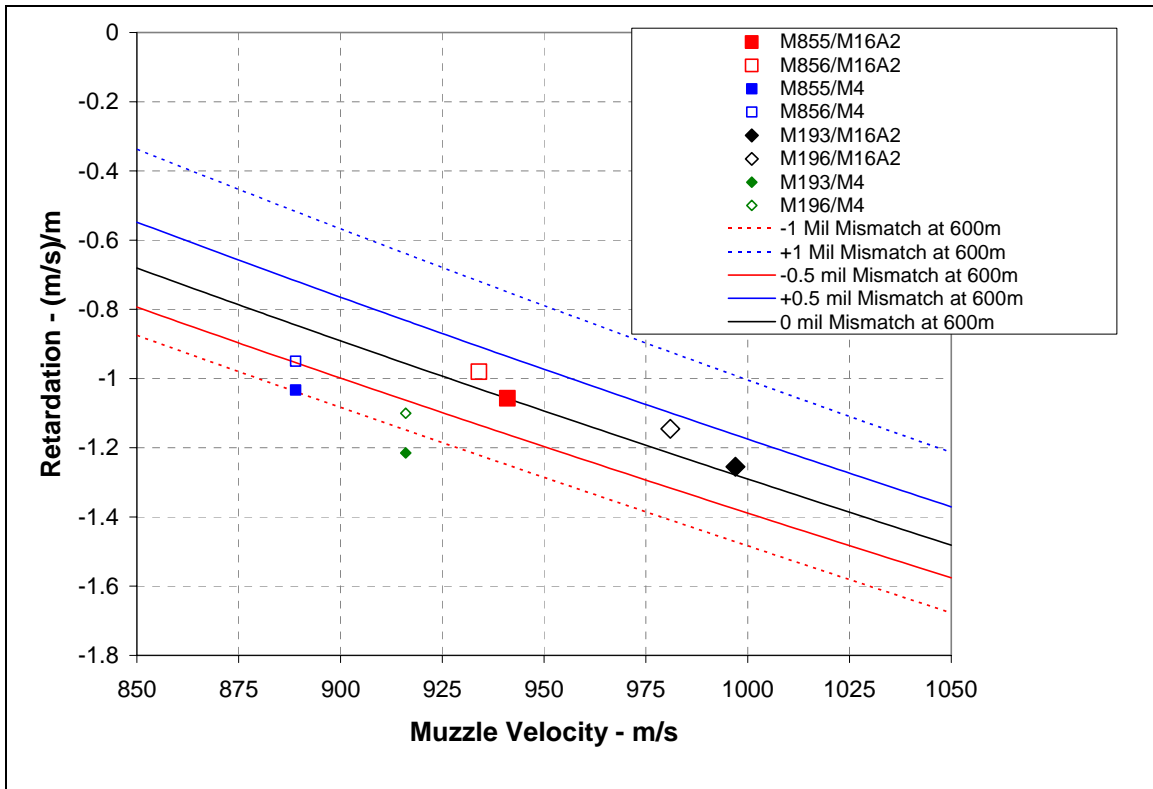
Figure 24. Muzzle velocity, muzzle retardation, and trajectory mismatch for M855 and M193 and their companion tracer rounds, M856 and M196, respectively.

Figures 25–27 show the predicted wind drift at 200, 300, and 600 m, respectively, relative to the M855 for constant values of the trajectory mismatch at 600 m. The results shown in figures 25–27 demonstrate that, for constant trajectory mismatch, the wind drift increases with increasing muzzle velocity. These trends are consistent across each of the ranges examined although the relative increase is larger at longer ranges. Although decreased wind sensitivity should be expected with increasing muzzle velocity, for constant mismatch, the muzzle retardation also increases (becomes more negative) with increasing muzzle velocity. The combined effects of increasing muzzle velocity and muzzle retardation result in increased wind sensitivity. The results also show that the target mismatch varies from −1.0 to +1.0 mils, the wind drift decreases. This trend is expected because, for a constant muzzle velocity, the muzzle retardation decreases (becomes less negative) as the mismatch varies from −1.0 to +1.0 mils, resulting in less wind sensitivity.

Results are also shown in figures 25–27 for the M855, M856, M193, and M196 fired from the M16A2 and M4 rifles. In each case, the M855 and M856 fired from the M16A2 produces the least wind sensitivity. A slight increase in wind sensitivity in the M855 and M856 is noted when fired from the M4 rifle as a result of the lower muzzle velocity. The M193 and M196 produce slightly more wind drift than the M855 and M856 when fired from the same rifle.

33
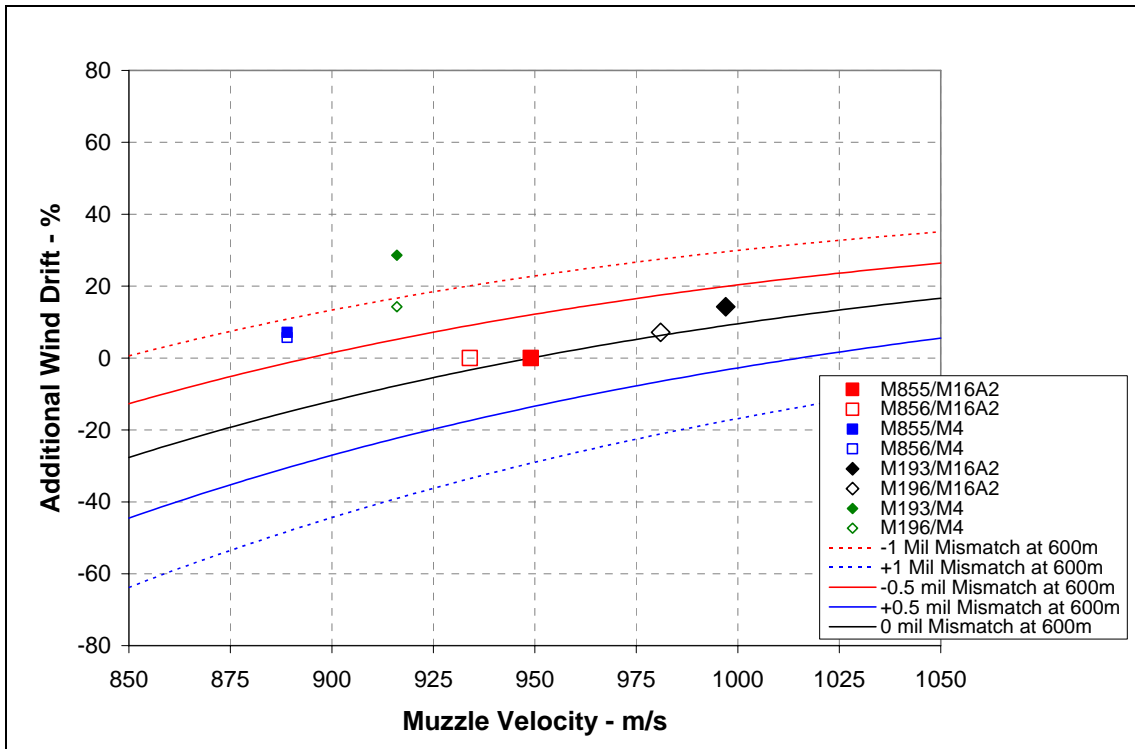
Figure 25. Percent increase or decrease in wind drift at 200 m relative to the M855 as a function of muzzle velocity for constant values trajectory mismatch at 600 m.
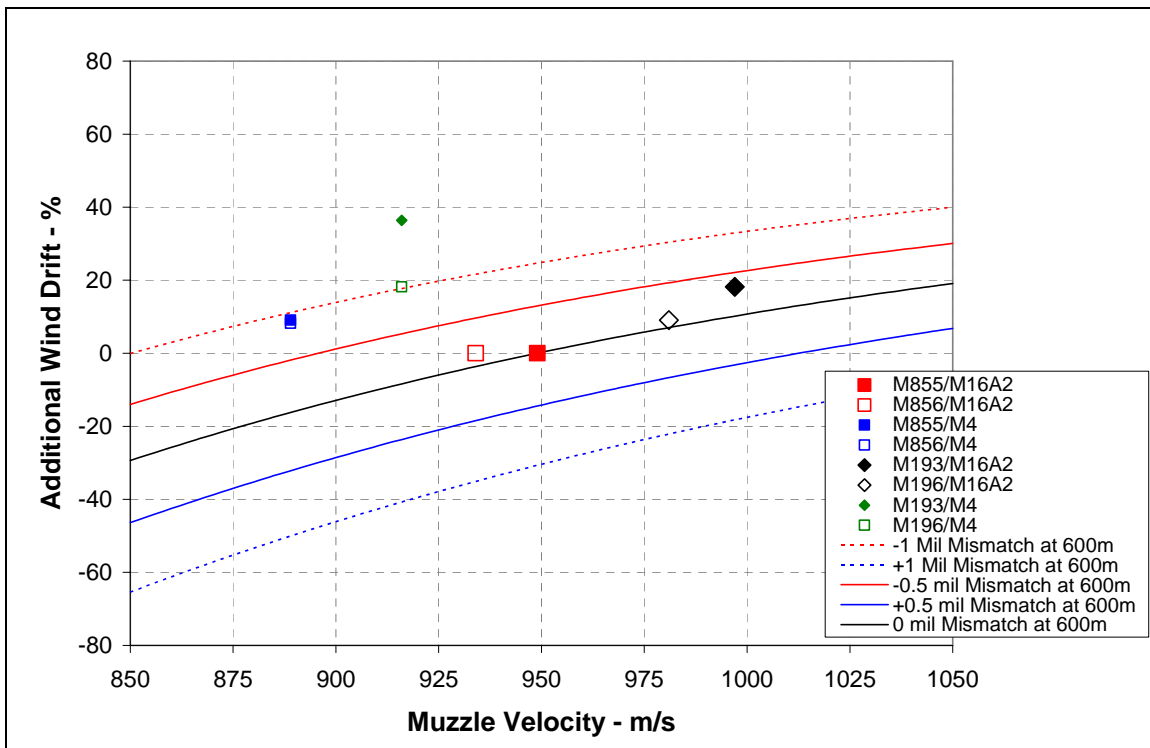
Figure 26. Percent increase or decrease in wind drift at 300 m relative to the M855 as a function of muzzle velocity for constant values trajectory mismatch at 600 m.
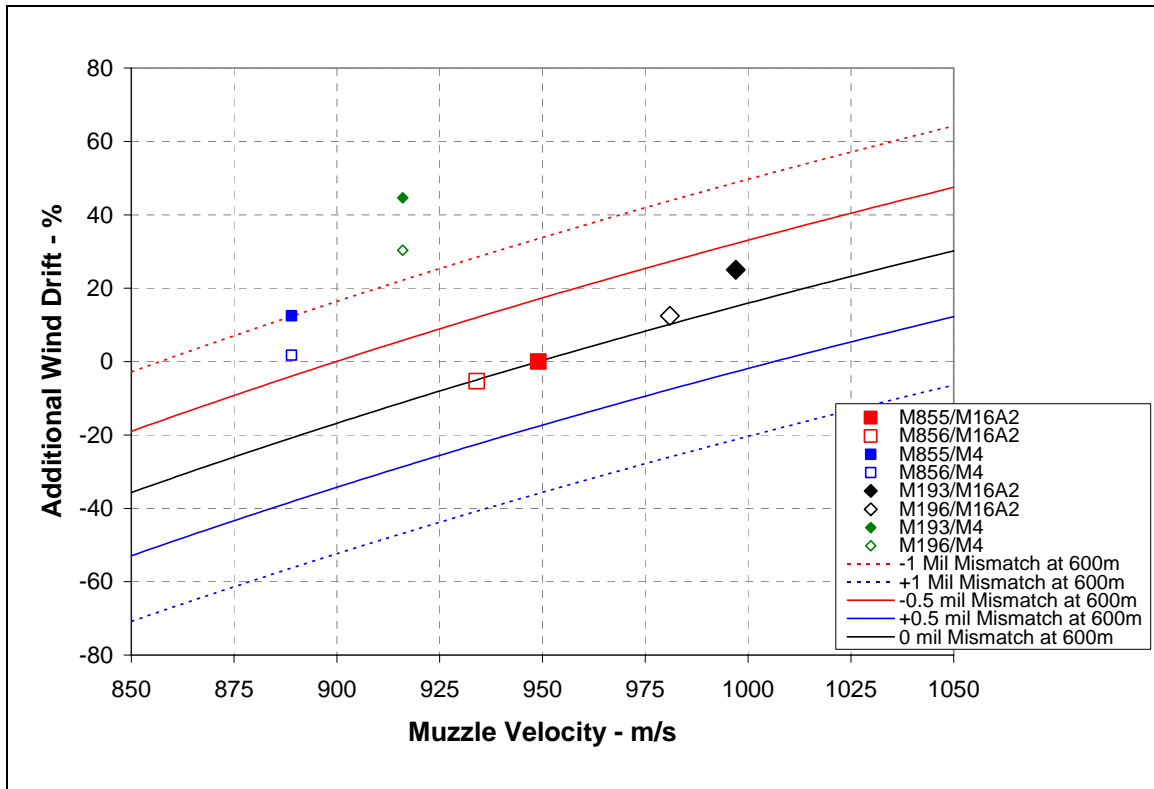
Figure 27. Percent increase or decrease in wind drift at 600 m relative to the M855 as a function of muzzle velocity for constant values trajectory mismatch at 600 m.

Because small arms rifles are zeroed at some specified range, it would be natural to question the necessity of the second part of the mismatch requirement that assumes the gun elevation is fixed for baseline and modified ammunition. The Rifle Marksmanship Field Manual (FM) (*12*) for the M16/M4 series rifle discusses various approaches for zeroing the rifle. Zeroing is typically performed at 25-m range. With proper marksmanship fundamentals, 25-m zeroing will allow the Soldier to hit all targets out to 300 m using the existing ammunition. Known distance (KD) zeroing at 300 m can also be performed to confirm or refine the 25-m zero. As stated in the FM, the zero for the 300-m target is more valid than the zero obtained on the 25-m range when the wind is properly compensated for. It would seem that the zeroing process at a known distance could eliminate some of the mismatch between the baseline and modified ammunition or allow greater flexibility in the selection of the muzzle velocity and muzzle retardation for the modified ammunition while still meeting the ±1.0 mil mismatch at 600 m. In other words, allowing zeroing at a known distance might be less restrictive than assuming that the gun elevation is fixed for the baseline and modified ammunition.

An analysis was performed allowing zeroing of the weapon at various intermediate ranges between 25 and 300 m so that both the baseline and modified ammunition had the same vertical impact location at the known distance downrange used for zeroing while allowing a ±1.0 mil mismatch for the modified ammunition at 600 m. For the baseline M855, the gun

elevation angle required to produce a vertical impact along a horizontal line-of-sight at the known distance range was computed using equations 5 and 6. Using this gun elevation angle, the vertical impact location was also computed at 600-m range. For the modified ammunition, the muzzle retardation required to produce a trajectory that satisfied the following two constraints was obtained for fixed values of the muzzle velocity. This trajectory had the identical vertical impact location as the M855 at the KD range used for zeroing and a ±1.0 mil mismatch at 600 m relative to the M855 impact. Similar to the trajectory mismatch results previously presented, an iterative procedure was used to determine the retardation of the modified ammunition required to meet these constraints. At each iteration step, the gravity drop and the gun elevation angle for the modified ammunition were computed using equations 5 and 6 to produce the identical vertical impact location at the KD range used for zeroing as for the baseline M855. Based on this gun elevation angle, the vertical impact locations were determined at 600-m range using equations 5 and 6. The retardation of the modified ammunition was adjusted until the proper vertical impact locations were obtained at both the KD range used for zeroing and at 600 m.

Figure 28 shows sample trajectories with KD zeroing for the M855 and the modified ammunition at a muzzle velocity of 949 m/s. For the sample trajectories shown in figure 28, the M855 and the modified ammunition have been rezeroed at either 200 or 300 m to produce the same vertical impact at the respective KD ranges. For each set of trajectories rezeroed at the same KD range, the impact locations at 600 m for the M855 and the modified ammunition differ by –1.0 mils. Figure 29 compares the gravity drop of the modified ammunition for rezeroing at 100, 200, and 300 m, with the gravity drop obtained when assuming both the M855 and the modified ammunition are fired with the same gun elevation angle. Also shown is the gravity drop for the baseline M855. There is very little difference in the gravity drop when rezeroing is allowed at ranges less than 300 m, compared to the results obtained by assuming the M855 and the modified ammunition are fired with the same gun elevation angle. These differences in gravity drop are due to the differences in the predicted muzzle retardation obtained using the procedure previously outlined. These results indicate that rezeroing at a known distance offers little difference in the modified ammunition performance compared with using the same gun elevation for both the modified and baseline ammunition.

Comparison of the values of the muzzle retardation obtained using rezeroing at 300 m, with the muzzle retardation values obtained assuming a fixed gun elevation angle, show less than a 2% difference for a muzzle velocity of 949 m/s. Similar results were obtained for muzzle velocities between 949 and 1050 m/s. Velocities below 949 m/s showed somewhat more sensitivity to rezeroing with differences in the predicted muzzle retardation of about 10% obtained for a muzzle velocity of 850 m/s. The differences in the predicted muzzle retardation decreased as the KD for rezeroing was decreased. The results indicate that the performance envelope of
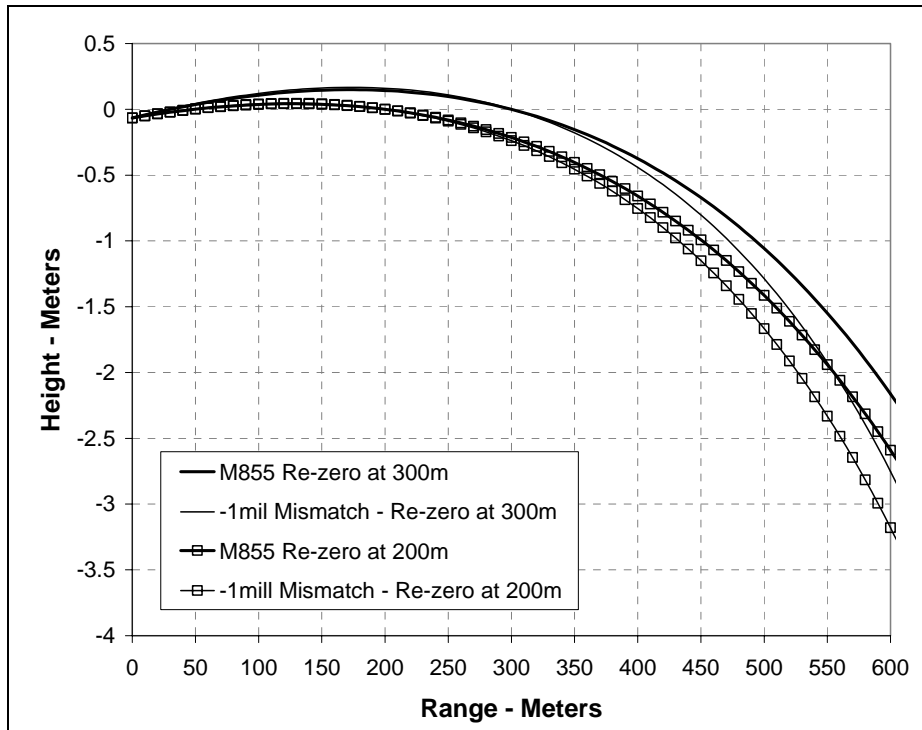
Figure 28. Trajectories for M855 and modified ammunition with –1.0 mil mismatch
   at 600 m with rezeroing at 200 and 300 m.
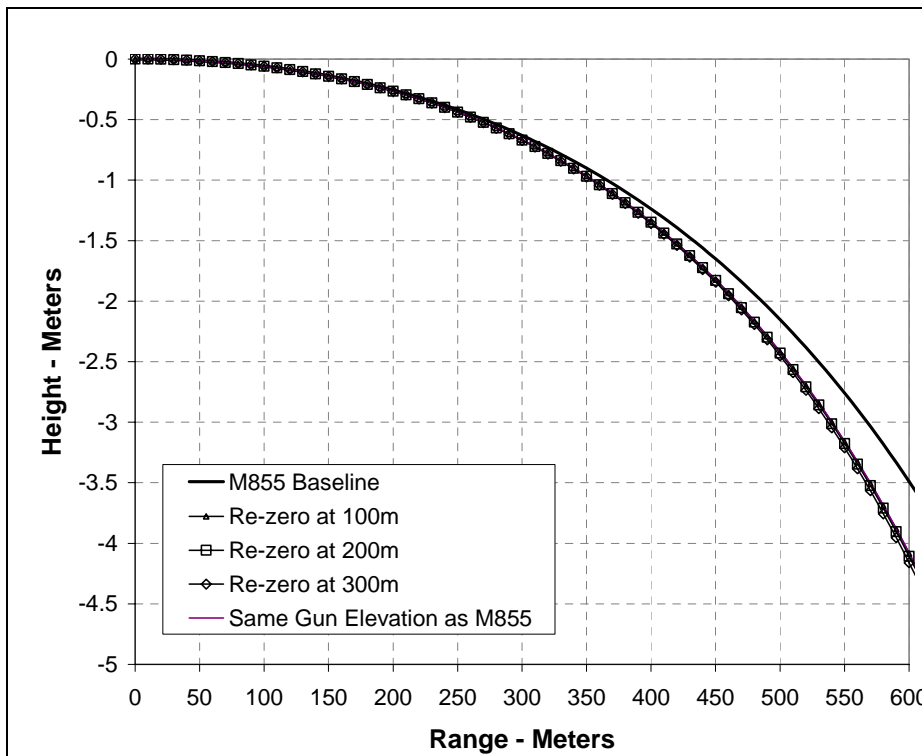
Figure 29. Gravity drop for M855 and modified ammunition with –1.0 mil mismatch
          at 600 m when fired at same gun elevation as M855 or zeroed at 100, 200,
          and 300 m.

allowable retardations (such as that shown in figure 22) for trajectory mismatches of ±1.0 mils is not significantly changed by allowing rezeroing at a KD. The results also show that the differences in the gun elevations between the M855 and modified ammunition are generally quite small when rezeroing is employed. For example, for the baseline muzzle velocity of 949 m/s, the largest differences in gun elevation occurs for the 300-m rezeroing case, but is less than 0.2 mils.

The results obtained for zeroing the rifle at 25 m were nearly identical to the results obtained by assuming the baseline M855 ammunition and the modified ammunition were fired at the same gun elevation angle. The differences in the gun elevation angle between the baseline M855 and the modified ammunition required to zero the rifle at 25 m were extremely small. Essentially, zeroing at 25 m is equivalent to assuming a constant gun elevation angle for the baseline and modified ammunition.   The predicted muzzle retardation for the modified ammunition obtained by allowing zeroing at 25 m was within 1% of the results obtained assuming the modified ammunition had the same gun elevation as the baseline M855 ammunition for muzzle velocities between 850 and 1050 m/s.

Clearly, the additional effort of considering rezeroing at ranges less than 300 m does not result in significant difference in the performance of the modified ammunition compared with the results obtained assuming both the M855 and the modified ammunition are fired at the same gun elevation angles. Thus, the second part of the ±1.0 mil mismatch requirement which assumes the same gun elevation for both the baseline ammunition and the modified ammunition simplifies the analysis process without adding any significant constraint to the modified ammunition design. Rezeroing at ranges beyond 300 m for the purpose of removing differences in the gravity drop between the baseline and modified ammunition appears to have more of an effect, although there is some question whether rezeroing at these ranges could be accomplished in practice.

It is important to note that the previous comments regarding rezeroing only apply to the requirements for trajectory mismatch. Zeroing the rifle remains an important approach for correcting other sources of inaccuracy produced by launch disturbances which are not considered here. It appears then that the requirement for 1.0 mil mismatch in impact location for ranges up to 600 m with the additional constraint of fixed gun elevation provides a meaningful but simple requirement for trajectory mismatch. It is relatively easy to implement both in practice and in engineering analysis and provides nearly the same performance envelope for the modified ammunition as requirements which involve rezeroing.

5. Combined Exterior and Interior Ballistics Results

The previous results show the possible bounds on muzzle velocity and muzzle retardation to meet the ±1 mil trajectory mismatch requirement. These results show that the best performance (in terms of reduced wind sensitivity and gravity drop and increased impact velocity and energy) is obtained by firing bullets with low retardation and high muzzle velocity. These results treat the muzzle velocity as an independent variable, but, in fact, the muzzle velocity itself is constrained by the interior ballistic constraints and considerations. In particular, for the M16 rifle, there are limitations on chamber pressure and charge mass. For example, the M855 attains nearly the maximum allowable chamber pressure during the interior ballistic cycle. If heavier variants of the M855 are fired with the existing charge, the maximum allowable chamber pressure would be exceeded resulting in possible catastrophic failure of the gun tube. The result is that lower charge weights must be utilized for heavier bullets so that the maximum allowable chamber pressure is not exceeded. This typically produces lower muzzle velocity as the projectile mass is increased. Additionally, for the M855, the volume available for propellant is nearly completely occupied by the current propellant load and it is difficult to add additional propellant to increase the current muzzle velocity of the round. This is particularly a problem for lighter bullets that can be fired with increased charge masses without exceeding the maximum chamber pressure. For these lighter variants of the M855, the maximum charge volume becomes the constraint limiting muzzle velocity rather than the maximum allowable chamber pressure. Efforts are underway to develop new propellants that will provide increased performance within the 5.56 constraints.

To demonstrate the effect that these constraints have on muzzle velocity and, subsequently, on the exterior ballistic performance, interior ballistics computations using the IBHVG2 interior ballistics code (*13*) were performed to obtain predictions of muzzle velocity for different projectile masses using the existing WC844 propellant. Two separate series of computations were run. The first series of computations constrained the chamber pressure to the maximum allowable chamber pressure while allowing the charge mass to vary. Predictions of the resulting muzzle velocity were obtained for each projectile mass. A second series of computations constrained the charge mass to the existing M855 charge mass while allowing the chamber pressure to vary. Again, predictions of the resulting muzzle velocity were obtained for each projectile mass. For both series of computations, the change in chamber volume due to projectile intrusion resulting from the varying projectile mass was taken into account by assuming that the change in projectile mass relative to the M855 was produced by a right circular cylinder with the density of lead. Validation of the model for the baseline M855 was obtained by comparing the predicted case mouth pressure with experimental measurements as shown in figure 30. The predictions are in excellent agreement with the experimental measurements. Also shown is the predicted breech pressure which represents one of the constraints on the M855 performance.
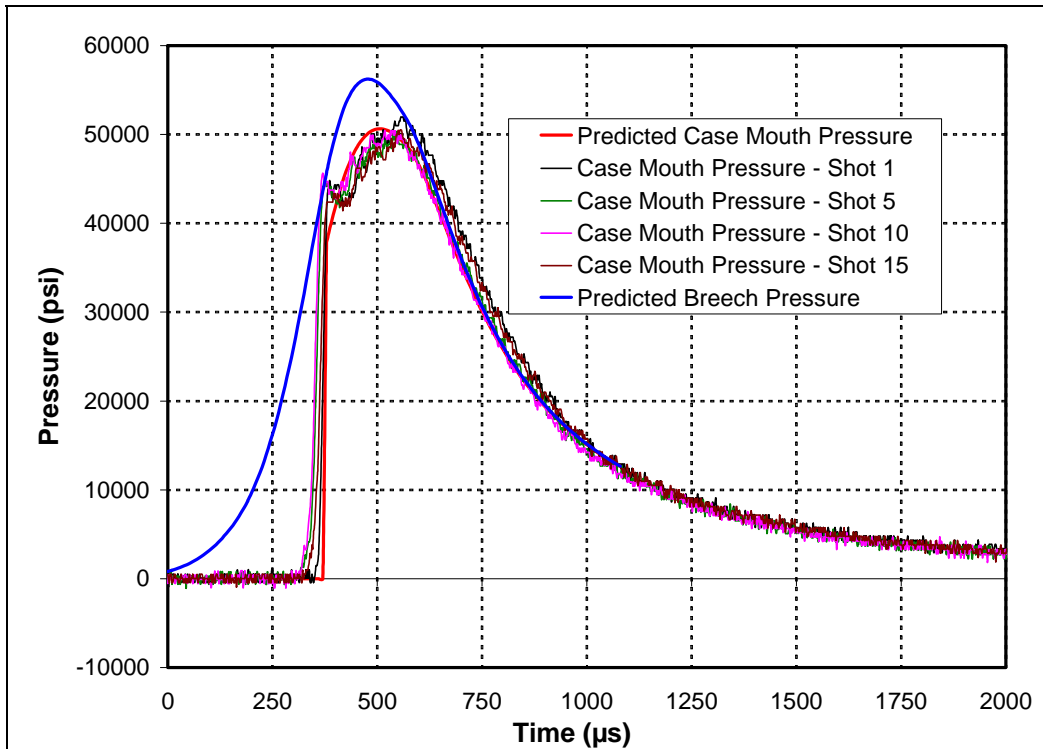
Figure 30. Predicted breech pressure and case mouth pressure (Gage 0.32 in) compared with measured case mouth pressure for standard M855 cartridge.

Figure 31 shows the predicted muzzle velocities as a function of projectile mass for both series of computations. As a benchmark for the results, muzzle velocity measurements for the 56-gr M193, the 62-gr M855, and the 77-gr Mk262 are plotted on the same graph. Additional experimental results are presented from a recent firing of 5.56-mm prototypes. All of the rounds from this set of firings were lighter or weighted the same as the existing M855 and were fired using the M855 charge mass. In general, the experimental results confirm the predictions for muzzle velocity.

Obviously, an acceptable charge is one that meets both constraints, so only muzzle velocities that are below both curves are acceptable. For the heavier projectiles, the muzzle velocity decreases with increasing projectile mass. For lighter projectiles, the muzzle velocity is relatively constant showing only a slight increase with decreasing projectile mass. It is interesting to note that the 62-gr projectile is close to the intersection of both performance constraints, meaning that the 62-gr projectile has nearly the maximum charge mass and attains a maximum chamber pressure that is close to the maximum allowable.

The interior ballistic performance yields the muzzle velocity as a function of projectile mass. The data shown in figure 31 was curve fit using a second-order polynomial to obtain a representation of the muzzle velocity vs. charge mass. These fits are shown in equations 18 and 19 where the velocity is in m/s and the projectile mass is in gr.

40
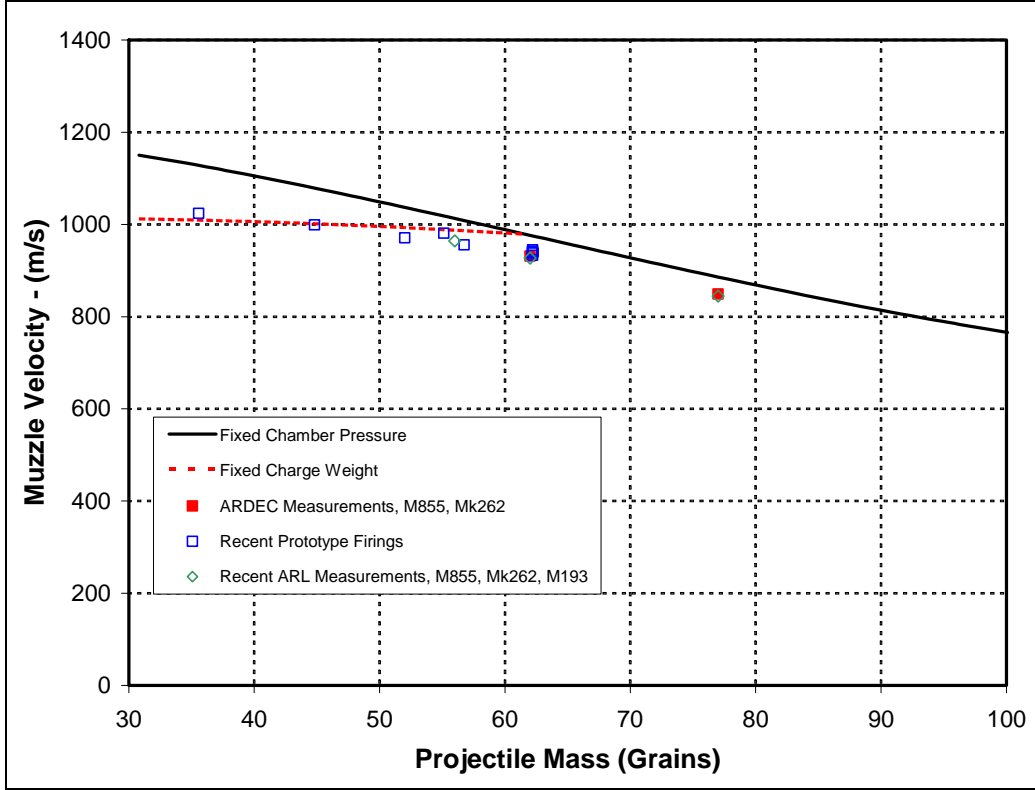
Figure 31. Muzzle velocity vs. charge mass for M855 cartridge and propellant.

$$V_0 \, (\text{m/s}) = -0.0191 \text{m}^2 + 0.6793 \text{m} + 1009.5 \quad \text{m} < 61.3 \, \text{gr.} \tag{18}$$

$$V_0 \, (\text{m/s}) = 0.0026 \text{m}^2 - 6.1077 \text{m} + 1344.2 \quad \text{m} > 61.3 \, \text{gr.} \tag{19}$$

These results can be used to predict exterior ballistic performance as a function of projectile mass. As previously discussed, the velocity history, gravity drop, and cross-wind drift can be obtained if the muzzle velocity, muzzle retardation, and exponent defining the shape of the drag curve are known. With the muzzle velocity known for each projectile mass, the muzzle retardation can be predicted using equation 8. For the prediction shown here, the standard atmospheric density of 1.22 kg/m^3 was used. The reference area is easily obtained as shown in equation 20 using a reference diameter of 5.56 mm.

$$S_{\text{ref}} = \frac{\pi}{4} D^2 . \tag{20}$$

The drag coefficient was computed as shown in equation 21.

$$C_D \big|_{V_0} = \left(\frac{V_{\text{Ref}}}{V_0} \right)^n i_{\text{Form}} C_{DG1} \big|_{V_{\text{Ref}}} . \tag{21}$$

The last two terms of equation 21 represent the drag coefficient as the product of the form factor i_{Form} and the drag coefficient of the standard G1 drag curve at a reference velocity of 3100 m/s. The G1 drag function is a standard drag function used within the commercial small arms community. These last two terms represent the drag coefficient of a given bullet geometry at the reference velocity of 3100 m/s. The form factor represents the ratio of the actual drag coefficient of a projectile to reference drag coefficient. (This is the same form factor that appears in the ballistic coefficient quoted for many commercial bullets.) In the current results, the form factor was treated as a parameter with results obtained for form factors of 0.6 and 0.8. As previously seen, the form factor of 0.6 represents the form factor for a low drag slender boattailed projectile with a long ogive. The form factor of 0.8 represents the form factor of a less streamlined projectile. A sampling of projectile shapes having form factors of 0.6 and 0.8 is shown in figure 32. The first term of equation 21 represents the variation of the drag coefficient with velocity (or Mach number) for a given bullet geometry. As previously shown, the exponent defining the shape of the drag curve can be estimated using the form factor using equation 13.


Bullets with I$_{form}$ =0.6   **Bullets with I$_{form}$ =0.8**
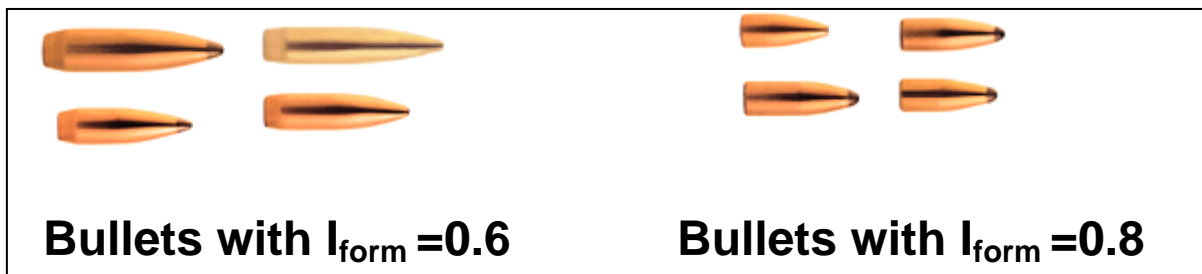
Figure 32. Typical projectile shapes for projectiles with form factors of 0.6 and 0.8; bullet photographs from Sierra Bullets (*8*).

Using the predicted muzzle velocity (equations 18 or 19), the muzzle retardation was obtained for each projectile mass using equation 8. Figure 33 shows the muzzle retardation as a function of projectile mass for form factors of 0.6 and 0.8 using the predicted dependence of the muzzle velocity on projectile mass. As seen in equation 8, the muzzle retardation varies explicitly with the inverse of the projectile mass. Because of the dependence of muzzle velocity on projectile mass, the muzzle retardation also has an additional implicit dependence on projectile mass through the muzzle velocity (equations 18 or 19) and drag coefficient (equation 21). The net effect is a decreasing trend of the muzzle retardation with projectile mass. The results for the form factor of 0.8 represent an increase in retardation of ~33% over the results for the form factor of 0.6. (Generally, the increase in muzzle retardation reflects the proportional increase in the factor factor, although this is a relatively minor effect due to small changes in the drag coefficient exponent due to form factor.) The results for the M193, M855, and Mk262 are reasonably well represented by the results for the form factor of 0.6.

With the muzzle velocity, muzzle retardation, and exponent characterizing the shape of the drag curve defined for each projectile mass, the velocity history, gravity drop, and cross-wind drift were predicted. Baseline results are presented for a form factor of 0.6 representing the expected
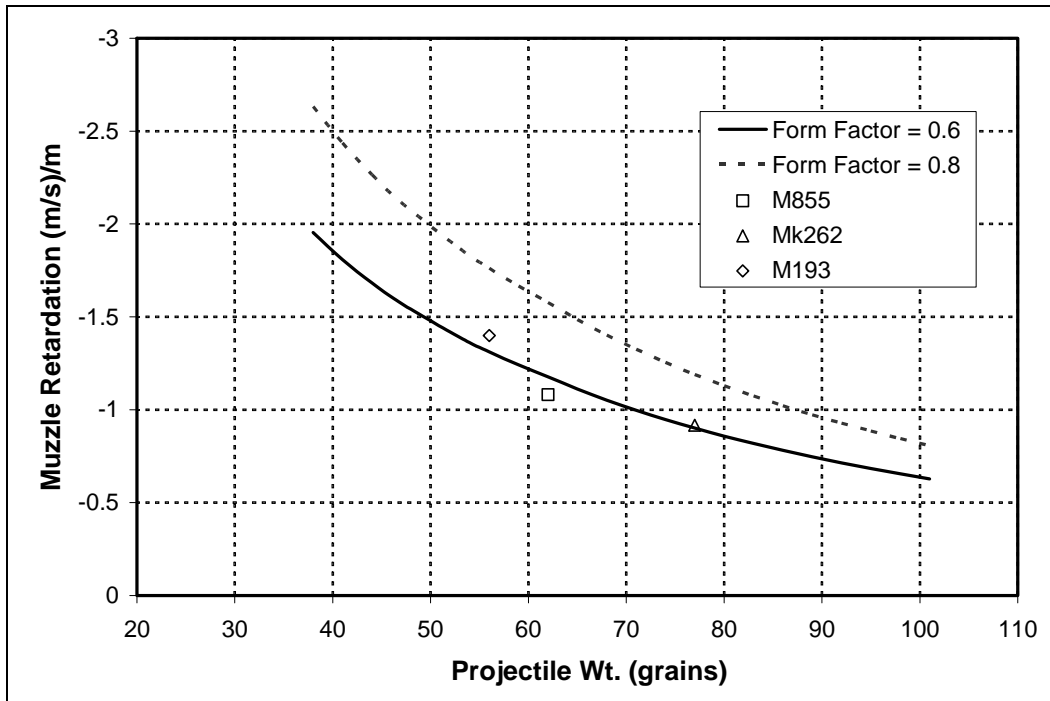
Figure 33. Muzzle retardation vs. projectile mass for form factors of 0.6 and 0.8 compared with retardation of M855, Mk262, and M193.

performance for a well-designed, low-drag, streamlined (typically boattailed) projectile. Additional results are presented for higher drag shape with a form factor of 0.8 to quantify the relative sensitivity of the results to form factor. Results for the dependent variables of interest are presented as a function of projectile mass. Each projectile mass is associated with a particular muzzle velocity by virtue of the results shown in figure 31.

Figure 34 shows the impact velocity as a function of projectile mass for ranges of 0, 150, 300, 450, and 600 m. The results at 0-m range are essentially the muzzle velocity results shown in figure 31. Corresponding results for short ranges are shown in figure 35. For short ranges, the lighter bullets have higher impact velocity due to the higher muzzle velocity, but these lighter bullets decelerate at a higher rate (due to the lighter mass) and the maximum impact velocity at a given range occurs for a progressively heavier bullet as the range increases. The impact velocity at 450–600 m shows relatively little variation with projectile mass for masses greater than 60 gr.

The sonic velocity for standard atmospheric conditions is also shown in figure 34. Some care must be taken in interpreting results that have impact velocities below the sonic velocity. The results presented here do not consider the significant decrease in drag that occurs in the transonic to subsonic velocity regime. The current results should overestimate the decrease in impact velocity below the sonic velocity. (It is possible to adapt the current approach to more accurately predict the flight behavior in this regime. However, this is beyond the scope of the current effort.) These comments also applied to the corresponding results for the impact energy, gravity

43
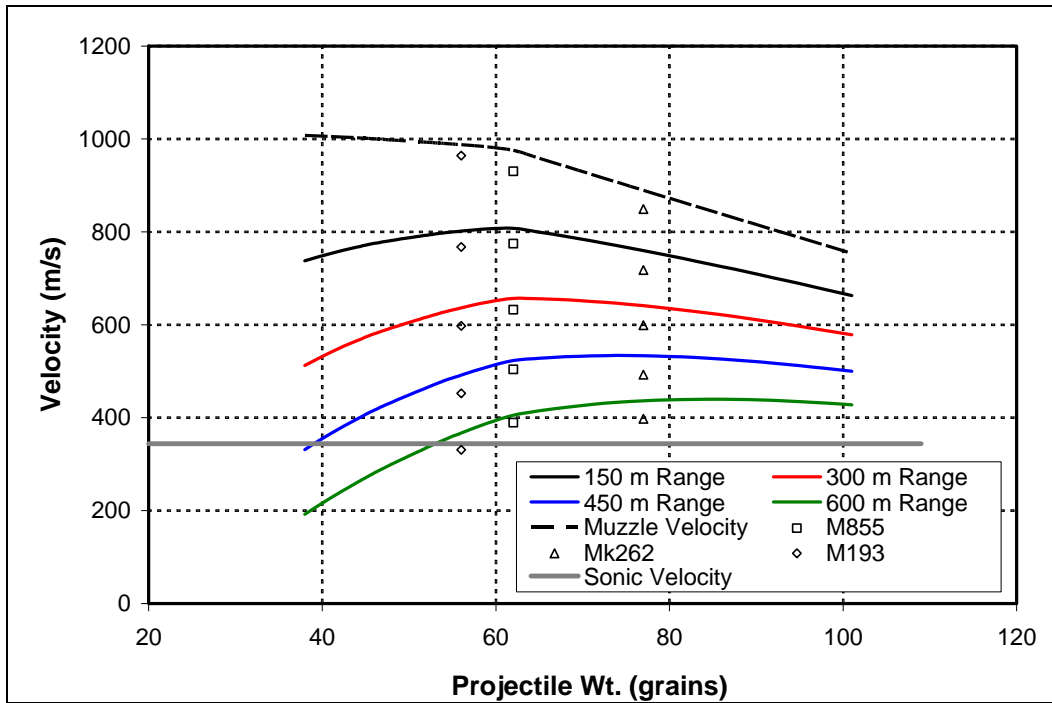
Figure 34. Impact velocity vs. projectile mass for ranges of 0, 150, 300, 450, and 600 m.
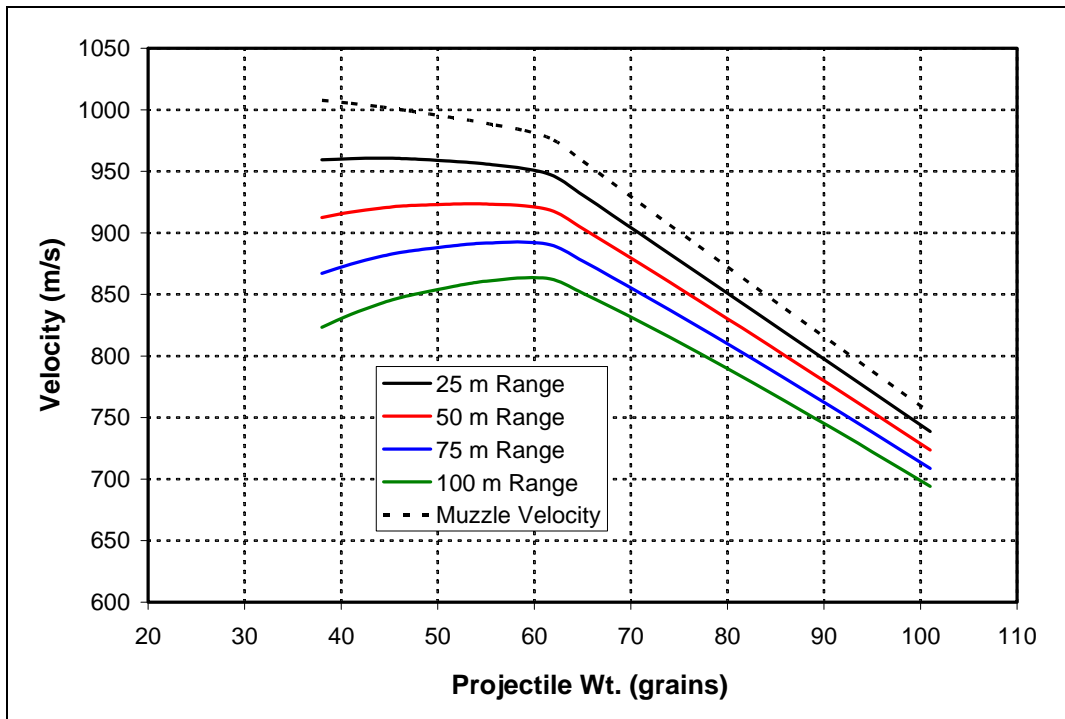

Figure 35. Impact velocity vs. projectile mass for ranges of 0, 25, 50, 75, and 100 m.

drop, and wind drift, which are derived from the same approach. The desirability of designs which result in impact velocities below the sonic velocity must also be carefully considered. Significant changes in projectile stability occur in the transonic velocity regime and these must be investigated as part of the design process to ensure projectile stability for those designs which operate in this flight regime. These issues can be avoided by considering only designs that fly at supersonic velocities within their operational ranges.

Results are also shown in figure 34 for the 56-gr M193, the 62-gr M855, and 77-gr Mk262 projectiles. Muzzle velocities used in the analysis for these rounds were experimentally determined from multiple sources using existing data (*14*) as well as recent in-house measurements. The experimentally determined muzzle velocities are slightly lower (2%, 3%, and 5% lower for M193, M855, and Mk262, respectively) than the predictions shown in figure 31. Actual values of form factor (0.65, 0.57, and 0.63, for the M193, M855, and Mk262, respectively) and drag coefficient exponent (0.40, 0.53, and 0.43, for the M193, M855, and Mk262, respectively) were used rather than the baseline form factor of 0.6 and the corresponding drag coefficient exponent of 0.46 computed from equation 13. The form factor and drag coefficient exponent for the Mk262 were derived from the 77-gr HPBT Match King ballistic coefficients published by Sierra Bullets (*7*) using an approach similar that that described in section 3. The form factor and drag coefficient for the M193 and the M855 was derived from the FTB aeropack data using the approach described in section 2. In general, the results for the M193, M855, and Mk262 are consistent with the results presented as a function of projectile mass, especially when the slight differences in muzzle velocity is taken into account.

Figure 36 shows the impact energy as a function of projectile mass for ranges of 0, 150, 300, 450, and 600 m. The impact energy at short range is shown in figure 37. The results show a relatively strong decrease in impact energy with decreasing projectile mass below a projectile mass of 62-gr due to the relatively constant muzzle velocity for these lighter bullets. The impact energy at the muzzle is relatively constant for the heavier bullets, but the heavier bullets have higher impact energies at longer ranges due to the lower decelerations associated with the heavy projectile mass. Also shown are the results for the M193, M855, and Mk262 projectiles. These results follow the general trends of the analysis when the slight differences in muzzle velocity are accounted for. The M855 and Mk262 show only minor differences in impact energy relative to each other.

A traditional qualitative measure of lethality has been the product of mass and velocity to the 3/2 power (*15*). Results for this metric are shown in figure 38 as a function of projectile mass for various ranges. Compared to the impact energy, this metric is slightly less dependent on velocity and shows increased values of the metric as the projectile mass increases.

Figure 39 shows the gravity drop as a function of projectile mass for ranges of 150, 300, 450, and 600 m. At shorter ranges, the heavier bullets show the most gravity drop due to their lower muzzle velocity and longer time of flight. However, as the range increases, the 62-gr
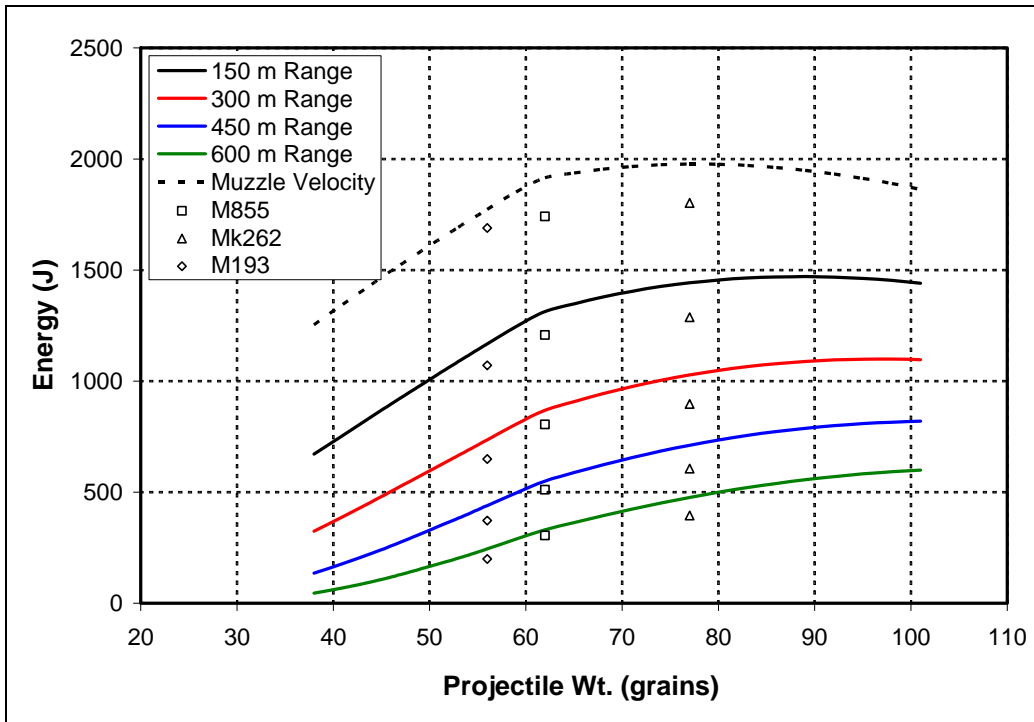
Figure 36. Impact energy vs. projectile mass for ranges of 0, 150, 300, 450, and 600 m.
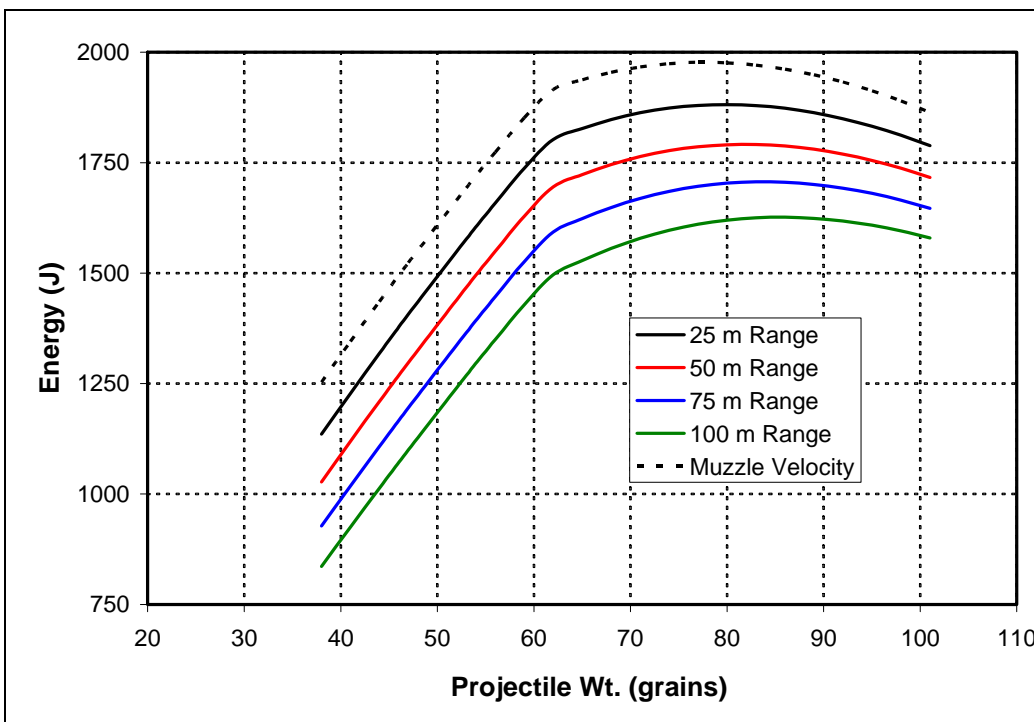
Figure 37. Impact energy vs. projectile mass for ranges of 0, 25, 50, 75, and 100 m.

46
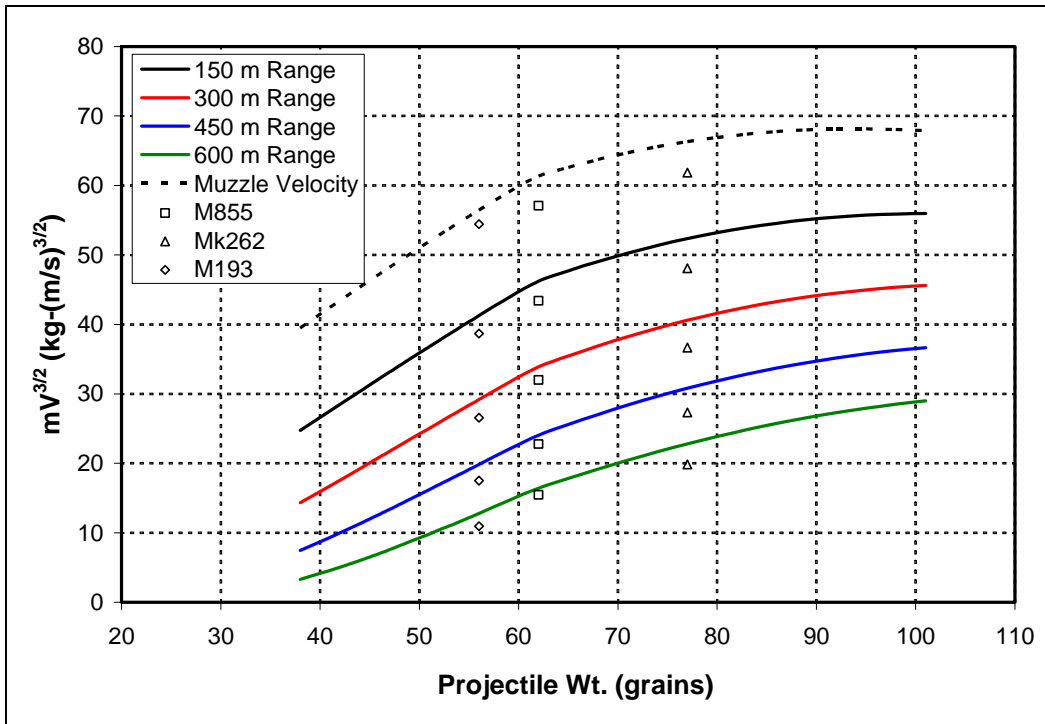
Figure 38. $mV^{3/2}$ vs. projectile mass for ranges of 150, 300, 450, and 600 m.
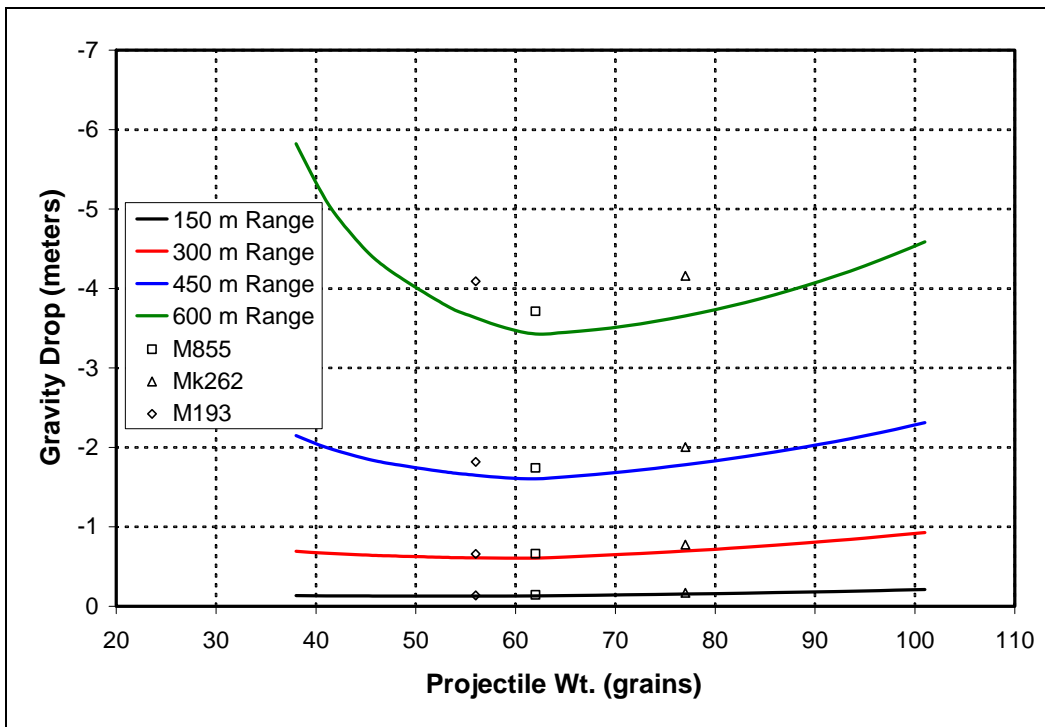

Figure 39. Gravity drop vs. projectile mass for ranges of 150, 300, 450, and 600 m.

bullet shows the lowest gravity drop due to the combination of higher muzzle velocity relative to the heavier bullets and lower retardation compared to the light bullets. Also shown are results for the M193, M855, and Mk262. After accounting for differences in muzzle velocity, these results compare relatively well with the predictions for the baseline form factor of 0.6. The Mk262 shows slightly higher gravity drop relative to the M855 as a result of its lower muzzle velocity. On the other hand, the M193 shows a slightly higher gravity drop due to its increased retardation (and relatively similar muzzle velocity) relative to the M855.

Figure 40 shows the gravity drop in mils relative to the M855 as a function of projectile mass. Projectile masses between 46 and 95 gr all meet the ±1.0 mil mismatch requirement relative to the M855. For projectile masses below 46 gr, the mismatch increases rapidly as the projectile mass decreases. The candidate designs which have projectile masses close to 62-gr impact above the M855 impacts due to the slight higher muzzle velocity of the candidate designs.
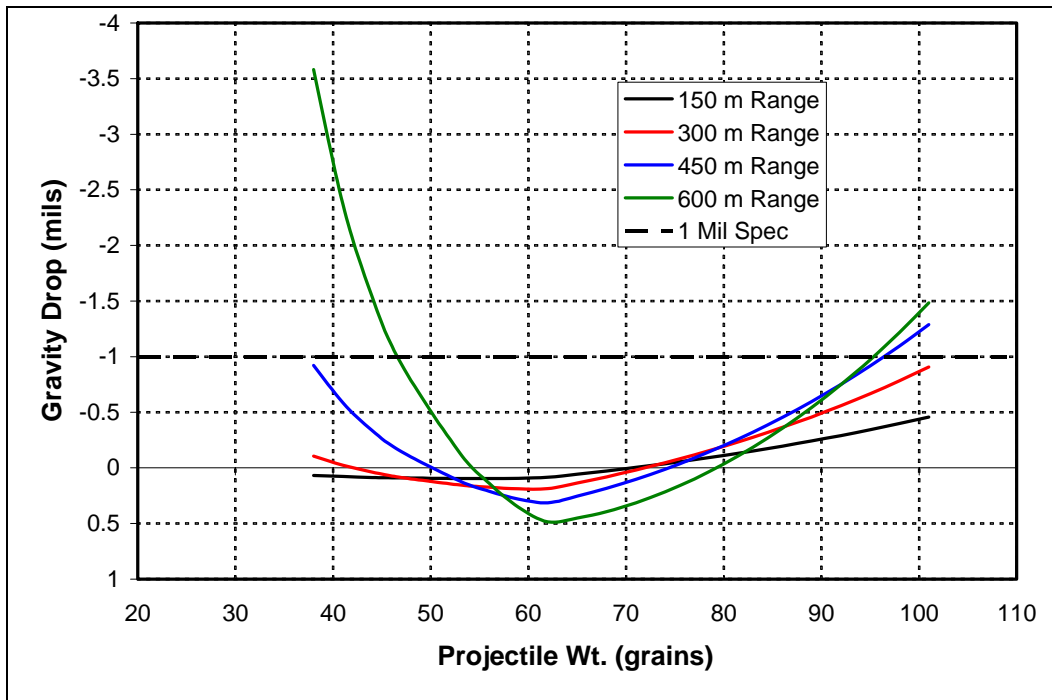
Figure 40. Gravity drop relative to M855 for ranges of 150, 300, 450, and 600 m.

The effect of gravity drop can be accounted for by proper aiming of the weapon. However, this requires the range to target to be correctly determined. Errors or uncertainty in determining range in turn will produce deviations from the desired vertical impact location. Ranging errors have been shown to be a significant source of impact errors at longer ranges (*16*). The deviation from the vertical impact location can be shown to be the product of the ranging error ε_R and the tangent of the angle of impact θ_I as shown in equation 22.

$$\Delta s_y = \varepsilon_R \tan \theta_I. \tag{22}$$

The ranging error may be dependent on range. One approach is to estimate the ranging error as a percentage of the range to target (*16*). However, in the current context, the ranging error should be fixed for a given range and only the tangent of the impact angle should vary as the projectile mass changes. Figure 41 shows the variation in the impact angle with projectile mass as a function of range. A strong variation in the tangent of the impact angle is seen at longer ranges for projectile masses below 60 gr. There is much less variation with projectile mass above 60 gr. If the ranging error can be estimated as a fraction of the range to target, the effect on the vertical miss distance as a function of range is increased significantly over the results in figure 41 which just consider the tangent of the impact angle. For ranges less than 150 m, the heavier projectiles show increased impact angle relative to the lighter projectiles. However, these trajectories are relatively flat and the trajectory is likely considered within point-blank range so that no adjustment for gravity drop is required.
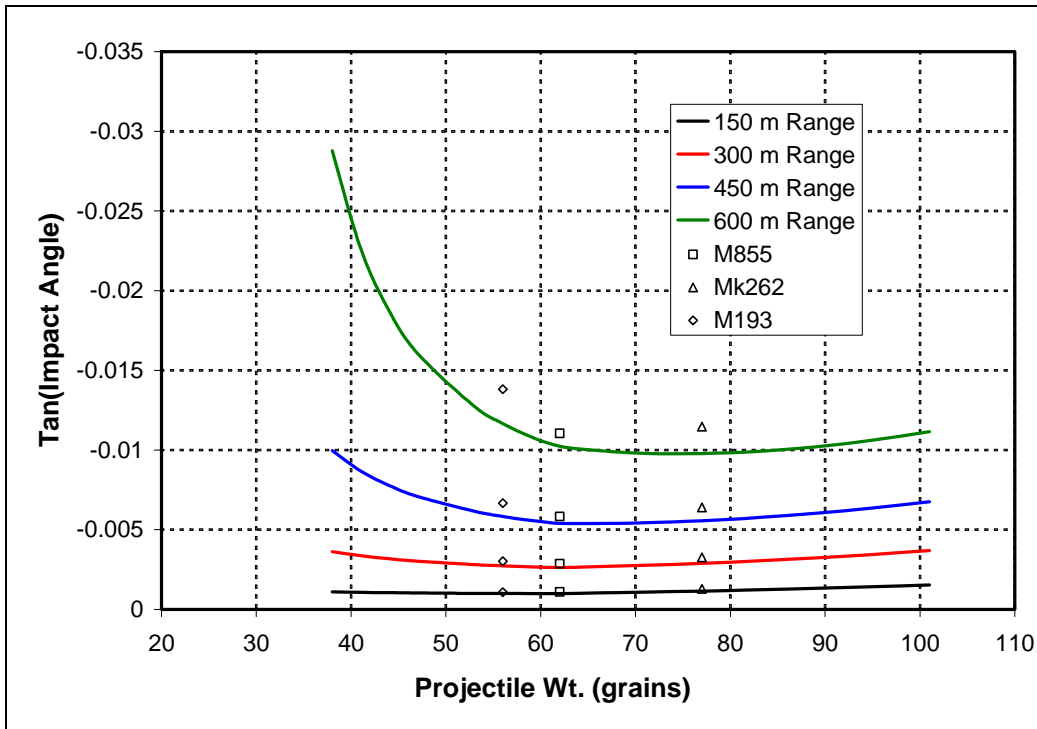
Figure 41. Tangent of impact angle vs. projectile mass for ranges of 150, 300, 450, and 600 m.

Figure 42 shows the cross-wind drift for a 10-m/s cross wind as a function of projectile mass for ranges of 150, 300, 450, and 600 m. Although the 10-m/s cross wind is relatively high, the cross-wind drift varies linearly with the cross-wind velocity, allowing the cross-wind drift for other wind velocities to be easily obtained from the presented results. The cross-wind drift increases significantly with range. The heavier bullets show less wind sensitivity than the lighter bullets particularly at longer ranges. This is because of the stronger influence of muzzle retardation compared with muzzle velocity (see equation 17). Results are also shown for the M193, M855, and Mk262. The M855 and Mk262 show nearly the same degree of wind

49
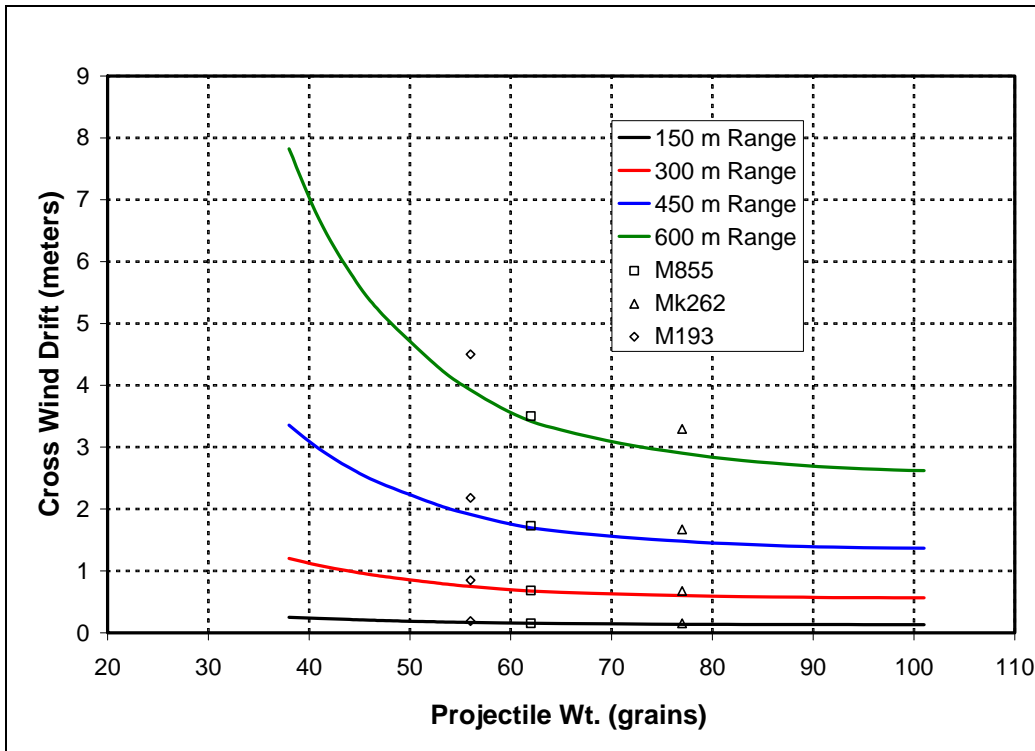
Figure 42. Cross-wind drift for 10-m/s cross wind vs. projectile mass for ranges of 150, 300, 450, and 600 m.

sensitivity. The M193 shows increase wind sensitivity compared to the M855 as a result of its increased retardation.

Figure 43 shows the percentage of cross-wind drift relative to the M855 as a function of projectile mass for ranges of 150, 300, 450, and 600 m. Bullets heavier than the M855 are less sensitive to cross winds. Correspondingly, bullets lighter than the M855 show increased sensitivity to cross winds. On a percentage basis, the difference in cross-wind drift relative to the M855 increases with range for a constant projectile mass.

Results were also obtained using a form factor 0.8 to compare with the baseline results obtained using a form factor of 0.6. Figure 44 compares the sensitivity of the impact velocity to form factor at various ranges as a function of projectile mass. The results show that the impact velocity decreases as the form factor increases from 0.6 to 0.8. This is primarily due to the increase in muzzle retardation that occurs as the form factor increases. (The results also show a slight dependence on the drag coefficient exponent produced by differences in the form factor.) The impact energy, shown in figure 45, is similarly affected by the change in form factor, although the differences are nearly twice that shown for the velocity because the impact energy varies with the square of the impact velocity.
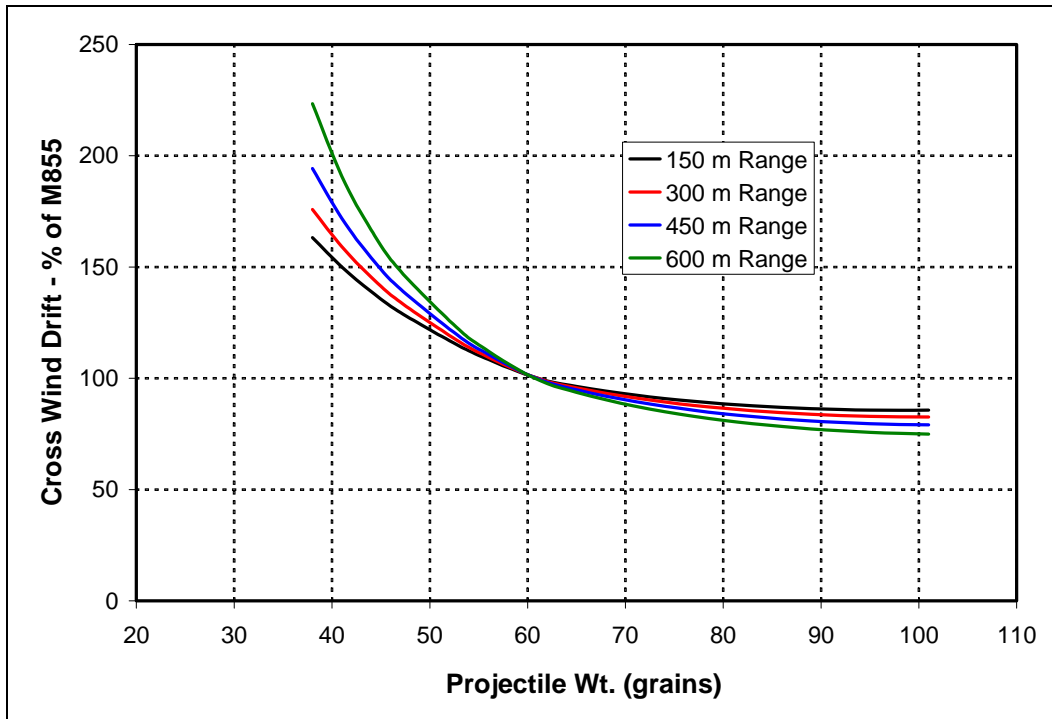
Figure 43. Cross-wind drift relative to M855 vs. projectile mass for ranges of 150, 300, 450, and 600 m.
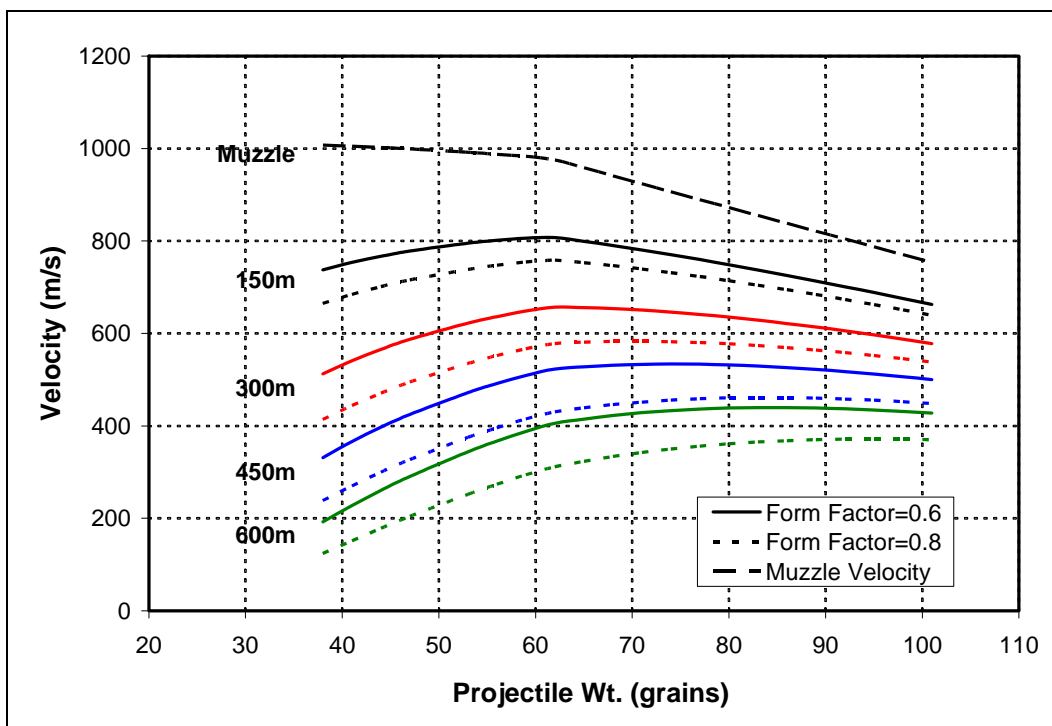

Figure 44. Impact velocity vs. projectile mass for form factors of 0.6 and 0.8 at ranges of 150, 300, 450, and 600 m.
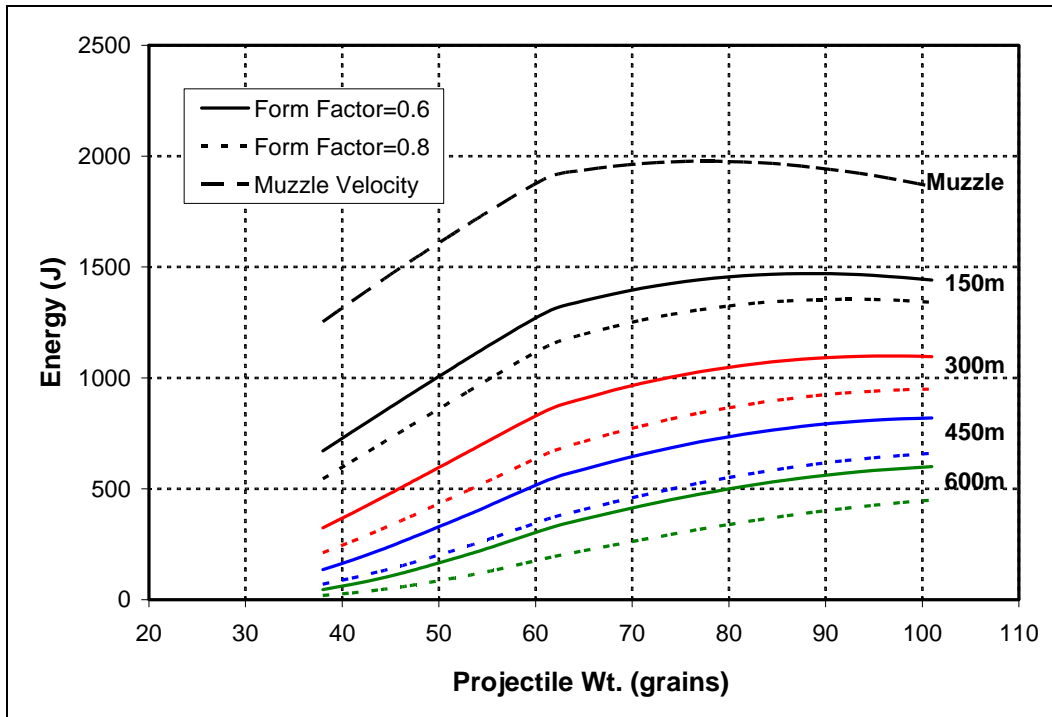
Figure 45. Impact energy vs. projectile mass for form factors of 0.6 and 0.8 at ranges of 150, 300, 450, and 600 m.

The gravity drop of projectiles with a form factor of 0.8 relative to the gravity drop of the M855 is shown in figure 46. The vertical impact location is nearly 1.0 mil or greater below the vertical impact location of M855 at 600 m for all projectile masses when the form factor is increased to 0.8. Given the predicted variation in the muzzle velocity with projectile mass, the form factor of 0.8 represents an upper limit for meeting ±1.0 mil mismatch requirement for projectile masses between 62 and 73 gr. A reduction in the form factor below 0.8 is required for projectile outside this range of projectile masses to meet the ±1.0 mil mismatch requirement.

Figure 47 shows the cross-wind drift of the projectile with a form factor of 0.8 as a percentage of the cross-wind drift of the M855. The cross-wind drift is greater than the M855 across the range of projectile masses considered here. For the 62-gr projectile, the increase in the form factor from 0.6 to 0.8 produces 35%–40% more cross-wind drift for ranges of 150–600 m. The relative effect decreases slightly as the projectile mass increases. The differences increase more substantially as the projectile mass decreases.

The results indicate some degree of sensitivity to the form factor associated with the drag coefficient. The survey of existing designs indicates that form factor of 0.6 can be reasonably accomplished, although significant reductions in form factor below 0.6 may be difficult. Projectile core configuration and mass distribution may result in designs with have drag form factors above 0.6. The current results provide a means of assessing the tradeoffs between
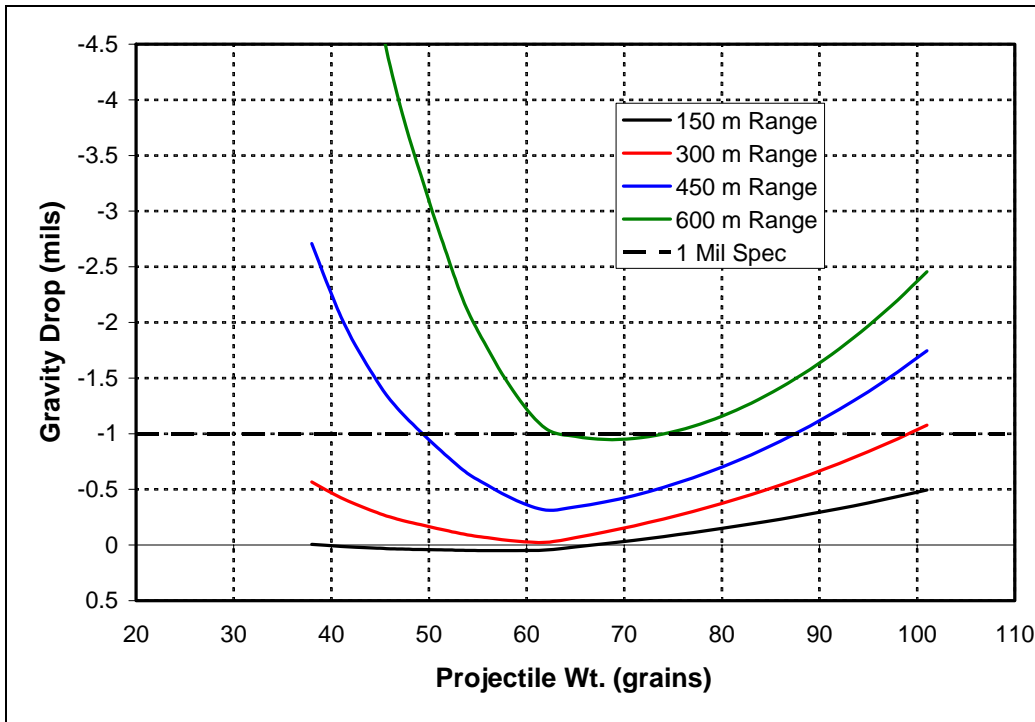
Figure 46. Gravity drop of projectiles with form factor of 0.8 relative to M855 vs. projectile mass for ranges of 150, 300, 450, and 600 m.
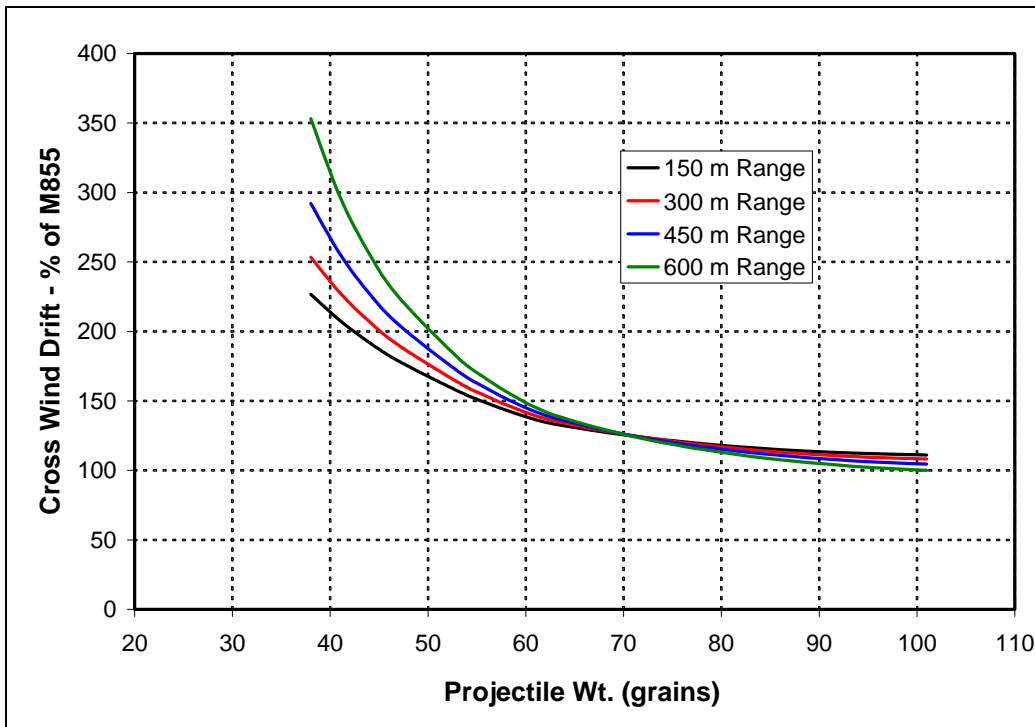

Figure 47. Cross-wind drift of projectiles with form factor of 0.8 relative to M855 vs. projectile mass for ranges of 150, 300, 450, and 600 m.

performance parameters associated with the point mass trajectory and the overall projectile effectiveness of the projectile.

5.1 Comparison of the Relative Performance of the M855 and Mk262

Currently within the U.S. Army there is discussion and perhaps some interest in use of the Mk262 in lieu of the M855. The Mk262 is based on the Sierra 77-gr match ammunition. The results shown here shed some light on the relative performance of the two rounds. In terms of impact velocity, impact energy, gravity drop, and cross-wind sensitivity, the Mk262 shows only marginal performance improvements in some cases (impact energy at long range, cross-wind drift) and slightly lower performance in other cases (gravity drop and impact velocity). These performance parameters represent an important subset of the complete set of performance parameters. Important considerations such as impact dispersion and lethality are not addressed here. Impact dispersion is influenced strongly by manufacturing considerations and there are significant differences in the manufacturing approaches and requirements for the high volume production of the M855 and the match grade Sierra 77-gr. Differences in the impact dispersion of the two rounds may exist. However, these differences must be considered in light of the other sources of delivery errors including cross wind and ranging errors that are directly related to the cross-wind sensitivity and gravity drop parameters examined here.

5.2 Copper and Steel-Cored M855 Variants

Environmental considerations have resulted in suggestions for removing the lead core of M855 and replacing it with alternative materials. One suggestion is to replace the lead core of the M855 with a steel core resulting in a projectile that weighs 52 gr. Another suggestion is to replace the lead core and steel penetrator with copper producing a projectile that weighs 57 gr. The current design approach can be used to predict the performance of potential designs.

The results show that over the first 150 m of flight, both the steel and copper variants have slightly impact higher velocity than the M855 because of the higher launch velocity. However, due to their lighter weight and correspondingly higher retardation, their impact velocity is lower at longer ranges and decreases to 83% and 92% of the impact velocity of the M855 at 600-m range. Because of the lighter weight of the both variants, the impact energy is less than the M855 across the trajectory. Both the copper- and steel-cored M855 variants have trajectories early in flight that are slightly above (less than 0.1 mil) the M855 due to the higher launch velocity, but the vertical impact point at 600 m is 0.1 mil and 0.5 mil, respectively, below the vertical impact point of the M855. The copper and steel cored M855 variants have 8%–12% and 18%–28% more cross-wind sensitivity, respectively, than the M855 over 150–600-m ranges, with the largest difference observed at the longest ranges.

6. Conclusion

A conceptual design approach for small-caliber munitions has been developed and applied to 5.56-mm ammunition. The method is based on an analytical approach for predicting the point mass trajectories for direct-fire munitions. The method utilizes a power law variation to characterize the variation of the drag coefficient with Mach number. High quality aerodynamic range data is used to demonstrate the validity of the power law approach for small-caliber munitions including the 5.56-mm M855. The method allows closed form solutions to be obtained for several important design quantities including the impact velocity and energy, gravity drop, and cross-wind drift. From the analytical method, it can be shown that these performance parameters are functions of three parameters: the muzzle velocity, muzzle retardation, and the exponent defining the power law drag variation. The analytical trajectory predictions has been validated by comparison with numerical predictions for the 5.56-mm M855 and excellent agreement is found.

An extensive database of trajectory data developed by a commercial small arms bullet manufacturer has been analyzed as part of the current study. From the database, a correlation that expresses the drag coefficient exponent as a function of the drag coefficient form factor has been developed for small arms bullets. The range of the form factor for low drag streamlined (typically boattailed) projectiles which represent likely candidates for tactical small arms bullets is also obtained from the database.

The method is then applied to investigate candidate designs for 5.56-mm ammunition. An initial set of results examines the performance of candidate designs in terms of muzzle velocity and muzzle retardation for a fixed value of the drag coefficient exponent. The results show the performance of candidate designs relative to the 5.56-mm M855 for a variety of performance metrics including trajectory mismatch and cross-wind sensitivity. In general, the results show that the best performance is obtained from projectiles which have high muzzle velocity and low muzzle retardation. The relative insensitivity of the results to the drag coefficient exponent is also demonstrated.

Recognizing that muzzle velocity is not truly an independent variable, but is dependent on launch mass and interior ballistic constraints, an additional set of results is obtained using interior ballistic computations to quantify the relationship between muzzle velocity and projectile mass. By considering designs with a drag coefficient form factor of 0.6, the performance of candidate designs can be assessed as a function of projectile mass. Performance parameters examined include impact velocity and energy, gravity drop, and cross-wind drift. For several performance parameters, the optimal performance is obtained for projectile masses close to that of the current 62-gr M855. Possible performance improvements are possible for some performance metrics with projectiles heavier than 62 gr. However, the performance gains

increase relatively slowly with increasing projectile mass, primarily because of the significant decrease in muzzle velocity with increasing projectile mass. Projectile designs lighter than 62 gr show improved performance for some metrics such as impact velocity at short range. However, the light weight and higher retardation associated with these rounds results generally results in poorer performance at ranges beyond 100–150 m.

The results documented here provide important design guidance for current efforts in 5.56-mm ammunition development. The results address primarily interior and exterior ballistic considerations, although some qualitative measures of terminal performance are predicted. Further analysis is required to ensure that the projectile designs are aerodynamically stable and have the required lethality. These considerations are being addressed in the next phase of the design effort.

7. References

1. Weinacht, P.; Cooper, G. R.; Newill, J. F. *Analytical Prediction of Trajectories for High-Velocity Direct-Fire Munitions*, ARL TR-3567; U.S. Army Research Laboratory: Aberdeen Proving Ground, MD, August 2005.

2. McCoy, R. L. *Modern Exterior Ballistics*; Schiffer Military History: Atglen, PA, 1999.

3. Tilghman, B. A. Firing Tables Branch, U.S. Army Armament Research, Development, and Engineering Center, Aberdeen Proving Ground, MD. Private communication, 8 December 2003.

4. McCoy, R. L. *Aerodynamic and Flight Dynamic Characteristics of the New Family of 5.56-mm NATO Ammunition*; BRL-MR-3476; U.S. Army Ballistics Research Laboratory: Aberdeen Proving Ground, MD, October 1985.

5. Arrow Tech Associates. *Prodas Users Manual*; Arrow Tech Associates: Burlington, VT, 2002.

6. Fourth Edition Rifle Exterior Ballistics Tables. http://www.exteriorballistics.com /ebexplained /4th-rifle_tables/index.cfm (accessed 28 February 2005).

7. Sierra Rifle Bullets Ballistic Coefficient Listing. http://www.exteriorballistics.com /ebexplained/riflecoefficients.cfm (accessed 28 February 2005).

8. Bullets. http://www.sierrabullets.com/index.cfm?section=bullets&page=bullets &bulletType=0 (accessed 28 February 2005).

9. Hoerner, S. F. *Fluid-Dynamic Drag*; Hoerner Fluid Dynamics: Brick Town, NJ, 1965.

10. Charters, A. C.; Stein, H. *The Drag of Projectiles with Truncated Cone Headshapes*; report no. 624; U.S. Army Ballistics Research Laboratories: Aberdeen Proving Ground, MD, March 1952.

11. *Firing Tables for Weapon, 5.56-mm, M16A1, Weapon, 5.56-mm, M16A2, Weapon, 5.56-mm, M249, Weapon, 5.56-mm, M4, Firing Cartridge, Ball, M855, Cartridge, Tracer, M856, Firing Cartridge, Ball, M193, Cartridge, Tracer, M196*; U.S. Army ARDEC Firing Tables; Aberdeen Proving Ground, MD, July 1996.

12. Department of the Army. *Rifle Marksmanship M16A1, M16A2/2, M16A4, and M4 Carbine*; Field Manual No. 3-22.9 (FM 23-9); Headquarters, Department of the Army: Washington, DC, 24 April 2003.

13. Anderson, R. D.; Fickie, K. D. *IBHVG2 (Interior Ballistics of High Velocity Guns, Version 2)—A User's Guide*; BRL-TR-2829; U.S. Army Ballistic Research Laboratory: Aberdeen Proving Ground, MD, July 1987.

14. Peterson, B. U.S. Army Research Laboratory, Aberdeen Proving Ground, MD. Private communication, 11 January 2005.

15. Kokinakis, W.; Sperrazza, J. *Criteria for Incapacitating Soldiers with Fragments and Flechettes*; BRL-1269; U.S. Army Ballistics Research Laboratory: Aberdeen Proving Ground, MD, January 1965.

16. Von Wahlde, R.; Metz, D. *Sniper Weapon Fire Control Error Budget Analysis*; ARL-TR-2065; U.S. Army Research Laboratory: Aberdeen Proving Ground, MD, August 1999.

List of Symbols, Abbreviations, and Acronyms

C	Ballistic coefficient
C_D	Drag coefficient
$C_D\big|_{V_0}$	Drag coefficient evaluated at the muzzle velocity
$C_D\big|_{V_{Ref}}$	Drag coefficient evaluated at the reference velocity
$C_{DG1}\big|_{V_{Ref}}$	Drag coefficient from G1 drag function evaluated at the reference velocity
D	Reference diameter
g	Gravitational acceleration
i_{Form}	Drag coefficient form factor
m	Projectile mass
M	Mach number
n	Exponent defining shape of the drag vs. Mach number curve
$\bar{s}$	Nondimensional range coordinate
SD	Sectional density, $\quad SD = \dfrac{m}{D^2}$
s_{g-drop}	Gravity drop
s_x, s_y	Horizontal and vertical displacement along trajectory
Δs_y	Deviation from intended vertical impact location due to ranging error
s_z	Out-of-plane displacement along trajectory (normal to *x-y* plane)
S_{ref}	Reference area, $S_{ref} = \dfrac{\pi D^2}{4}$
t	Time of flight
V	Total velocity
V_0	Muzzle velocity

V_{Ref} Reference velocity for comparison of form factor and retardation

$\left(\dfrac{dV}{ds} \right)_0$ Muzzle retardation

$\left(\dfrac{dV}{ds} \right)_{V_{Ref}}$ Retardation evaluated at reference velocity

w_z Cross-wind velocity

Greek Symbols

ε_R Ranging error

θ_0 Initial gun elevation angle

θ_I Trajectory impact angle

ρ Atmospheric density

No. of Copies	Organization	No. of Copies	Organization
1	ARROW TECH ASSOC 1233 SHELBURNE RD D8 W HATHAWAY SOUTH BURLINGTON VT 05403	1	ALLIANT TECHSYS INC MN07 LW54 D KAMDAR 4700 NATHAN LANE N PLYMOUTH MN 55442-2512
1	OREGON STATE UNIV DEPT OF MECHANICAL ENGR M COSTELLO CORVALLIS OR 97331	1	ATK ORDNANCE SYS MN07 MW44 B BECKER 4700 NATHAN LANE N PLYMOUTH MN 55442-2512
1	PRODUCT MGR SMALL AND MED CALIBER AMMO SFAE AMO MAS SMC M BULTER BLDG 354 PICATINNY ARSENAL NJ 07806-5000	1	US ARMY TACOM ARDEC CCAC AMSTA AR CCL C G FLEMING BLDG 65N PICATINNY ARSENAL NJ 07806-5000
1	PROJECT MGR MANEUVER AMMO SYS SFAE AMO MAS SMC R KOWALSKI BLDG 354 PICATINNY ARSENAL NJ 07806-5000	1	US ARMY TACOM-ARDEC CCAC AMSTA AR CCL B J MIDDLETON BLDG 65N PICATINNY ARSENAL NJ 07806-5000
3	ATK MN07 LW54 C AAKHUS R DOHRN M JANTSCHER 4700 NATHAN LANE N PLYMOUTH MN 55442	1	US ARMY TACOM ARDEC ASIC PROGRAM INTEGRATION OFC J A RESCH BLDG 1 PICATINNY ARSENAL NJ 07801
1	ATK LAKE CITY K ENLOW PO BOX 1000 INDEPENDENCE MO 64051-1000	3	US ARMY TACOM ARDEC M D MINISI S SPICKERT-FULTON M NICOLICH BLDG 65 PICATINNY ARSENAL NJ 07806-5000
5	ATK LAKE CITY SMALL CALIBER AMMO LAKE CITY ARMY AMMO PLANT MANSFIELD BOX 1000 DEPENDENCE MO 64051-1000	1	US ARMY TACOM ARDEC AMSTA AR CCH A S J MUSALLI BLDG 65S PICATINNY ARSENAL NJ 07806-5000
1	ATK LAKE CITY SMALL CALIBER AMMO MO10 003 LAKE CITY ARMY AMMO PLANT J WESTBROOK PO BOX 1000 INDEPENDENCE MO 64051-1000	1	US ARMY TACOM ARDEC AMSRD AAR AEM I R MAZESKI BLDG 65N PICATINNY ARSENAL NJ 07806-5000

1   US ARMY TACOM ARDEC
A P FARINA
BLDG 95
PICATINNY ARSENAL NJ 07806-5000

1   US ARMY TACOM ARDEC
CCAC
AMSTA AR CCL B
D J CONWAY
BLDG 65N
PICATINNY ARSENAL NJ 07806-5000

1   US ARMY TACOM ARDEC
AMSTA AR FSF T
H HUDGINS
BLDG 382
PICATINNY ARSENAL NJ 07806-5000

1   US ARMY TACOM ARDEC
CCAC AMSTA AR CCL D
F HANZL
BLDG 354
PICATINNY ARSENAL NJ 07806-5000

1   US ARMY TACOM ARDEC
P RIGGS
BLDG 65N
PICATINNY ARSENAL NJ 07806-5000

1   OPM MAS
SFAE AMO MAS MC
G DEROSA
BLDG 354
PICATINNY ARSENAL NJ 07806-5000

1   SIERRA BULLETS
P DALY
1400 W HENRY ST
SEDALIA MO 65302-0818

1   COMMANDER
US ARMY TACOM ARDEC
AMSTR AR FSF X
W TOLEDO
BUILDING 95 S
PICATINNY ARSENAL NJ 07806-5000

1   AEROPREDICTION INC
F MOORE
9449 GROVER DR STE 201
KING GEORGE VA 22485

1   US ARMY AMRDEC
AMSAM RD SS AT
R W KRETZSCHMAR
BLDG 5400
REDSTONE ARSENAL AL 35898-5000

3   ST MARKS POWDER
GENERAL DYNAMICS
J DRUMMOND
J HOWARD
R PULVER
7121 COASTAL HWY
CRAWFORDVILLE FL 32327

3   RADFORD ARMY AMMO PLANT
K BROWN
W J WERRRELL
H ZIEGLER
PO BOX 1 ROUTE 114
RADFORD VA 24143

ABERDEEN PROVING GROUND

2   COMMANDER
US ARMY ARDEC
FIRING TABLES AND
BALLISTICS DIV
AMSRD AAR AEF T
B TILGHMAN
F MIRABELLE
2201 ABERDEEN BLVD
APG MD 21005-5001

28   DIR USARL
AMSRD ARL WM
  J SMITH
AMSRD ARL WM B
  T ROSENBERGER
AMSRD ARL WM BA
  D LYON
AMSRD ARL WM BC
  M BUNDY
  J DESPIRITO
  J GARNER
  B GUIDOS
  K HEAVEY
  J NEWILL
  P PLOSTINS
  J SAHU
  S SILTON
  D WEBB
  P WEINACHT (3 CPS)

63

NO. OF
COPIES ORGANIZATION

AMSRD ARL WM BD
  A BRANT
  P CONROY
  B FORCH
  M NUSCA
  T WILLIAMS
AMSRD ARL WM BF
  R PEARSON
  W OBERLE
  S WILKERSON
  E RIGAS
AMSRD ARL WM TA
  M BURKINS
AMSRD ARL WM TC
  B PETERSON
  L MAGNESS